

**Charles University  
1st Faculty of Medicine**

Study programme: Experimental surgery



**UNIVERZITA KARLOVA  
1. lékařská fakulta**

**MUDr. Vladimír Koucký**

**Immunological aspects of head and neck cancer in relation to etiology**

*Imunologické aspekty maligních nádorů hlavy a krku ve vztahu k etiologii*

PhD Thesis

Supervisor: doc. MUDr. Jan Bouček, Ph.D.

Consultant: RNDr. Anna Fialová, Ph.D.

Prague, 2022

**Declaration:**

I, Vladimír Koucký, declare that the final thesis was prepared on my own and I properly cited all the sources used in the text. Also, I confirm that the thesis was not used to achieve any other or similar academic title.

I agree with the permanent archiving of the electronic form of the thesis in the database Theses.cz for the purpose of constant plagiarism control of academic documents.

Prague, 26.08.2022

MUDr. Vladimír Koucký

Signature

**Identification record:**

KOUCKÝ, Vladimír. *Immunological aspects of head and neck cancer in relation to etiology [Imunologické aspekty maligních nádorů hlavy a krku ve vztahu k etiologii]*. Praha, 2022. 107 s. Disertační práce (PhD Thesis). Univerzita Karlova, 1. lékařská fakulta, Klinika otorinolaryngologie a chirurgie hlavy a krku 1.LF UK a FN v Motole. Vedoucí závěrečné práce Bouček, Jan.

## **Acknowledgements:**

First and foremost, I would like to express my sincere gratitude to my supervisors doc. MUDr. Jan Bouček, Ph.D. and RNDr. Anna Fialová, Ph.D. for their time, constant support and guiding not only through my PhD studies, but also during first steps and early years of my professional life.

A special thanks belongs to the head of the Department of Otorhinolaryngology, Head and Neck Surgery, First Medical Faculty and Motol University Hospital prof. MUDr. Jan Plzák, Ph.D, and to the director of Sotio a.s. prof. MUDr. Radek Špíšek, Ph.D. for the great opportunity to be a part of their teams and for their helpfulness whenever needed.

Also, I am deeply indebted to my colleagues at scientific department of Sotio a.s. that selflessly provided me their research skills, knowledge and personal support. Last but not least I would like to thank to the medical and nursery staff of the Department of Otorhinolaryngology, Head and Neck Surgery, First Medical Faculty and Motol University Hospital for their assistance and obligingness in sample collection and management of the patients.

## Abstrakt

Nádorová imunologie je progresivně se rozvíjející multidisciplinární vědní obor. Výsledky základního výzkumu již navíc byly úspěšně přeneseny do klinické praxe a okamžitý úspěch nových imunoterapeutických přípravků, především blokátorů kontrolních bodů imunitního systému, dále vede k podpoře a růstu výzkumu v této problematice. V případě karcinomů hlavy a krku (HNSCC) byly identifikovány některé složky imunitní odpovědi, jako například  $CD8^+$  T lymfocyty, které hrají významnou roli v průběhu onemocnění. HNSCC je navíc rozmanitá skupina nádorů, kdy významná část z nich je indukována vysoce rizikovými kmeny lidského papilomaviru (HPV). HPV-asociované nádory ( $HPV^+$ ) mají lepší odpověď na standardní léčbu a právě imunitní odpověď byla identifikována jako jeden z hlavních faktorů zodpovědných za tento jev. V naší práci jsme se zaměřili na analýzu fenotypu, funkčních vlastností a prognostické hodnoty tumor-infiltrujících leukocytů u pacientů s HNSCC se zohledněním HPV statusu tumoru. Detekovali jsme  $CD8^+$  tumor-infiltrující T lymfocyty reaktivní vůči antigenům HPV16 u většiny  $HPV^+$  orofaryngeálních karcinomů. Tyto T lymfocyty byly schopny po specifické stimulaci HPV-derivovanými peptidy produkovat důležité prozánětlivé cytokiny,  $IFN\gamma$  a  $TNF\alpha$ . Produkce cytokinů pak byla umocněna kombinovanou blokádou dvou důležitých kontrolních bodů imunitního systému - receptorů PD-1 a TIM-3. Tyto výsledky tak podporují myšlenku kombinované imunoterapie u těchto nádorů. V naší imunohistochemické studii jsme identifikovali silnou pozitivní prognostickou hodnotu tumor-infiltrujících B lymfocytů (TIL-Bs) u pacientů s karcinomy orofaryngu. Ještě silnějším prognostickým faktorem se pak ukázaly být membránové interakce mezi TIL-Bs a  $CD8^+$  T lymfocyty. V naší poslední práci jsme analyzovali funkční kapacitu tumor-infiltrujících plasmacytoidních dendritických buněk (pDCs) u HNSCC, podskupiny dendritických buněk hrající zásadní roli v protivirové imunitě. Zjistili jsme, že narození od  $HPV^+$  nádorů inhibuje cytokinové prostředí HPV-negativních tumorů produkci  $IFN\alpha$  plasmacytoidními DC a takto suprimované pDCs indukují proliferaci regulačních T lymfocytů v nádorovém mikroprostředí. Našimi poznatky jsme významně přispěli ke znalostem o imunologické diverzitě HNSCC a identifikovali B lymfocyty jako důležitý biomarker s klinickým potenciálem.

**Klíčová slova:** dlaždicobuněčný karcinom hlavy a krku, lidský papilomavirus, nádorová imunologie, tumor-infiltrující lymfocyty, plasmacytoidní dendritické buňky

## **Abstract**

Tumor immunology is a progressively developing, multidisciplinary branch of biology. Results of basic research have already been successfully translated to clinical practice. The immediate success of new immunotherapeutic drugs, especially immune checkpoint inhibitors, has further supported the expansion of basic and clinical research in this field. In the case of head and neck squamous cell carcinoma (HNSCC), some immune system elements, such as CD8<sup>+</sup> T cells, were shown to play an important role in the progression of the disease. Importantly, HNSCC is a diverse group of diseases, and a significant number of the tumors are induced by high-risk strains of human papillomavirus (HPV). HPV-associated tumors (HPV<sup>+</sup>) respond better to standard therapy, and the immune system was shown to be one of the crucial factors in this phenomenon. We focused on the analysis of phenotype, function, and prognostic value in tumor-infiltrating immune cells in HNSCC patients regarding the HPV status of the tumor. We were able to detect CD8<sup>+</sup> tumor-infiltrating T cells reacting to HPV16 antigens in the majority of HPV<sup>+</sup> oropharyngeal cancers. Moreover, activity of these T cells was enhanced after blockade of both PD-1 and TIM-3 immune-checkpoint pathways, supporting a concept of combined immunotherapy. In our immunohistochemical analysis, we identified a strong prognostic role of tumor-infiltrating B lymphocytes (TIL-Bs) in oropharyngeal cancer patients. Furthermore, visible cell-to-cell interactions between TIL-Bs and CD8<sup>+</sup> T cells were a superior prognostic marker. Finally, we analyzed the functional capacity of tumor-infiltrating plasmacytoid dendritic cells (pDCs) in HNSCC, a subset of DCs that is essential for antiviral immunity. We showed that, compared with HPV<sup>+</sup> HNSCC, the cytokine milieu of HPV<sup>-</sup> tumors significantly impacted production of IFN $\alpha$  by pDCs and favored induction of regulatory T cells in the tumor microenvironment. We significantly contributed to the knowledge of the HNSCC immunological diversity and described B cells as an important new biomarker with translational potential.

**Key words:** head and neck squamous cell carcinoma, human papillomavirus, tumor immunology, tumor-infiltrating lymphocytes, plasmacytoid dendritic cells

## Table of contents

List of Abbreviations.....	9
1. Introduction.....	12
1.1 Head and neck cancer overview.....	13
1.1.1 Epidemiology and classification.....	13
1.1.2 Etiology and association with HPV.....	14
1.1.3 Symptoms and diagnostic workup.....	15
1.1.4 Therapy and prognosis.....	16
1.2 Carcinogenic effect of human papillomaviruses.....	17
1.2.1 Transmission and prevalence of HPV infection.....	18
1.2.2 HPV cell cycle and oncoproteins.....	19
1.2.3 Genetic changes associated with HPV-induced tumors.....	20
1.2.4 HPV detection.....	21
1.2 Immune microenvironment of head and neck cancer.....	22
1.3.1. General principles of antitumor immunity.....	23
1.3.2 Components of the HNSCC tumor microenvironment and its shaping by HPV.....	26
1.3.2.1 Cancer-associated fibroblasts and extracellular matrix.....	26
1.3.2.2 Cytokine and chemokine milieu.....	27
1.3.2.3 T lymphocytes.....	28
1.3.2.4 Immune-checkpoint molecules.....	29
1.3.2.5 B lymphocytes.....	31
1.3.2.6 Dendritic cells.....	32
1.3.2.7 Other leukocyte subgroups.....	33
1.4 Head and neck cancer immunotherapy.....	34
2. Aims of the study and hypotheses.....	38
2.1 Study of HPV-specific tumor-infiltrating T cells in oropharyngeal cancer (Study 1) ...	38
2.2 Study of tumor-infiltrating B cells in oropharyngeal cancer (Study 2).....	38
2.3 Study of tumor-infiltrating plasmacytoid dendritic cells in head and neck cancer (Study 3).....	39
3. Materials and methods.....	40
3.1 Patient cohorts.....	40
3.1.1 Study of HPV-specific tumor-infiltrating T cells in oropharyngeal cancer (Study 1).....	40
3.1.2 Study of tumor-infiltrating B cells in oropharyngeal cancer (Study 2).....	41
3.1.3 Study of tumor-infiltrating plasmacytoid dendritic cells in head and neck cancer..	41

(Study 3).....	41
3.2 Tumor tissue and blood processing .....	45
3.3 Flow cytometric analysis .....	45
3.4 Immunohistochemistry .....	47
3.5 Quantitative real-time PCR .....	48
3.6 Cytokine and chemokine detection.....	49
3.7 HPV detection.....	49
3.8 Functional cell experiments .....	50
3.8.1 Study of HPV-specific tumor-infiltrating T cells in oropharyngeal cancer (Study 1) .....	50
3.8.2 Study of tumor-infiltrating B cells in oropharyngeal cancer (Study 2) .....	52
3.8.3 Study of tumor-infiltrating plasmacytoid dendritic cells in head and neck cancer (Study 3).....	52
3.9 Statistical analysis and graph editing.....	53
4. Results .....	54
4.1 Study of HPV-specific tumor-infiltrating T cells in oropharyngeal cancer (Study 1) .	54
4.2 Study of tumor-infiltrating B cells in oropharyngeal cancer (Study 2) .....	63
4.3 Study of tumor-infiltrating plasmacytoid dendritic cells in head and neck cancer (Study 3).....	78
5. Discussion .....	90
6. Conclusions .....	97
References .....	98

## List of Abbreviations

AJCC	American Joint Committee on Cancer
APC	antigen presenting cells
BCL2L1	BCL2-like 1 protein
BDCA-2	blood dendritic cell antigen 2
BMP	bone morphogenetic protein
Bregs	B regulatory cells
CAF	cancer-associated fibroblasts
CCL	C-C motif chemokine ligand
CD	cluster of differentiation
CDK	cyclin-dependent kinase
CpG ODN	CpG oligodeoxynucleotides
CTLA-4	cytotoxic T-lymphocyte-associated protein 4
cTNM	clinical TNM classification
CXCL	C-X-C motif chemokine ligand
DAMPs	damage-associated molecular patterns
DCs	dendritic cells
DC-LAMP	dendritic cell lysosomal associated membrane glycoprotein
DNA	deoxyribonucleic acid
EDTA	ethylenediaminetetraacetic acid
EGFR	epidermal growth factor receptor
ELISA	enzyme-linked immuno sorbent assay
FFPE	formalin-fixed, paraffin-embedded
FLT3L	FMS-like tyrosine kinase 3 ligand
FoxP3	forkhead box P3
HLA	human leukocyte antigen
HMGB1	high-mobility group box 1 protein
HNSCC	head and neck squamous cell carcinoma
HPV	human papillomavirus
ICI	immune checkpoint inhibitors

ICOS/ ICOS-L	inducible costimulator / inducible costimulator ligand
IDO	indoleamine 2,3-dioxygenase
IFN	interferon
IgD	immunoglobulin D
IGF	insuline-like growth factor
IgG	immunoglobulin G
IgM	immunoglobulin M
IHC	immunohistochemistry
IL	interleukin
IMQ	imiquimod
ISH	in situ hybridization
LAG-3	lymphocyte-activation gene 3
mAb	monoclonal antibody
MAMPs	microbe-associated molecular patterns
mDCs	myeloid dendritic cells
MDSC	myeloid-derived suppressor cells
MFI	mean fluorescence intensity
MHC	major histocompatibility complex
mRNA	messenger ribonucleic acid
NCCN	National Comprehensive Cancer Network
NK	natural killer
OPSCC	oropharyngeal squamous cell carcinoma
p16 <sup>inkA4</sup>	cyclin-dependent kinase inhibitor 2A
PBMC	peripheral blood mononuclear cells
PBS	phosphate-buffered saline
PCR	polymerase chain reaction
PD-1	programed cell death 1
pDCs	plasmacytoid dendritic cells
PD-L1/2	programed cell death ligand 1/2
PIK3	phosphoinositide 3-kinase
PMA	phorbol 12-myristate 13-acetate
pTNM	pathological TNM classification

RB	retinoblastoma protein
SD	standard deviation
SEM	standard error of the mean
TAA	tumor-associated antigens
TCR	T-cell receptor
TGF	tumor growth factor
TIGIT	T-cell immunoreceptor with Ig and ITIM domains
TIL-Bs	tumor-infiltrating B lymphocytes
TILs	tumor-infiltrating lymphocytes
TIM-3	T-cell immunoglobulin and mucin-domain containing-3
TLR	toll-like receptor
TLS	tertiary lymphoid structures
TME	tumor microenvironment
TNF $\alpha$	tumor necrosis factor alpha
TP53	tumor protein 53
TRAIL	TNF-related apoptosis-inducing ligand
Tregs	T regulatory cells
TSA	tumor specific antigens
VEGF	Vascular endothelial growth factor

## 1. Introduction

Malignant tumors are the second most common cause of death worldwide after cardiovascular diseases. Although a small number of cancers have an inherited, monogenic background, most malignancies have multifactorial etiology, including polygenic dispositions, epigenetic influences, and environmental factors. Therefore, some tumor types may be at least partially preventable. An example are tumors that are strongly associated with smoking, a habit that is responsible for approximately 30% all cancer deaths in developed countries [Peto et al. 1992]. Other preventable diseases are virally-induced tumors. Discovery of human papillomavirus (HPV) as an important etiological agent of cervical cancer in women led to the development of vaccine prophylaxis and the subsequent decrease in high-grade cervical lesion incidence in highly vaccinated populations [Guo et al. 2018, Gargano et al. 2019]. Both etiological agents, smoking and HPV, are also significantly associated with head and neck cancer induction, making it a group of diseases that has a significant potential for lowered incidence using preventive approaches. Unfortunately, these and many other preventive efforts are insufficient; therefore, cancer-targeted research and treatment development are one of the primary goals of medicine. All the essential mainstays of cancer treatment, namely surgery, radiotherapy, and chemotherapy, have made significant progress in previous decades. However, in many diagnoses, these modalities have reached their limits and a new paradigm of cancer treatment is needed. Over the last few years, we have had a chance to witness a rise of a new cancer treatment strategy that is based on the activation of the patient's immune system. The success of new immunotherapeutic drugs, especially immune checkpoint inhibitors (ICIs), provided a dose of optimism for tumor immunology, which has become one of the leading topics in cancer research. Despite the achievements of current immune-based approaches, there is still much to elucidate regarding the immunity-cancer relationship to improve and further evolve the treatment of patients.

The first, theoretic part of the thesis summarizes the topic of head and neck cancer, with emphasis on the carcinogenic role of HPV and its biology. In addition, the current knowledge on innate and adaptive immune responses in the tumor microenvironment (TME) of head and neck carcinomas and their therapeutic implications are discussed. In the second part of the thesis, our original research on the head and neck squamous cell carcinoma (HNSCC) TME is presented.

## 1.1 Head and neck cancer overview

Head and neck carcinomas are burdened with high morbidity and mortality; however, they are exciting from an immunological point of view. These carcinomas are a heterogeneous group of malignant tumors comprising a variety of histological subtypes and different locations of occurrence. Nevertheless, more than 90% of these tumors are HNSCCs whose progression can differ significantly according to the anatomic locality and etiology. The main sublocations of HNSCCs are the oral cavity, oropharynx, hypopharynx, larynx, paranasal sinuses, and nasopharynx. The thyroid gland and salivary gland tumors are clinically important among head and neck cancers; however, squamous cell carcinoma is a rare entity in these locations, and it will not be discussed in this thesis.

### 1.1.1 Epidemiology and classification

The annual incidence of HNSCC was reported to be 890 000 cases worldwide in 2018 [Bray et al. 2018], with more than 450 000 cases of cancer-associated death [Bray et al. 2018]. To the final count of affected people, we can include a significant number of patients suffering from severe morbidity due to the aggressive treatment that is part of standard protocols. In the Czech Republic, the incidence of head and neck cancer in 2017 was around 2 200 cases. The most common sublocations were the oral cavity, oropharynx, and larynx. Concerning oropharyngeal cancer, most of the cases (420 patients) were located in the palatine tonsil. The other anatomic regions, such as paranasal sinuses, nasopharynx, and hypopharynx, accounted for less than 300 cases altogether. The incidence and mortality dynamics have significantly changed since 2000 and differ between the subsites; there was an increase in oral cavity cancer (excluding salivary gland tumors) from approximately 4.5 to 6.6/100 000 cases and a slight mortality increase from 2.47 to 2.79/100 000 cases. Data for laryngeal cancer have been stable since 2000, accounting for an incidence of 5/100 000 and a mortality rate of 2.6/100 000. Importantly, we have observed a striking increase in age-dependent incidence and mortality in the case of oropharyngeal tumors. Incidence of palatine tonsil cancer increased from 1.85 to 4/100 000, and the mortality rate increased from 0.9 to 1.5/100 000. Similarly, the second most common oropharyngeal subsite, the base of the tongue, experienced an incidence increase from 0.85 to 1.5/100 000, with a relatively stable mortality rate fluctuating around 0.55/100 000. The peak of oropharyngeal cancer incidence is between 55 and 64 years; however, it has shifted to

younger patients in last 2 decades. Concerning gender predilection, all these tumors are two (oropharynx) to nine (larynx) times more common in men than women. The data for the Czech population were extracted from databases based on national oncologic register data and were obtained from [www.svod.cz](http://www.svod.cz).

### 1.1.2 Etiology and association with HPV

The epidemiological data are far more interesting when the main etiological factors are taken into consideration. Originally, well-established dispositions for the development of HNSCC were heavy tobacco smoking and alcohol intake. Smoking is a sufficient cause; however, alcohol intake significantly multiplies the risk of HNSCC. Whether this increase in risk is due to a systemic metabolic effect, local irritation, dissolution of cigarette carcinogens, or all the mechanisms combined, remains unclear [Hashibe et al. 2009]. The duration of smoking history and number of cigarettes per day correlate with head and neck cancer risk; however, there are reports showing increased incidence of HNSCC in weaker smokers who smoked for a longer time compared with stronger smokers who smoked for a shorter period [Tomar 2020]. Active smoking is also a factor that is significantly associated with treatment failure and disease relapse [Chen et al. 2011]. In contrast, the incidence of tobacco-related tumors is decreasing slightly in developed countries, and the rise of oropharyngeal cancer, which we can observe in the Czech Republic, is due to the carcinogenic action of high-risk strains of HPV, especially HPV16. On average, more than 50% of all oropharyngeal squamous cell carcinomas (OPSCCs) are currently driven by HPV (varying from 10% to 90% in different populations) [Marur et al. 2010]. Data from the USA show an increase in HPV prevalence in OPSCCs from 16.3% in the 1980s to 72.2% in the 2000s [Chaturvedi et al. 2011]. There are studies showing increased hazard or odds ratios for HNSCC according to the number of sexual partners, oral sex partners, and earlier age at sexual debut [Gillison et al. 2015]. Importantly, patients with HPV-associated tumors show markedly better response to standard treatment protocols, regardless of the chosen modality, and significantly improved overall survival [Ang et al. 2010, Licitra et al. 2006, Fakhry et al. 2008]. These factors led to the actualization of TNM staging of HNSCC by AJCC and UICC in 2017. The 8<sup>th</sup> edition of the TNM classification categorized OPSCC on HPV-negative (HPV<sup>-</sup>) and HPV-positive (HPV<sup>+</sup>) subgroups based on p16 protein positivity on immunohistochemical staining [James D. Brierley 2017]. The cut-off value for p16 expression was estimated as positivity of more than 70% of the cancer cells. For p16-positive tumors, there

is a difference in clinical (cTNM) and pathological (pTNM) classification, especially in case of nodal status. According to the new staging system, most HPV<sup>+</sup> patients originally classified as stage III or IV have been shifted to stage I and II. In the case of pathological N status, there is no prognostic role of size of the metastases; however, the number of metastatic lymph nodes is considered, regardless of unilateral or bilateral neck involvement. Nevertheless, based on current knowledge, it is evident that HPV<sup>+</sup> patients are not a uniform group of patients and there are individuals with highly aggressive disease and unfavorable prognosis. Several hazard-risk models were proposed for the purpose of stratification of HPV<sup>+</sup> patients. For example, Ang et al. reported a well-known model of low-, intermediate-, and high-risk patient groups based on their smoking pack-year values [Ang et al. 2010]. However, in 2022, there was still no valid, generally accepted biomarker that could further stratify HPV<sup>+</sup> patients. Furthermore, the treatment strategies for both HPV<sup>+</sup> and HPV<sup>-</sup> OPSCC are nearly identical, and possible deintensification of treatment in prognostically favorable patients is currently under investigation. The oncogenic effects of HPV at other anatomic head and neck sublocations are not well established; the topic is mostly studied in oral squamous cell carcinoma, and there are inconsistent reports regarding the detection methods and clinical outcomes.

### 1.1.3 Symptoms and diagnostic workup

The main symptoms, such as pain, dysphagia, or hoarseness, manifest based on the site of the lesion. Despite adequate access to the upper aerodigestive tract and possible self-evaluation of mucosal infiltration by visualization, patients present to the clinic at an advanced stage in more than 60% of cases [Chow 2020]. The other important manifestation of head and neck malignancy is a neck lump caused by a metastatic lymph node. A small primary tumor accompanied by large, cystic metastatic lymph nodes is a typical finding on imaging that is characteristic for HPV<sup>+</sup> oropharyngeal cancer, emphasizing the biological distinction of HPV-associated tumors [Goldenberg et al. 2008]. However, the cystic lymph nodes are more prone to false-negative findings when fine-needle aspiration biopsy is used for evaluation. In some cases, the primary tumor lesion is not evident due to involution of the tumor or because it is restricted to the deep tonsillar crypts and the neck masses are the main target of the diagnostic process. When the originally unknown primary tumor is located using PET CT and/or endoscopic evaluation under general anesthesia accompanied with diagnostic tonsillectomy, it is HPV<sup>+</sup> in most cases [Axelsson et al. 2017, Motz et al. 2016]. This finding further highlights

the different behavior and clinical presentation of the HPV-induced tumors. Evaluation of p16 is obligatory in all the OPSCC to enable evaluation of the tumor, according to the 8<sup>th</sup> edition of the TNM classification. Other detection methods, such as HPV16 *in situ* hybridization or polymerase chain reaction, are recommended for confirmation of viral etiology but are not obligatory.

#### 1.1.4 Therapy and prognosis

Head and neck cancer management is a highly specialized topic that should be restricted to high-volume centers. The accessibility of a multidisciplinary team, supportive medical branches, and trained nursing staff have proven to influence patient prognosis [David et al. 2017]. The treatment of HNSCC not only targets the location of the primary tumor, but also the lymphatic vessels and lymph nodes of the neck, despite a lack of clinical suspicion of disease dissemination. Lymph node involvement is one the most important predictors of survival [Jones et al. 1993]; even clinically, N0 necks are suspicious of occult metastases in up to 30% of patients, depending on the primary tumor site. In case of metastasis to distant organs, such as the lungs and liver, the prognosis is usually fatal and, except for in the case of solitary metastases, systemic therapy has palliative intention. The mainstays of HNSCC therapy are surgery, radiotherapy, cisplatin-based chemotherapy, anti-EGFR targeted therapy with cetuximab, and combinations of these modalities. Stages I and II can be treated by surgery or radiotherapy alone or surgery with adjuvant radiotherapy, depending on the tumor location, accessibility, and histopathological risk factors. Locally advanced disease (i.e. stages III to IV) is treated by a multimodal approach, such as definitive concurrent chemoradiotherapy or surgery with adjuvant chemoradiation. Despite favorable treatment results in HPV-associated OPSCC, where even advanced stages have a 5-year overall survival (OS) rate of more than 80%, in general, more than half of HNSCC patients develop local recurrence and/or distant metastasis, and the 5-year OS of advanced stages is less than 50% [Chow 2020]. Recurrent and metastatic disease should be treated by salvage surgery and radiotherapy when possible. However, because of distant dissemination and previous radiation dose load, systemic treatment is the only option in many patients. Standard of care in these cases was the EXTREME protocol, combining cetuximab, fluorouracil, and cis/carboplatin [Vermorken et al. 2008]; however, the approach to these patients changed dramatically when the efficacy of the new immunotherapeutic drugs nivolumab and pembrolizumab was proven in clinical trials [Ferris

et al. 2016, Cohen et al. 2019]. The immunotherapy of head and neck cancer is described in detail in Chapter 1.4.

Concerning HPV<sup>+</sup> OPSCC, the optimistic survival results of most of the patients are nevertheless associated with high morbidity and decreased quality of life due to the aggressive therapy. Two large prospective randomized studies, DeEscalate and RTOG 1016, examined a deintensification protocol in which cisplatin chemotherapy was replaced by cetuximab. The studies had to be prematurely halted due to the clearly observed worsening survival of the patients in the experimental arm [Mehanna et al. 2019, Gillison et al. 2019]. In view of these results, deeper stratification of HPV<sup>+</sup> patients is needed. In contrast, in developed countries, we can expect decreasing incidence of HPV<sup>+</sup> OPSCC because of anti-HPV vaccination programs that already shown their effectiveness in anogenital cancers. However, the proposed time estimate of the vaccination campaign impact is 40 years [Gillison et al. 2015].

## **1.2 Carcinogenic effect of human papillomaviruses**

HPVs are a large group of non-enveloped double-stranded DNA viruses best known for their ability to cause both benign and highly malignant disease of cutaneous and mucosal surfaces. There are more than 200 identified genotypes of HPV; however, only a fraction can cause serious diseases. The subtypes belonging to Beta, Gamma, and Mu phylogenetic genera penetrate mainly the skin and can lead to wart formation or have no manifestations. In contrast, genotypes of the Alpha genus have affinity for anogenital epithelial surfaces and are currently the most common sexually transmitted disease [Schiffman et al. 2016]. To date, 14 high-risk strains of HPV that can lead to cancer development in case of persistent infection have been identified. The reasons why a persistent infection will stay productive or become cell-transforming are not yet fully elucidated. The most common HPV-induced malignancy is cervical cancer, with a worldwide burden of more than 550 000 cases per year and 300 000 cancer-associated deaths [Bray et al. 2018]. The number of patients diagnosed with HPV-induced OPSCC worldwide was estimated to be 30 000 cases per year [de Martel et al. 2017]. However, the incidence varies significantly among countries, with increasing numbers in high-income societies. The HPV16 subtype is the most prevalent high-risk strain that is responsible for the majority of both cervical and oropharyngeal cancers; it makes HPV one of the most important human carcinogens. The discovery of high-risk HPV as a crucial agent in cancer

development by Harald Zur Hausen was awarded the Nobel prize in 2008. Generally, it is estimated that almost 30% of infection-related malignancies are associated with HPV, which highlights the medical and socio-economic importance of this virus [Bouvard et al. 2009].

### 1.2.1 Transmission and prevalence of HPV infection

Sexual intercourse, penetrative or non-penetrative, represents a method of HPV transmission. In the cervix, the most susceptible tissue is the squamocolumnar junction. In the oropharynx, the reticulated epithelium of deep tonsillar crypts is the most common location of viral invasion. Both these locations are characterized by different expression profiles compared with their surrounding epithelium, notably overexpression of cytokeratin 7 [Herfs et al. 2012]. The incidence of the infection significantly increases after the average age at which individuals begin their sex lives in different populations. The prevalence of anogenital HPV is highly variable among different populations; however, there are estimates from the pre-vaccination era of a 12% global prevalence of high-risk HPV infection among women [Bruni et al. 2010]. In case of both high- and low-risk HPV subtypes, the anogenital infection prevalence was reported to be up to 40% in both men and women in USA [McQuillan et al. 2017]. In contrast, oral HPV prevalence in healthy men and women was approximately 4–7% [McQuillan et al. 2017] [Kreimer et al. 2011] [Tam et al. 2018]. In the Czech Republic, HPV prevalence in oral rinses in the unvaccinated population was reported to be 8.8% [Malerova et al. 2020]. In case of high-risk strains, such as HPV16, the oral prevalence in healthy men was approximately 1% [Kreimer et al. 2011, Tam et al. 2018]. Despite different prevalence rates and less data concerning oral and oropharyngeal HPV infection, there are similarities in infection persistence to anogenital HPV infection. Data show that pre-existing HPV16 infection at the baseline of the study is more likely to persist compared with newly acquired infection. Therefore, long-term infections are more prone to becoming persistent and the higher prevalence of oral HPV16 in older men is thus not due to an increased new-infection rate [Pierce Campbell et al. 2015]. This observation corresponds with HPV infection in the cervix [Mollers et al. 2013]. Moreover, it was shown that women with persistent HPV infection in the cervix also have longer persistence of oral HPV. Factors influencing viral persistency, such as viral attributes, immune response, and behavior co-factors, are not well elucidated; however, it seems these factors are similar between the cervix and head and neck regions [Pierce Campbell et al. 2015]. One of the discussed co-factors is smoking. Whereas some studies reported higher likelihood of infection acquisition

and higher persistence rate in smokers [Kero et al. 2014, D'Souza et al. 2007], others did not confirm this finding [Pierce Campbell et al. 2015]. Nevertheless, it is necessary to distinguish between the prevalence results based on oral cavity rinses/smears and tonsillar tissue specimens prepared from resected tonsils. The studies using selected tonsillar tissue generally reported lower rates of HPV detection, with 0–3.9% of samples being positive for high-risk HPV [Mordechai et al. 2019, Palmer et al. 2014, Rieth et al. 2018].

### 1.2.2 HPV cell cycle and oncoproteins

HPV infects the basal layer of the stratified epithelium, and its DNA is established in the form of episomes in the cell cytoplasm [Lechner et al. 2022]. However, in a majority of HPV-induced cancers and high-grade precancerous lesions, the HPV16 and HPV18 DNA are found to be integrated into the genome of host cell [McBride et al. 2017]. Early episomal gene expression initiates deregulated expression of integrated genes, such as E6 and E7. Infected cells proliferate and enter more superficial layers of the epithelium. While HPV genome amplification occurs mainly in the middle layers of the epithelium, the assembly of new virions and their release occurs near the epithelial surface [Schwartz 2013]. Low-risk HPV strains, such as HPV9 and HPV11, use similar mechanisms for deregulation of the cell cycle to a much lesser extent and without the capability to induce cell proliferation in basal layers [Schiffman et al. 2016]. Nevertheless, even benign diseases induced by these viruses could cause serious health problems and consequences. An example is recurrent laryngeal papillomatosis, which could lead to total laryngectomy as a definitive treatment in the most severe cases.

The HPV genome contains approximately eight kilobase pairs encoding six early-phase genes (E1, E2, E4, E5, E6, E7) and two late-phase genes (L1, L2). E1, E2, L1 and L2 can also be called “core genes” as they have an essential role in DNA replication (E1, E2), capsid formation (L1), and virion assembly (L2) by binding the capsid to viral DNA [Schiffman et al. 2016]. The accessory proteins E4–E7 modify the cell cycle of infected cells and facilitate viral amplification [Doorbar et al. 2012]. The key elements in sustained viral replication and in acquisition of malignant potential are the oncogenes E6 and E7. The E6 protein can bind directly to p53 and prevent its activity, or it can mobilize E3 ubiquitin ligase E6-associated protein that forms a complex with p53 and causes its degradation [Thomas et al. 1999]. The E7

protein binds to retinoblastoma (RB) tumor-suppressor protein, which is an important regulator of the E2F family of transcription factors [Boyer et al. 1996]. RB binds to E2F and thereby controls transition from G1 to S phase. When RB is phosphorylated by cyclin-dependent kinase 4 and 6 (CDK4/6) at the end of G1 phase, RB releases from E2F and induces transcription of genes necessary for S phase. The binding of E7 to RB disrupts RB–E2F complexes and leads to continuous activation and premature entrance to S phase, which results in uncontrolled replication [Doorbar et al. 2012]. E7 also supports CDK2 activity by blocking p21 and p27 and neutralizes their inhibitory effects on CDK2, which is also important for transition from G1 to S phase [Estevao et al. 2019]. Via a negative feedback mechanism, CDK inhibitor 2A (CDKN2A), which encodes the p16<sup>INK4A</sup> protein, is upregulated, and as a result we can observe p16 overexpression, one of the essential, but not specific, markers of HPV infection via immunohistochemical staining. Under physiological conditions, p16<sup>INK4A</sup> binds to CDK4 and 6, inhibiting CDK4/6-mediated phosphorylation of RB family members and maintaining its hypophosphorylated state [Doorbar et al. 2012]. Consequently, the progression of the cell to S phase is blocked.

The mechanisms responsible for malignant transformation of HPV-infected cells are more complex. In addition to the aforementioned main processes, another important step in cell immortalization is telomerase activation, which is mainly caused by E6 interactions; however, E7 alone can lead to telomere maintenance [Panczyszyn et al. 2018]. Furthermore, E6 and E7 cooperate to interfere with apoptotic pathways induced by inhibitory cytokines, such as TNF $\alpha$ , through binding to TNF receptor 1, TRAIL, or CD95 [Jiang et al. 2014].

### 1.2.3 Genetic changes associated with HPV-induced tumors

The persistent E6 and E7 expression and their actions lead to accumulation of somatic mutations. HPV-induced head and neck cancer have one of the highest mutational loads from all the solid tumors [Alexandrov et al. 2013]. This is an important attribute as the mutational landscape clearly corresponds with the immunogenicity of the tumor. The overall mutational burden is similar between HPV<sup>+</sup> and HPV<sup>-</sup> HNSCC, but the spectrum of mutated genes differs significantly between the groups and emphasizes distinct biological and clinical behavior of these tumors [Seiwert et al. 2015]. The most common genetic alteration in HPV<sup>+</sup> tumors affects PIK3 pathway. Amplification and activating mutations of the *PIK3CA* oncogene are found in

approximately 20% of samples [Seiwert et al. 2015, Leemans et al. 2011]. PIK3 pathway is one of the major regulators of tumorigenesis in HNSCC; it affects cell survival and its alteration is found in a significant number of HPV<sup>-</sup> tumors [Kiessling et al. 2018].

Tobacco smoking, in general, increases mutational burden, independent of HPV status. Biologically important mutation of TP53 is significantly associated with smoking [Seiwert et al. 2015]. *TP53* gene mutations are found in up to 80% of HPV<sup>-</sup> HNSCCs but are rare in HPV-induced tumors [Leemans et al. 2011]. p53 dysfunction in HPV<sup>+</sup> tumors is not caused by its mutation, but rather by its E6-mediated degradation [Steenbergen et al. 2014].

#### 1.2.4 HPV detection

Detection of HPV-induced precancerous lesions is the main goal of cervical cancer screening, and in addition to the vaccination program, it is an essential in reducing the incidence and mortality of this disease. There are two options in the screening of cervical cancer: cytology or HPV-DNA testing. Direct HPV testing was proven to be superior to cytology and showed a higher sensitivity for identification of precancerous lesions and a significantly higher negative predictive value, allowing for longer screening intervals [Ronco et al. 2014]. Unfortunately, in the case of the oropharynx, the prevalence of high-risk HPV is very low and there are no clear premalignant lesions that can be detected. Moreover, it is difficult to select a population at high risk of oropharyngeal cancer development; therefore, the applicability of an analogous screening program is currently not possible. HPV detection in the head and neck is limited to the determination of the etiology of the already-diagnosed primary tumor or metastatic disease.

HPV E6 and E7 mRNA detection by reverse-transcription PCR or *in situ* hybridization is considered to be the most accurate method for identification of HPV as an etiological agent of tumors [Prigge et al. 2017]. However, despite the diagnostic accuracy, these tests are relatively expensive and technically challenging for routine clinical testing. The internationally recommended and widely used assay for assessment of HPV etiology of OPSCC is p16 immunohistochemistry (IHC). p16 is a surrogate marker of the infection rather than a direct indicator of active HPV involvement; however, it shows a high correlation with specific HPV-targeted tests in the case of oropharyngeal cancer, where a cut-off value of positivity in >70% of cancer cells with evident cytoplasmic and nuclear staining is applied [Lewis et al. 2018]. In

contrast, p16 could be overexpressed because of somatic mutations in the aforementioned tumor-suppressor pathways and not due to the viral E7 protein activity [Romagosa et al. 2011]. Therefore, despite the correlation of p16 positivity with patient prognosis, p16 IHC has a higher sensitivity than specificity, and there are subgroups of patients with p16<sup>+</sup>/HPV-DNA<sup>-</sup> disease and vice versa [Albers et al. 2017]. Some studies report a prognosis for p16<sup>+</sup>/HPV-DNA<sup>-</sup> patients that is worse than true HPV<sup>+</sup> patients, but better than double-negative or p16<sup>-</sup>/HPV-DNA<sup>+</sup> patients [Albers et al. 2017]. In contrast, post hoc analyses from the DeEscalate study showed no difference in survival between p16<sup>+</sup>/HPV-DNA ISH<sup>+</sup> and p16<sup>+</sup>/HPV-DNA ISH<sup>-</sup> patients [Mehanna et al. 2019]. A combined approach for HPV testing that includes p16 IHC and HPV-DNA PCR has shown a sensitivity and specificity above 90% [Prigge et al. 2017]; current TNM and NCCN guidelines recommend p16 IHC as the only necessary marker for estimation of HPV status, and HPV DNA evaluation is only a recommendation [Pfister et al. 2020]. Sequential testing of HPV DNA in p16-positive samples could represent an option in the future. Immunohistochemical analysis of p16 expression in squamous cell carcinomas from other head and neck sublocations is not generally recommended in a clinical setting as there is no defined cut-off for positivity and no clinical impact for the patient.

## **1.2 Immune microenvironment of head and neck cancer**

The employment of the immune system in cancer therapy has become a focus since the approval of anti-PD-1 and anti-CTLA-4 monoclonal antibodies, so-called checkpoint inhibitors, in 2014. However, the importance of the immune system in cancer development was theorized much earlier. Originally, the theory of immunosurveillance was proposed by Paul Ehrlich in the first half of 20<sup>th</sup> century and further defined by Sir MacFarlane Burnet and Lewis Thomas [Burnet 1957]. In the early 21<sup>st</sup> century, Schreiber and colleagues improved on the idea of immunosurveillance emphasizing the dual role of the immune system in cancer development [Dunn et al. 2002]. There had already been sufficient evidence to determine that the immune system could support progression of tumors, and the authors introduced a new term: “cancer immunoediting”. They divided the process of cancer immunoediting into three phases: the first phase was “elimination”, during which the effector cells of the immune system destroyed developing tumor cells; the second phase was an “equilibrium” that could last for years; and the final phase, “escape”, when selected tumor clones overcame immune mechanisms and clinically apparent tumor developed. In 2011, Weinberg and colleagues published an updated

version of their highly-rated *Hallmarks of Cancer* article [Hanahan et al. 2011]. The ability of cancer to evade the immune response was determined as an emerging factor in cancer growth. One decade later, it is clear that immune response is one of the essential factors affecting all the aspects of the cancer cycle, from its development to its response to therapy, both in a positive and a negative way. The following paragraphs discuss the most important aspects of antitumor immune response in head and neck cancer, with emphasis on local immunity and tumor-infiltrating immune cell populations that are further analyzed in the experimental part of this thesis.

### 1.3.1. General principles of antitumor immunity

The human immune system consists of a complex network of cells, cytokines, and their interactions. The elements of both innate and adaptive immunity participate and communicate with each other. Today, immuno-oncology research is predominantly focused on the study of local immune response and analysis of the processes in the TME. The local immune response shows a more specific reflection of the immunity setting in case of a malignant tumor compared with peripheral blood, which could be affected by many additional factors. Nevertheless, the tumor-infiltrating immune cells need to be replenished from peripheral blood and central lymphoid organs; therefore, for an effective immune response with intact communication and coordination between the local microenvironment and periphery is essential.

Concerning the systemic immune response, there are many reports showing disrupted hematopoiesis in different cancer types. Expansion of immature neutrophils and monocytic cells that may migrate to the tumor site and provide an immunosuppressive effect is characteristic of cancer [Hiam-Galvez et al. 2021]. These cells were identified as myeloid-derived suppressor cells (MDSCs) and their frequency in peripheral blood is higher in HNSCC patients than in healthy controls [Almand et al. 2001, Lang et al. 2018]. In contrast, myeloid dendritic cells (mDCs), the most important antigen-presenting cells (APCs), are decreased in the peripheral blood of the HNSCC patients [Hoffmann et al. 2002]. Peripheral blood-derived regulatory T cells (Tregs) are also a well-studied population in HNSCC. As shown in a systematic review by O'Higgins et al., most of the studies reported elevated levels of Tregs in the blood; however, there are contradictory results concerning their effect on patient survival

and correlation with intratumoral Treg infiltration [O'Higgins et al. 2018]. Interestingly, in different solid tumor types, it was shown that the T cell receptor (TCR) repertoire of circulating Tregs corresponded with the TCRs of tumor-infiltrating Tregs, suggesting that a significant portion of intratumoral Tregs was derived from thymic Tregs and not via peripheral induction by naive CD4<sup>+</sup> T cells [Ahmadzadeh et al. 2019]. The study of the systemic immune response is attractive due to the ease of sample collection. Unfortunately, despite the aforementioned findings, a specific biomarker suitable for HNSCC patient stratification has not yet been identified in the peripheral blood. In contrast, there are widely accepted positive prognostic markers, such as a high level of tumor-infiltrating CD8<sup>+</sup> T cells, based on the evaluation of tumor tissue samples across different tumor types [Kawai et al. 2008, Al-Saleh et al. 2017, Sato et al. 2005]. Nevertheless, these markers are neither validated nor routinely used in clinical practice. The most promising is the use of immune response-based staging of the tumor in colorectal carcinoma (CRC) patients. Jerome Galon and colleagues showed that an abundance of tumor-infiltrating CD8<sup>+</sup> and CD3<sup>+</sup> cells (Immunoscore) was a better prognosticator for CRC than international TNM classification [Galon et al. 2020]. However, basic and translational research in the field surpasses simple quantification of tumor-infiltrating lymphocytes (TILs). Functional capacity and proportional representation of immune cell populations might better reflect the immune setting of the TME.

As mentioned previously, both the innate and adaptive immunity play an important role in development of an anti-tumor immune response. Cells of innate immunity can promote direct effector responses against tumor cells and they can induce and amplify the adaptive immune response. A connecting link between innate and adaptive immunity is DCs. Adaptive immunity is generally dependent on antigen presentation by DCs followed by clonal expansion and activation of effector T lymphocytes. Tumor antigens can be divided into tumor-associated antigens (TAAs), which can be expressed on normal cells, and tumor-specific antigens (TSAs), which comprise viral and abnormal cell proteins (neoantigens). Consequently, levels of these neoantigens are associated with the number of somatic mutations in tumor cells (Figure 2) [Alexandrov et al. 2013]. This also corresponds with the finding that, in a wide spectrum of malignancies, tumors with a higher mutational load have more prominent immune infiltration; however, this phenomenon is not universal [Maleki Vareki 2018]. Exceptions have been reported, such as a subgroup of HNSCC with a strong genetic signature associated with smoking [Seiwert et al. 2015]. These tumors have a high mutational and neoantigen load, but

poor immune infiltration and prognosis. In contrast, tumor mutational load was shown to correlate with response to immunotherapy in lung cancer and melanoma [Nathanson et al. 2017]. In addition, chromosomal microsatellite instability was recently approved as a biomarker for ICIs (i.e., anti-PD1) in colorectal carcinoma. HNSCCs are tumors with a high mutational load and, consequently, with a high abundance of TILs. This phenomenon is even more evident in HPV<sup>+</sup> tumors, most of which can be classified as immunologically “hot” tumors (Figure 3) [Partlova et al. 2015].

Despite expression of an antitumor immune response, immune cells are unable to clear fully-developed cancer. Tumor cells use multiple escape mechanisms to impede their eradication. The most prominent are reduction of expression of major histocompatibility complexes (MHCs) and other co-stimulatory molecules, secretion of immunosuppressive cytokines (e.g., TGFβ, IL-10), induction of immunosuppressive immune populations, such as Tregs and MDSCs, and expression or activation of immune checkpoints.

Figure 2

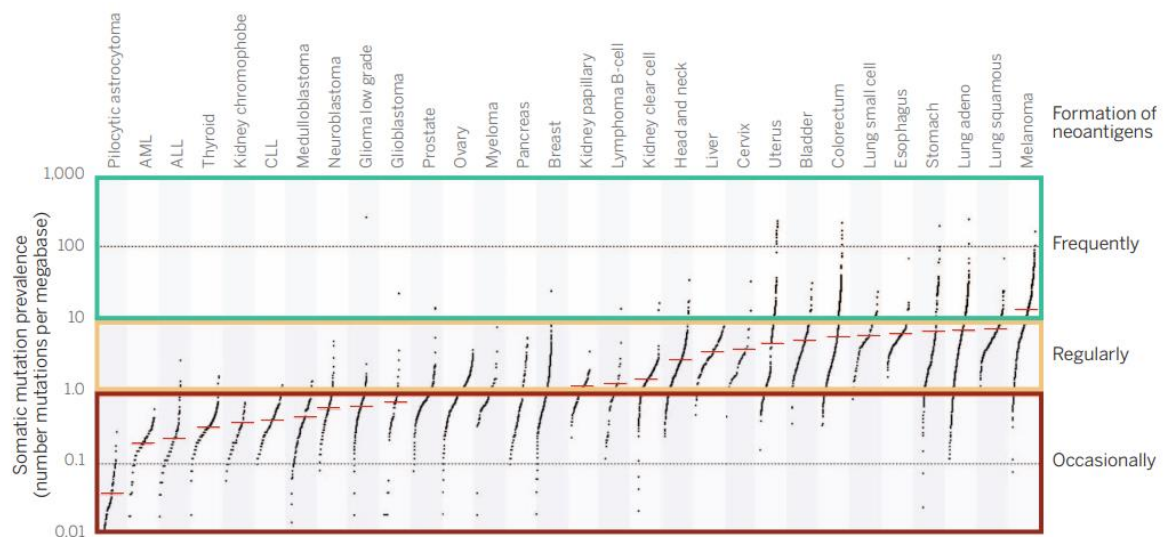
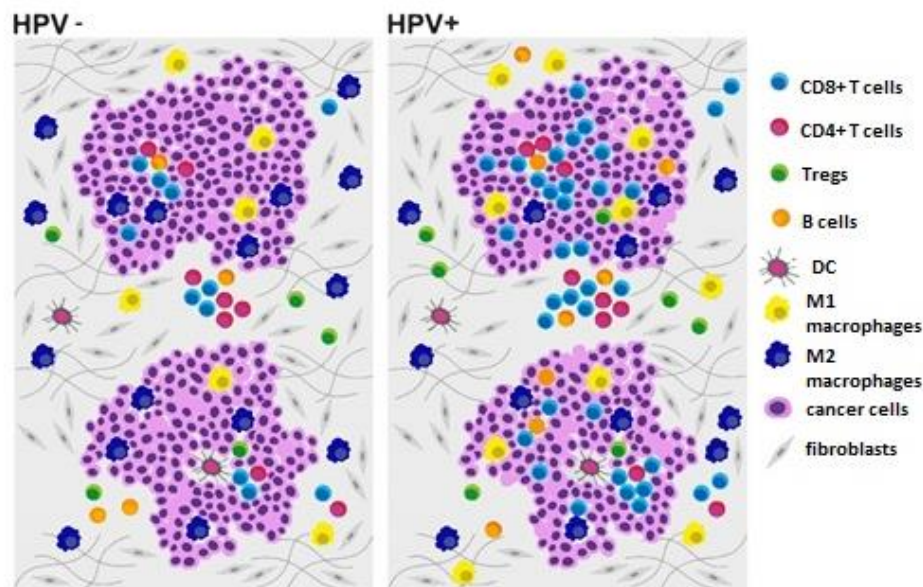


Figure shows association of mutational load of selected tumors with likelihood of neoantigen formation. Adapted from Alexandrov et al. 2013

Figure 3



*Figure illustrates differences in selected TILs populations between HPV<sup>+</sup> and HPV<sup>-</sup> HNSCC based on the current knowledge. Adapted and modified from Fialová et al. 2020*

### 1.3.2 Components of the HNSCC tumor microenvironment and its shaping by HPV

The following paragraphs report essential findings on the role of selected tumor-infiltrating cell populations and their products in HNSCC and provide indispensable theoretical background for the experimental part of the thesis.

#### 1.3.2.1 Cancer-associated fibroblasts and extracellular matrix

In addition to TILs, other non-immune cell groups and their secretory products are engaged in the complicated network of interactions in the TME. Cancer-associated fibroblasts (CAFs) are a highly studied cell subpopulation that is known to affect the migratory activity of cancer cells and progression of the disease. In general, their increased abundance is associated with negative prognosis in HNSCC [Takahashi et al. 2017]. CAFs can develop by epithelial-to-mesenchymal transition of epithelial cells, by differentiation of mesenchymal stem cells that migrate to the tumor from bone marrow, or by transformation of “regular” fibroblasts at the location of the

tumor. CAFs affect the microenvironment by producing cytokines and growth factors, such as IL-10, TGF- $\beta$ , VEGF, BMP4, and IGF-2 [Joshi et al. 2021]. Moreover, they synthesize components of the extracellular matrix, which is not only a space filler in human tissues, but also an important factor that provides intercellular communication and affects cell proliferation and migration. In HNSCC, multiadhesive matrix glycoprotein tenascin C was found to support cell invasion and proliferation in oral cancer [Berndt et al. 2015]. Expression of another glycoprotein, fibronectin 1, is associated with lymph node metastases and worse overall survival in oral cancer patients [Mhaweche et al. 2005]. Important immunomodulatory function was found in galectin 1, a member of a family of endogenous carbohydrate-binding proteins that can support an immunosuppressive environment by inducing apoptosis in activated T cells. Galectins were shown to play an important role in angiogenesis, cell proliferation, and invasion [Plzak et al. 2019]. According to this observation, inhibition of galectin 1 was found to reduce CAF-driven tumor growth and metastasis in oral squamous cell carcinoma [Wu et al. 2011]. Furthermore, galectin 3 was suggested to play a prognostic role in HNSCC; however, the data are contradictory [Honjo et al. 2000, Tokmak et al. 2021].

#### 1.3.2.2 Cytokine and chemokine milieu

Cytokines are soluble proteins with pleiotropic functions that play a major role in intercellular interactions. Chemokines are cytokines that are characteristic for their chemotactic properties. In the TME, they are produced by immune, mesenchymal, and cancer cells and affect vital processes, such as proliferation, migration, apoptosis, differentiation, and angiogenesis. In relation to the modulation and induction of immune responses, these factors can be divided into proinflammatory, Th1-type cytokines, and immunosuppressive, Th2-type cytokines. In many tumors, including HNSCC, a shift towards a Th2 response was observed and was associated with elevated levels of IL-4 and IL-10 and decreased levels of IL-2 and IFN $\gamma$  [Sparano et al. 2004]. IL-6 and IL-10 are regarded as important pro-tumorigenic factors, and their plasma levels are elevated in HNSCC patients compared with controls [Lathers et al. 2003]. IL-6 serum levels were associated with later stages of the disease and negatively correlated with patient prognosis [Duffy et al. 2008]. Similarly, detectable serum levels of IL-10 were associated with later stages of laryngeal and hypopharyngeal cancer [Jebreel et al. 2007]. Concerning the effect of HPV, studies with cell culture supernatants showed inconsistent differences in IL-6 and IL-10 production between HPV<sup>+</sup> and HPV<sup>-</sup> HNSCC. However, Partlova et al. reported increased

production of T-cell stimulatory and chemoattractant cytokines, such as IL-2, IL-17, IFN $\gamma$ , CXCL9, CCL17, and CCL21, indicating a proinflammatory, immunologically hot TME in HPV<sup>+</sup> HNSCC compared with HPV<sup>-</sup> tumors [Partlova et al. 2015].

### 1.3.2.3 T lymphocytes

Current immuno-oncologic research and immunotherapeutic approaches (e.g., checkpoint inhibitors, adoptive cellular transfer, CAR T cells) are mainly focused on the most important effector cells of adaptive immunity: T lymphocytes. CD8<sup>+</sup> cytotoxic T cells are an especially valuable target because of their cell-killing capacity that involves mechanisms such as secretion of perforin and granzyme, induction of apoptosis by Fas ligand expression, and secretion of cytokines TNF $\alpha$  and IFN $\gamma$  that can have direct cytotoxic effects. In head and neck cancer (and many other malignancies), increased abundance of CD8<sup>+</sup> T cells in the TME has often been reported as a positive prognostic marker [Balermipas et al. 2016, Nasman et al. 2012, Solomon et al. 2018]. As mentioned previously, HPV<sup>+</sup> HNSCCs generally have higher levels of tumor-infiltrating immune cells, including T lymphocytes [Chen et al. 2018, Gameiro et al. 2018]. However, Ward et al. identified an HPV<sup>+</sup> HNSCC patient subgroup with sparse T-cell infiltration that had the same survival characteristics as HPV<sup>-</sup> patients [Ward et al. 2014]. Proper antigen recognition and costimulatory signals are necessary for T-cell activity. Therefore, the constitutive expression of HPV antigens, which are recognized by the immune system as foreign, could explain the higher immunogenicity of HPV-associated OPSCCs. T cells specific for HPV antigens E6 and E7 have previously been detected in OPSCC tissues and represent a promising therapeutic target [Welters et al. 2018, Heusinkveld et al. 2012]. Furthermore, current clinical trials with checkpoint inhibitors in metastatic and recurrent HNSCC have reported improved response to therapy in patients with significant CD8<sup>+</sup> T-cell infiltration [Hanna et al. 2018]. In contrast, some studies have found no significant effect of CD8<sup>+</sup> T-cell abundance on overall or disease-specific survival [Wolf et al. 2015]. This discrepancy could be partially explained by different counts of CD8<sup>+</sup> T cells relative to other important T-cell subtypes in the tumor tissue, and CD8<sup>+</sup>/CD4<sup>+</sup> and CD8<sup>+</sup>/Treg ratios might better describe the overall TME setting.

The data describing the role of tumor-infiltrating CD4<sup>+</sup> T cells are less clear. CD4<sup>+</sup> T cells are a heterogeneous group that comprises of T-helper cells (Th1, Th2, Th17), T-follicular helper cells

(Tfh), and Tregs. Gameiro and Cillo showed higher abundance of Tregs and Tfh cells in HPV<sup>+</sup> tumors *in silico* and suggested a positive prognostic role of Tfh cells [Gameiro et al. 2018, Cillo et al. 2020]. However, HPV<sup>+</sup> HNSCCs are mainly OPSCCs in most of the studies, while HPV<sup>-</sup> HNSCCs are a mix of different head and neck subregions. This might also partly explain the opposing results concerning the survival benefit of patients with high levels of tumor-infiltrating CD4<sup>+</sup> T cells [Wondergem et al. 2020].

One subtype of CD4<sup>+</sup> T cells has been highly studied and discussed in cancer immunology, namely Tregs. These cells mediate self-tolerance, silencing of over-reactive immune responses, and prevention of autoimmunity. Tregs can develop either in the thymus during T-cell maturation and selection and can subsequently be attracted to the tumor site or they can be induced in peripheral tissues. The cytokines IL-10 and TGFβ play an important role in the development of Tregs [Togashi et al. 2019]. Another important mechanism of Treg induction in the TME is expression of indoleamine-2,3-dioxygenase (IDO) by DCs that promote differentiation of naïve CD4<sup>+</sup> T cells into Tregs [Munn et al. 2007]. One of the essential markers currently used for the identification of Tregs is expression of FoxP3, which is necessary for Treg development [Hori et al. 2003]. Based on the immunosuppressive function of Tregs, we can assume their protumoral effect in HNSCC; however, there are confronting results showing both the positive and negative prognostic value of Tregs [Sun et al. 2012, Bron et al. 2013, Seminerio et al. 2019, Liang et al. 2011]. One of the explanations is that higher Treg counts could reflect higher T-cell infiltration in general, as shown in some studies, and that the ratio of FoxP3<sup>+</sup> Tregs to other effector immune cells, especially CD8<sup>+</sup> T cells, signifies the true setting of the TME [Partlova et al. 2015, Chen et al. 2018]. Moreover, Feng et al. reported, in their immunohistochemical study using samples from oral cancer patients, that colocalization of Tregs and CD8<sup>+</sup> T cells was an important factor negatively affecting patient survival [Feng et al. 2017].

#### 1.3.2.4 Immune-checkpoint molecules

Immune-checkpoint molecules belong to the most important group of factors that regulate the immune response. Their constant activation in the TME leads to diminished antitumor activity of the immune machinery and subsequently to cancer progression. Exhaustion of T cells following continuous antigen stimulation was first reported in chronic viral infections, and the

same phenomenon was later described in tumors [Zajac et al. 1998]. Exhausted T cells show a decreased ability to produce inflammatory cytokines (IFN $\gamma$ , TNF $\alpha$ , IL-2) and lower proliferative and cytotoxic properties [Wherry 2011]. The main identification marker of exhausted T cells is increased expression of immune-checkpoint molecules that transfer inhibitory signals [Wang et al. 2005]. The first-described and the most studied immune checkpoints are cytotoxic T-lymphocyte-associated antigen 4 (CTLA-4) and programmed cell-death protein 1 (PD-1). Inhibition of these molecules has become the fourth pillar of cancer therapy, as discussed in Chapter 1.4.

CTLA-4 has a similar structure to CD28, an essential receptor for co-stimulatory molecules CD80 and CD86 expressed on professional APCs. CTLA-4 competes with CD28 and therefore reduces activating signals for T cells. Increased expression of CTLA-4 is characteristic for Tregs and serves as one of the tools of their immunosuppressive functions [Togashi et al. 2019]. In HNSCC samples, CTLA-4 is increased compared with control tissue; however, only inconclusive results were found concerning correlation with clinical or pathological characteristics of patients [Veigas et al. 2021].

In contrast to CTLA-4, which emerges early in the process of antigen stimulation, PD-1 is expressed on T cells following their activation and mediates its inhibitory effect in the periphery when its ligands are encountered. Two PD-1 ligands were identified, PD-L1 and PD-L2, that are expressed on many cell types, including tumor cells. In HNSCC, higher PD-1 and PD-L1 expression was found in more aggressive tumors [Karpathiou et al. 2017]; however, reports concerning correlation with patient prognosis are contradictory [Yang et al. 2018]. Interestingly, the abundance of tumor-infiltrating CD4<sup>+</sup> T lymphocytes expressing PD-1 was reported to be a positive prognostic factor in HPV<sup>+</sup> HNSCC, suggesting that PD-1 is not necessarily a marker of exhaustion but might also reflect T-cell activation [Badoual et al. 2013].

Following CTLA-4 and PD-1, other immune checkpoints with therapeutic potential were discovered. Among the newly emerging checkpoints, T-cell immunoglobulin and mucin-domain containing 3 (TIM-3), lymphocyte-activation gene 3 (LAG 3), and T-cell immunoreceptor with Ig and ITIM domains (TIGIT) are the most studied. TIM-3 was reported as an important factor mediating and signifying immunosuppression in the TME of HNSCC [Oweida et al. 2018, Shayan et al. 2017]. It is a transmembrane receptor expressed on many immune cells, including T cells, B cells, and DCs. There are four known ligands for TIM-3: galectin 9, high-mobility group protein B1 (HMGB1), carcinoembryonic antigen cell-adhesion molecule 1 (ceacam-1), and phosphatidyl serine [Du et al. 2017]. Galectin 9 is considered the

major TIM-3 ligand in the TME that induces T-lymphocyte exhaustion or apoptosis based on the receptor with which it interacts [Yang et al. 2021]. Furthermore, recent data have shown that higher TIM-3 expression correlates with worse survival in HNSCC patients [Yang et al. 2021].

#### 1.3.2.5 B lymphocytes

Until recently, the role of B lymphocytes in cancer has been underestimated. However, in recent years, the significant prognostic role of tumor-infiltrating B cells (TIL-Bs) was reported in a wide range of solid tumors. Importantly, B cells have been shown to be a predictor of response to checkpoint inhibitors [Griss et al. 2019]. Despite these optimistic reports, both the pro- and anti-tumoral effects of B cells were shown in different studies. Two potential mechanisms by which B cells support antitumor immunity are discussed. First, B cells express MHC class II molecules and co-stimulatory molecules, such as CD70, CD80, and CD86; therefore, they can serve as APCs stimulating CD8<sup>+</sup> and CD4<sup>+</sup> T-cell responses [Tsou et al. 2016]. Second, after T cell-dependent or independent activation, B cells differentiate into plasmablasts and long-lived plasma cells that are able to produce antibodies. Antibodies directed against tumor-associated antigens can activate NK cells that can kill cancer cells via antibody-dependent cell-mediated cytotoxicity (ADCC) [Fridman et al. 2021]. In addition, Fc portions of antibodies activate Fc receptors expressed by macrophages, DCs, and neutrophils. The effect of B cells in the TME of a patient depends on the phenotype and functionality of different B-cell subpopulations; however, these aspects have yet to be fully elucidated. Nevertheless, a recently described immunosuppressive subpopulation of B regulatory cells (Bregs), were characterized by production of IL-10 and were shown to be associated with poor prognosis in patients with hepatocellular and gastric cancers [Murakami et al. 2019, Shao et al. 2014].

In HNSCC, increased B-cell infiltration was reported in HPV-induced tumors based on both immunohistochemical and flow cytometry studies [Lechner et al. 2019, Russell et al. 2013]. Furthermore, the activated and antigen-experienced memory phenotype was shown to be enriched in the TME. There are few studies reporting the prognostic importance of TIL-Bs. Distel et al. that reported that the survival of a low-risk group of HNSCC patients showed a positive correlation with CD20<sup>+</sup> infiltration; in contrast, high-risk patients with low CD20<sup>+</sup> counts had significantly better survival [Distel et al. 2009]. Furthermore, Zhou et al. reported a

negative correlation between the level of IL10<sup>+</sup> Breg infiltration and survival of patients with tongue cancer [Zhou et al. 2016].

#### 1.3.2.6 Dendritic cells

DCs are the most efficient APCs, and they represent a link between innate and adaptive immunity. DCs can be found in almost all human tissues, and despite their low numbers, they are a crucial element in the initiation of the adaptive immune response. Upon stimulation by danger-associated molecular patterns (DAMPs) or microbe-associated molecular patterns (MAMPs), DCs mature and express high levels of MHC class II and co-stimulatory molecules that are necessary for activation of naive CD4<sup>+</sup> T cells. Based on their expression profiles and functional characteristics, DCs can be divided into various sub-populations. The functionally distinct populations are classical or mDCs and plasmacytoid DCs (pDCs).

mDCs are a heterogeneous subpopulation that comprises cells primarily responsible for antigen presentation. mDCs can be further separated into the mDC1 subset, which expresses CD141 and has the ability to cross-present antigens to CD8<sup>+</sup> T cells, and the mDC2 subset, which expresses CD1c [Wculek et al. 2020]. In the TME, mDC recruitment and differentiation is abolished by reduced expression of the main DC chemokine, CCL4, and by reduction of FLT3L, an important factor in mDC development [Wculek et al. 2020]. Furthermore, mDC signaling pathways and antigen processing can be impeded by tumor cell actions, such as the production of immunosuppressive cytokines and accumulation of truncated fatty acids and half-degraded lipids. The role of mDCs in HNSCC has not yet been fully elucidated. A positive prognostic role of mDCs was shown in oral, tongue, and laryngeal cancers; however, several studies failed to confirm these findings [Karpathiou et al. 2017, Reichert et al. 2001, Goldman et al. 1998, O'Donnell et al. 2007]. Increased mDC infiltration was reported in HPV<sup>+</sup> HNSCC; however, it did not show a correlation with clinical parameters and patient outcome [Partlova et al. 2015].

The main function of pDCs is the production of IFN $\alpha$  upon TLR7/9 stimulation, although they also possess antigen-presenting properties [Koucky et al. 2019]. pDCs are essential players in antiviral immunity; however, their important role in cancer immunology, both pro- and anti-tumorigenic, has also been reported [Koucky et al. 2019]. A decreased capacity of pDCs to produce IFN $\alpha$  was observed in many tumors, including ovarian and breast cancer, where the

levels of pDCs correlated with worse prognosis [Sisirak et al. 2012, Labidi-Galy et al. 2011]. An important pro-tumorigenic effect of pDCs is their capability of inducing Tregs *in situ* through the ICOS/ICOS-L pathway and inducing IDO expression under the influence of the TME [Chen et al. 2008]. In contrast, *in vitro* and mouse model experiments showed that TLR7/9-stimulated pDCs were able to directly lyse tumor cell lines in a mechanism dependent on TRAIL and granzyme B expression [Wu et al. 2017]. Furthermore, the main secretory product of pDCs, IFN $\alpha$ , is known to have both direct and indirect tumoricidal effects. As in other malignancies, pDCs were reported to have a diminished capacity to produce IFN $\alpha$  in HNSCC [Hartmann et al. 2003]. Moreover, Han et al. observed a correlation between a high density of tumor-infiltrating pDCs with poor prognosis in patients with oral cancer [Han et al. 2017]. However, the functional capacity of pDCs in HPV-associated HNSCC has not yet been evaluated.

#### 1.3.2.7 Other leukocyte subgroups

In addition to the aforementioned cell populations, other leukocytes, such as macrophages, NK cells, and neutrophils, have been studied in the context of their prognostic significance in HNSCC. Macrophages are important effector cells of innate immunity, producing a wide range of cytokines. They have antigen-presenting capabilities and are necessary for the promotion of a T cell-dependent immune response. Under the influence of IFN $\gamma$ , they can polarize into a proinflammatory M1 subset and produce high levels of IL-1, IL-12, and TNF $\alpha$ , supporting a Th1 immune response. In contrast, the exposure of macrophages to IL-4 leads to polarization into an M2 subset, producing immunosuppressive cytokines, such as TGF $\beta$  and IL10 that are known to support tumor progression [Martinez et al. 2014]. Activated macrophages may also contribute to immunosuppression via upregulation of PD-L1 and IDO, production of TGF $\beta$ , and support tumor promotion via induction of angiogenesis [Zhou et al. 2020]. Both in HPV<sup>+</sup> and HPV<sup>-</sup> HNSCC, higher M1/M2 ratios were associated with better prognosis [Chen et al. 2018]. Moreover, increased infiltration of an M2 subset of macrophages was repeatedly reported in HPV<sup>-</sup> HNSCC compared with HPV<sup>+</sup> tumors [Gameiro et al. 2018, Saloura et al. 2019].

NK cells are leukocytes with strong direct cytotoxic activity that play an important role in antiviral and antitumoral immunity, mainly through sensing abnormalities in MHC I expression

on infected or mutated cells. Their effect is mediated through secretion of granzyme, perforin, and IFN $\gamma$ , nevertheless, a suppressive subpopulation characterized by low CD16 and high CD56 expression has also been described [Cooper et al. 2001]. Although tumor-infiltrating NK cells comprise only a small fraction (<1%) of leukocytes in the TME, their positive prognostic value has been reported in HNSCC regardless of HPV status [Wagner et al. 2016, Mandal et al. 2016].

There are few studies focused on tumor-infiltrating neutrophils in HNSCC despite neutrophils being the most numerous leukocyte population in humans. In studies published by Chen et al. and Dumitru et al., higher neutrophils counts were associated with worse prognosis in oropharyngeal and hypopharyngeal cancers [Chen et al. 2018, Dumitru et al. 2013]. An overview of the prognostic role of various TILs is summarized in Table 1.

Table 1. *Prognostic role of selected TILs in HNSCC. Adapted and modified from Fialová et al 2020.*

<b>Marker</b>	<b>Prognostic role in HPV- HNSCC</b>	<b>Prognostic role HPV+ HNSCC</b>
<b>CD8<sup>+</sup> T lymphocytes</b>	Positive	Positive
<b>CD4<sup>+</sup> T lymphocytes</b>	None	None
<b>Tregs</b>	Contradictory	Contradictory
<b>B lymphocytes</b>	NA	Positive
<b>IL-10<sup>+</sup> B regulatory lymphocytes</b>	<i>Negative</i>	<i>NA</i>
<b>mDCs</b>	Positive	None
<b>pDCs</b>	<i>Negative</i>	NA
<b>Neutrophils</b>	None	<i>Negative</i>
<b>MDSC</b>	NA	NA
<b>High M1/M2 ratio</b>	Positive	Positive
<b>NK cells</b>	Positive	NA

#### 1.4 Head and neck cancer immunotherapy

For several reasons HNSCC is an attractive target for immunotherapy. As discussed above, many reports show the prevalent immunosuppressive setting of the HNSCC TME that supports tumor growth. Furthermore, a high mutational burden in HNSCC predicts the existence of a wide spectrum of neoantigens. Finally, a significant portion of HNSCCs are associated with

oncoviruses (HPV in the case of oropharyngeal cancer and Epstein-Barr virus in the case of nasopharyngeal cancer) that can provide additional antigen-specific stimulation. Despite references to HNSCC as one entity in most of the clinical trials, it is a heterogeneous group of diseases. Different molecular backgrounds and TME compositions among HNSCC subgroups adds to the variability of treatment responses. In view of this fact, finding generally applicable biomarkers predicting treatment response is as equally important as the development of the therapy itself.

Basic immunotherapeutic approaches in cancer therapy can be categorized as follows: monoclonal antibodies, cancer vaccines, adoptive cell therapy, oncolytic virotherapy, and recombinant cytokines.

ICIs are the only approved immunotherapy for HNSCC. ICIs are monoclonal antibody-based treatment targeting immune checkpoint molecule PD-1, which was discussed in previous chapters. Although inhibitors of PD-1 and other checkpoint molecules revolutionized treatment and prognosis in melanoma and lung cancer, response rates in HNSCC are low and its application is reserved for recurrent and/or metastatic HNSCC (R/M HNSCC). The anti-PD-1 antibody nivolumab was approved in 2016 based on the results of the CheckMate 141 clinical trial. The response rate was 13.3% in the nivolumab group versus 5.8% in the standard-therapy group, and median overall survival was 7.5 months versus 5.1 months, respectively [Ferris et al. 2016]. There was no significant relationship between patient survival and the level of PD-L1 or p16 expression. Pembrolizumab, the second anti-PD-1 antibody treatment for HNSCC, was approved in 2017 based on the non-randomized Keynote 012 study. The efficacy of pembrolizumab against standard treatment was confirmed in Keynote 040. The study reported a median overall survival 8.4 months with pembrolizumab and 6.9 months with standard chemotherapy [Cohen et al. 2019]. In this case, the treatment effect was greater in patients with a PD-L1 combined positive score (CPS, number of PD-L1<sup>+</sup> tumor cells and lymphocytes relative to all viable tumor cells)  $\geq 1\%$ , especially in the group with CPS  $\geq 50\%$ . Although PD-L1 expression on both tumor cells and TILs is used as a biomarker for anti-PD-1 treatment and most of the studies show higher efficacy in PD-L1-expressing patients, it is not a sufficient predictor of treatment response in HNSCC. PD-L1 expression is detected in a significant portion of HNSCCs, and treatment response can be observed in approximately 20% of patients, including patients considered non-expressors [Evrard et al. 2020]. Interestingly, PFS and OS rates of non-expressors is comparable to PD-L1-expressing patients [Evrard et al. 2020]. Furthermore, a recent metanalysis by Yang et al. showed no survival benefit of PD-L1

expression in HNSCC [Yang et al. 2018]. The technical parameters (i.e., antibody, method of evaluation) of PD-L1 detection and the established cut-off values among the studies differed. Moreover, conflicting results can even be found for PD-1 expression in TILs. Despite being considered a marker of exhaustion, Badoual et al. reported positive correlation between PD-1 expression and survival in HNSCC, suggesting that PD-1 might also represent cell activation [Badoual et al. 2013]. There are ongoing clinical trials testing the efficacy of other ICIs in HNSCC, such as anti-CTLA4, PD-L1, and their combinations with each other or with radiotherapy and chemotherapy. Combined therapy might represent a way to overcome the process of adaptive resistance to ICI. Adaptive resistance is a dynamic process of upregulation of other suppressor pathways following PD-1/PD-L1 blockade. An overexpression of TIM-3 especially was reported *in vitro* in HNSCC patients who progressed following an initially favorable response to anti-PD1 treatment [Shayan et al. 2017]. However, available data on the ICI combination tremelimumab (anti-CTLA4) plus durvalumab (anti-PD-L1) did not show a clinical benefit over treatment with a single agent [Ferris et al. 2020, Siu et al. 2019].

Cancer vaccines might be another promising strategy, both in HPV<sup>-</sup> and HPV<sup>+</sup> HNSCC, especially in combination with other immune-based agents that can help to overlap immunosuppressive mechanisms (checkpoint molecules, immunosuppressive cell populations, and chemokines) that may impede vaccine effectiveness. In HPV<sup>-</sup> tumors, there is a necessity to find appropriate TAAs and TSAs. Mucin I and human telomerase reverse transcriptase are vaccine targets currently being tested in clinical trials [Cheng et al. 2021]. In HPV<sup>+</sup> HNSCC, it is possible to design vaccines based on the well-defined HPV antigens E6 and E7. These oncoproteins are associated with malignant transformation of epithelial cells in the oropharynx and were shown to be able to elicit a specific T-cell response [Heusinkveld et al. 2012]. Clinical trial NCT02426892 combining the HPV vaccine with nivolumab showed a better response rate (33%) than ICI alone in a group of 24 patients with incurable HPV-induced cancer [Massarelli et al. 2019]. The NCT03162224 clinical trial included 35 R/M HNSCC patients and tested a combination of the HPV vaccine and anti-PD-L1 antibody durvalumab. The reported response rate was 22.2%, with an acceptable degree of side effects. Other studies are currently testing different types of HPV vaccines in combination with immunomodulatory agents, such as anti-CD40 or anti-CD137 costimulatory antibodies. Nevertheless, there are currently no therapeutical vaccines approved for use in clinical practice. The same statement applies to other immunotherapeutic approaches, such as adoptive cell therapy or recombinant cytokine therapy, that are in phases I clinical trials testing their safety and preliminary efficacy.

In conclusion, the future direction of immunotherapy in HNSCC is a combination of different immunotherapeutic techniques that may influence more of the mechanisms that tumors use to evade the immune response.

## **2. Aims of the study and hypotheses**

Immune system response is one of the major factors influencing HNSCC patient prognosis. Indeed, new immune-targeted drugs already showed their high efficacy in cancer treatment, exceeding classic treatment modalities in some tumor types. Our research focuses on profound analysis of immune infiltration in HNSCC in relation to HPV carcinogenetic influence. In our studies we analyzed three tumor-infiltrating leukocyte subgroups: T lymphocytes, B lymphocytes and pDCs. The aim of the studies was to describe phenotype and functional characteristics of these immune cells and find their possible prognostic and therapeutic value in HNSCC patients. Aims and hypotheses of each of the project are stated below.

### **2.1 Study of HPV-specific tumor-infiltrating T cells in oropharyngeal cancer (Study 1)**

The aim of the study was to describe proportions, phenotype and functional capacity of tumor-infiltrating T cells in OPSCC specific to HPV16 antigens and evaluate effect of blocking PD-1 and TIM-3 immune checkpoint pathways on T-cell characteristics.

Hypothesis:

- Expression of immune checkpoint molecules and a process of adaptive resistance negatively affects anti-tumor immune response mediated by HPV-specific tumor-infiltrating lymphocytes with exhausted phenotype.

### **2.2 Study of tumor-infiltrating B cells in oropharyngeal cancer (Study 2)**

The aim of the study was analysis of frequency, phenotype and tissue distribution of tumor-infiltrating B lymphocytes in OPSCC and evaluate their prognostic significance.

Hypotheses:

- Tumor-infiltrating B lymphocytes have a prognostic role in OPSCC patients.
- Tumor-infiltrating B lymphocytes support antigen-specific CD8<sup>+</sup> T cell-mediated anti-tumor immune response in HPV<sup>+</sup> OPSCC.

### **2.3 Study of tumor-infiltrating plasmacytoid dendritic cells in head and neck cancer (Study 3)**

The aim of the study was to analyze frequency, phenotype, tissue distribution, functional characteristics and prognostic role of tumor-infiltrating pDCs in HPV<sup>-</sup> and HPV<sup>+</sup> HNSCC.

Hypotheses:

- pDCs infiltrating HNSCC have negative prognostic impact on overall survival of the patients.
- Tumor microenvironment affects function of tumor-infiltrating pDCs.

### **3. Materials and methods**

#### **3.1 Patient cohorts**

All the patient native tumor tissue, control and blood samples were obtained at the Department of Otorhinolaryngology, Head and Neck Surgery, First Medical Faculty, Motol University Hospital, between 2015 – 2020. Tumor samples were separated from the resected tissue by an experienced pathologist or head and neck surgeon immediately after tumor resection. The specimens were left without fixation solution till the experimental samples were collected. Concerning the surgery technique, patients underwent surgical resection of the primary tumor using external or peroral approach always complemented with therapeutic or prophylactic neck lymph node dissection. None of the cancer patients enrolled in the studies have had received any neoadjuvant treatment. All of the patients signed an informed consent approved by the Ethics Committee of the Motol University Hospital. Pathologic staging of the disease was performed by an experienced pathologist in coordination with a head and neck surgeon. Because of the change in staging system of head and neck cancer in 2018, the older specimens and samples for immunohistochemistry analysis were re-classified according to the present TNM classification standards that have higher prognostic value in HPV-associated oropharyngeal cancer.

Formalin-fixed paraffin embedded (FFPE) samples for immunohistochemistry staining were obtained from the Department of Pathology and Molecular Medicine, Second Medical Faculty, Motol University Hospital and the Fingerland Department of Pathology, Faculty of Medicine in Hradec Králové and University Hospital Hradec Králové.

##### **3.1.1 Study of HPV-specific tumor-infiltrating T cells in oropharyngeal cancer (Study 1)**

Primary oropharyngeal squamous cell carcinoma (OPSCC) specimens and paired blood samples from 51 patients were collected. The clinical and pathological characteristics of the patient cohort are summarized in Table 1. Four cervical cancer tissue specimens were received from the Department of Gynecology and Obstetrics, Third Faculty of Medicine, University Hospital Královské Vinohrady.

### 3.1.2 Study of tumor-infiltrating B cells in oropharyngeal cancer (Study 2)

For the purpose of this study we analyzed 3 patient cohorts. The retrospective cohort 1 consisted of FFPE samples of primary OPSCC specimens that were obtained from 72 patients who underwent radical surgery at the University Hospital Hradec Králové between 2001 and 2014. Cohort 2 consisted of 21 primary fresh OPSCC tissues and matching FFPE tumor sections, that were obtained from patients after therapeutic surgery at the Motol University Hospital between 2015 and 2016. Prospective cohort 3 composed of 21 fresh primary OPSCC specimens and matched blood samples obtained after therapeutic surgery at the Motol University Hospital, between 2018 and 2019. Healthy tonsils specimens used as a control tissue were obtained from 6 healthy donors undergoing surgery for sleep apnea syndrome at the Motol University Hospital. The clinical and pathological characteristics of the patients are summarized in Table 2.

### 3.1.3 Study of tumor-infiltrating plasmacytoid dendritic cells in head and neck cancer (Study 3)

Freshly resected primary head and neck squamous cell carcinoma specimens from 76 patients, who underwent therapeutic surgery at the Motol University Hospital in Prague, were collected between 2016 and 2019. Control peritumoral, macroscopically tumor-free mucosa was obtained from 9 patients. Control tonsillar tissue specimens were obtained from 9 healthy age-matched donors undergoing surgery for a sleep apnea syndrome. The clinical and pathological characteristics of the patients are summarized in Table 3.

Table 1 (modified from Hladíková et. al, 2018)

<b>Variable</b>	<b>No.</b>	<b>%</b>
<b>Total no. of patients</b>	51	
<b>Age</b>		
<b>Mean</b>	59	
<b>Range</b>	36-75	
<b>Sex</b>		
<b>Male</b>	36	70.6
<b>Female</b>	15	29.4
<b>Nodal status</b>		
<b>N0</b>	9	17.6
<b>N1-N3</b>	42	82.4
<b>Stage</b>		
<b>I</b>	1	1.9
<b>II</b>	8	15.7
<b>III</b>	13	25.5
<b>IV</b>	29	56.9
<b>Tumor site</b>		
<b>Palatine tonsil</b>	32	62.7
<b>Base of tongue</b>	10	19.6
<b>Oropharynx NS</b>	9	17.7
<b>HPV status</b>		
<b>HPV<sup>+</sup></b>	41	80.4
<b>HPV<sup>-</sup></b>	10	19.6

Table 2 (modified from Hladíková et. al, 2019)

Variable	Cohort No. 1		Cohort No. 2		Cohort No. 3	
	No.	%	No.	%	No.	%
<b>Total No. of Patients</b>	63		21		21	
<b>Age</b>						
Mean	58.5		60		63	
Range	41 - 76		40 - 73		41 - 75	
<b>Sex</b>						
Male	47	72.3	16	76.2	13	61.9
Female	16	25.7	5	23.8	8	38.1
<b>Tumor site</b>						
Palatine tonsil	53	84.1	18	85.7	14	66.7
Base of tongue	10	15.9	2	9.5	4	19
Oropharynx NS	0	0	1	4.8	3	14.3
<b>T status</b>						
T1	16	25.4	6	28.6	6	28.6
T2	32	50.8	11	52.4	12	57.1
T3	11	17.5	4	19	3	14.3
T4	4	6.3	0	0	0	0
<b>N status</b>						
N0	1	1.6	4	19	1	4.8
N1	51	81	17	81	16	76.2
N2	7	11.1	0	0	4	19.
N3	4	6.3	0	0	0	0
<b>Stage</b>						
I	42	66.7	17	81	15	71.4
II	10	15.9	4	19	6	28.6
III	4	6.3	0	0	0	0
IV	7	11.1	0	0	0	0
<b>HPV status</b>						
HPV <sup>+</sup>	56	86.2	21	100	21	100
HPV <sup>-</sup>	9	13.8	0	0	0	0

Table 3 (modified from Koucký et. al, 2021)

<b>Variable</b>	<b>No.</b>	<b>%</b>
<b>Total No. of Patients</b>	76	
<b>Age</b>		
Mean	61	
Range	38 - 80	
<b>Sex</b>		
Male	63	80.3
Female	15	19.7
<b>Tumor site</b>		
Palatine tonsil	19	25
Base of tongue	12	15.8
Oropharynx NS	6	7.9
Body/margin of tongue	7	9.2
Base of mouth	5	6.6
Hypopharynx	5	6.6
Larynx	22	28.9
<b>T status</b>		
T1	7	9.2
T2	38	50
T3	16	21.1
T4	15	19.7
<b>N status</b>		
N0	26	34.2
N1	28	36.8
N2	22	29
N3	0	0
<b>Stage</b>		
I	22	29
II	12	15.8
III	15	19.7
IV	27	35.5
<b>HPV status</b>		
HPV <sup>+</sup>	32	42.1
HPV <sup>-</sup>	44	57.7

### **3.2 Tumor tissue and blood processing**

Fresh tumor tissue samples were transported in a physiologic solution. In a laminar box the samples were mechanically minced into small pieces using scissors and tweezers. After that the tissue was enzymatically digested in 5ml of RPMI 1640 (Thermo Fisher Scientific) with addition of 1 mg/ml of Collagenase D (Roche) and 0.05 mg/ml of DNase I (Roche). After 30 min of incubation at 37°C with continuous gentle rocking the specimens were passed through a 100- $\mu$ m nylon cell strainer (BD Biosciences) and washed with PBS (Lonza). Subsequently, cell counts were determined using Trypan blue staining and Bürker chamber. The same protocol was used for control tonsillar tissues, healthy oral mucosa and peritumoral mucosa.

Blood samples were collected on the day of the surgery by the nursery staff. EDTA 9ml tubes (Vacuette) were used for the purpose. Blood was diluted 1:1 with PBS EDTA (Sigma) and underwent centrifugation on a Ficoll-Paque density gradient (GE Healthcare). After centrifugation a ring of peripheral blood mononuclear cells (PBMCs) was harvested with 1 ml automatic pipette and washed two times with PBS EDTA and one time in PBS. Cell counts were determined using Trypan blue staining and Bürker chamber.

### **3.3 Flow cytometric analysis**

Single cell suspensions derived from tumor tissues and blood-derived PBMC were incubated and labeled with different panels of fluorescent-marked monoclonal antibodies for 20min in 5°C. Afterwards the cells were washed in PBS and analyzed on a BD LSR Fortessa (BD Biosciences). For final evaluation FlowJo software (TreeStar) was used. When intracellular detection of cytokines and other intracellular markers was needed, after extracellular staining the cells were fixed with Fixation/Permeabilization Buffer Set (eBioscience) for 30min in 5°C, two times washed with Permeabilization buffer (eBioscience) and intracellularly labeled with 50ul solution of primary antibodies diluted in permeabilization buffer. The incubation period was 30 min. All the fluorescent-labeled monoclonal antibodies used in the studies are listed in Table 4.

Table 4

<b>Antigen</b>	<b>Fluorochrome</b>	<b>Clone</b>	<b>Producer</b>
CD3	FITC	OKT3	eBioscience
CD3	AmCyan	SK7	BD Biosciences
CD4	Pe/Dazzle	OKT4	Biologend
CD4	Pe-Cy7	RPA-T4	eBioscience
CD5	PE/Dazzle 594	UCHT2	Biologend
CD8a	PE-DyLight 594	MEM31	Exbio
CD14	FITC	MEM15	Exbio
CD16	FITC	LNK16	Exbio
CD19	FITC	LT19	Exbio
CD20	FITC	LT20	Exbio
CD20	Alexa Fluor 700	2H7	Exbio
CD21	PerCP-Cy 5.5	Bu32	Biologend
CD24	PerCP-Cy 5.5	ML5	Biologend
CD25	Alexa Fluor 700	M-A251	Biologend
CD27	APC	M-T271	Biologend
CD28	Pe-Cy7	CD28.2	Biologend
CD38	Alexa Fluor 700	HB-7	Biologend
CD40	Brilliant Violet 421	5C3	Biologend
CD45	Alexa Fluor 700	HI30	Biologend
CD45	Pe-Cy7	HI30	Biologend
CD56	FITC	MEM188	Biologend
CD70	PE	Ki-24	BD Biosciences
CD80	Pe-Cy 7	2D10	Biologend
CD86	PE	HA5.2B7	Immunotech
CD123	APC	6H6	Biologend
CD127	Alexa Fluor 647	A019D5	Biologend
BDCA-2	PerCP-Cy 5.5	201A	Biologend
FoxP3	Alexa Fluor 488	259D/C7	BD Biosciences
Granzyme A	Alexa Fluor 700	CB9	Biologend
Granzyme B	Alexa Fluor 700	GB11	BD Biosciences
Granzyme B	Brilliant Violet 421	GB11	BD Biosciences
HLA-A,B,C	Alexa Fluor 700	W6/32	Biologend
HLA-DR	Brilliant Violet 421	L243	Biologend
IDO	Pe-Cy7	eyedio	eBioscience
IFN $\alpha$	PE	7N4-1	BD Biosciences
IFN $\gamma$	FITC	B27	BD Biosciences
IFN $\gamma$	Pe-Cy 7	4S.B3	eBioscience
IgD	Brilliant Violet 421	IA6-2	Biologend
IgG	PerCP-Cy 5.5	HP6017	Biologend
IgM	PerCP-Cy 5.5	MHM-88	Biologend
IL-6	PerCP-Cy 5.5	MQ2-13A5	Biologend
IL-10	PE	JES3-9D7	Biologend
Ki-67	Pe-Cy 7	Ki-67	Biologend
LAG-3	Pe-Cy 7	11C3C65	Biologend
NKp44	Pacific Blue	44.189	eBioscience

PD-1	APC	EH12.2H7	Biolegend
TIM-3	PE	F38-2E2	Biolegend
TIM-3	Pe-Cy7	F38-2E2	Biolegend
TLR7	PE	533707	R&D systems
TLR9	PE	eB72-1665	BD Biosciences
TNF $\alpha$	Pacific Blue	Mab11	Biolegend
TNF $\alpha$	PerCP-Cy 5.5	Mab11	Biolegend
TRAIL	PE	RIK-2	Biolegend

---

### 3.4 Immunohistochemistry

Acquired FFPE were stored in 5°C. Sections were deparaffinized with xylene solution for 3 x 5 minutes and rehydrated in decreasing concentrations of ethanol (100% - 95% - 70% - 50%). Afterwards, antigen retrieval was performed with incubation of slides in Tris/EDTA retrieval solution (pH 8; Dako) in water bath in 97°C for 30 min. Sections were cooled at room temperature for 30 minutes. Endogenous peroxidase activity was blocked using 150ul of 3% hydrogen peroxide per slide for 15 min. After peroxidase blocking, sections were incubated with 150ul of protein block (DAKO) for 20 min and stained with diluted primary antibodies against CD8 (SP16, Spring Bioscience), CD20 (L26, Dako), DC-LAMP (1010E1.01, Dendritics), BDCA-2 (polyclonal goat IgG, R&D Systems) and FoxP3 (monoclonal mouse IgG1, Abcam). After 1h incubation, polymer detection kits were used (ImPress AP, Vector Laboratories; VisUcyte, RD Systems). After 30min incubation, depending on the antibody used, corresponding chromogens were added followed by either 30 sec of Mayer's hematoxylin (Dako) or 10 min of Nuclear Fast Red (Vector Laboratories) counterstaining. Slides were washed in tap water and mounted in Glycerol Mounting Medium (Dako). The images were acquired using a Leica Aperio AT2 scanner (Leica).

We thoroughly inspected each section and evaluated the number of stained immune cells in the tumor nest and the tumor stroma in 10 representative visual fields at 10 $\times$  magnification or at 20x magnification in 20 representative fields in case of Study 3. Aperio ImageScope (Leica) or Ventana Image Viewer software were used.

In Study 2 a semiquantitative analysis of CD20<sup>+</sup>/CD8<sup>+</sup> cell-cell interactions was performed (-, negative sections; +, sections positive for B cell/CD8<sup>+</sup> T cell interactions in 1-5 visual fields; ++, sections positive for interactions in > 5 visual fields). The cell-to-cell interaction was

estimated as a direct cell-to-cell contact of CD20<sup>+</sup> B cells and CD8<sup>+</sup> T cells in a group of 20 – 100 cells or in a distance up to 100 µm from a margin of the aggregate.

### **3.5 Quantitative real-time PCR**

Bulk HNSCC-derived cells suspensions or magnetically isolated tumor-infiltrating CD8<sup>+</sup> cells were used for RNA extraction. At least 1 x 10<sup>6</sup> cells per specimen were lysed in RLT buffer and frozen in -20°C until used. RNA isolation was performed with RNA Easy Mini Kit (Qiagen) according to the manufacturer's instructions. The concentration and purity of the extracted nucleic acid was evaluated with NanoDrop© 2000c (Thermo Scientific) UV-Vis spectrophotometer. RNA integrity was controlled with a 2100 Bioanalyzer (Agilent). For synthesis of complementary DNA we applied prefabricated product iScript cDNA Synthesis Kit (BIO-RAD) on 100ng of total RNA. Complementary DNA (cDNA) was diluted with RNA-free water depending on the RNA integrity before the reaction.

For the quantitative real-time PCR itself, 2ul of synthesized cDNA and selected forward and reversed primers were pipetted to the 96-well plate together with Kappa Fast qPCR Master Mix (Kapabiosystems). The gene expression levels of PD-1, PD-L1, CTLA-4, TIM-3, LAG-3, TIGIT and BTLA were evaluated in Study 1. Gene expression of IL-2, IL-2R, BCL2L1, CD40L and CD27 were evaluated in the Study 2 and gene expression levels of TNF $\alpha$ , TGF $\beta$ , IL-10 were evaluated for Study 3. In all the studies,  $\beta$ -actin was used as a reference gene for normalization of target gene expression. All the experiments were performed with CFX 96™ Real-Time System (BIO-RAD).

In the Study 2 following RNA extraction and cDNA synthesis described before, we analyzed gene expression of immune response-associated genes with TaqMan low-density array cards (Applied Biosystems). The TaqMan low-density array cards were run on a Vii7 instrument (Applied Biosystems) using Taq-Man® Universal Master Mix II (Applied Biosystems).  $\Delta\Delta$ Ct method for relative gene expression levels was used.

### 3.6 Cytokine and chemokine detection

For detection of cytokines and chemokines in tumor-derived supernatants, ELISA and Luminex techniques were performed. We cultivated tumor-derived single cell suspensions at the concentration of  $1 \times 10^6$  cells/ml in a 96- U – well plate in RPMI1640 complemented with 1% L-glutamine, 10% heat-inactivated FCS and 1% penicillin-streptomycin in 37°C. After 24h of incubation, cell supernatants were collected and frozen in -80°C until used.

In Study 1 we evaluated concentrations of IL-4, IL-6, IL-10, IL-17A, IFN $\gamma$  and TNF $\alpha$  in culture supernatants, using Luminex based MILLIPLEX™ Human Cytokine Kit (Merck). PD-1 Human ELISA Kit (Thermo Fisher Scientific), Free Fatty Acid Quantification Kit (Abcam) and Adenosine Assay Kit (BioVision, Milpitas, USA) were used for determination of soluble PD-1, free fatty acids and adenosine levels, respectively. Assays were performed according to the manufacturer's instructions.

In Study 2 we used Luminex based MILLIPLEX™ Human Cytokine Kit (Merck) for detection of levels of IL-6, IL-10, IL-12, CXCL9, CXCL13, IFN $\gamma$ , TNF $\alpha$  and TNF $\beta$  in cell culture supernatants. In some samples we performed magnetically mediated B cell depletion with CD19 MicroBeads (Miltenyi Biotech) before 24h incubation.

Luminex-based MILLIPLEX™ Human Cytokine Kit (Merck) was also used in the Study 3 for evaluation of concentrations of IL-3, IL-4, IL-6, IL-10, IL-12 $\alpha$ , IL-17, IFN $\alpha$ , IFN $\gamma$  and TNF $\alpha$  in the supernatants. IFN $\alpha$  released into the culture supernatants in functional test was detected with Verikine Human IFN $\alpha$  ELISA Kit (PBL Assay Science). Detection of HMGB1 was performed using HMGB1 ELISA Kit (IBL International).

### 3.7 HPV detection

For determination of HPV etiology of the HNSCC we did both p16 protein immunohistochemical staining and PCR for detection of HPV DNA or 16E6\*I mRNA. Only the samples positive for 16E6\*I mRNA expression in case of Study 1 or samples positive for both HPV DNA and p16 in Study 2 and Study 3 were considered as HPV-induced tumors.

The antibody p16<sup>INK4a</sup> (monoclonal mouse anti-human p16, Clone G175-405, BD Pharmingen, dilution 1:100) or the CINtec Histology Kit (Roche) were used. The location of the signal,

whether cytoplasmic or/and nuclear, was also specified. Samples that were estimated as p16 positive had to show more than 70% cells that reveal nuclear and/or cytoplasmic staining. The staining was performed by a hospital laboratory technician. The results were interpreted by an experienced histopathologist.

For HPV DNA detection, the nucleic acid was obtained from paraffin-embedded sections with MagCore Genomic DNA FFPE One-Step Kit (RBC Bioscience). Further, qualitative real-time PCR with use of the AmoyDx Human Papillomavirus Genotyping Detection Kit (Amoy Diagnostics) was performed. The test is able to detect and genotype 19 high-risk strains of HPV (16, 18, 26, 31, 33, 35, 39, 45, 51, 52, 53, 56, 58, 59, 66, 68, 70, 73, and 82) and 2 low-risk strains of HPV (6 and 11). The test sensitivity is 100 copies of HPV DNA per reaction. In Study 1 we performed RNA extraction from paraffin-embedded sections, synthesized complementary DNA and ran quantitative real-time PCR with amplification of 16E6\*I mRNA oncoprotein using primers specific for the 86-bp fragment.

### **3.8 Functional cell experiments**

#### **3.8.1 Study of HPV-specific tumor-infiltrating T cells in oropharyngeal cancer (Study 1)**

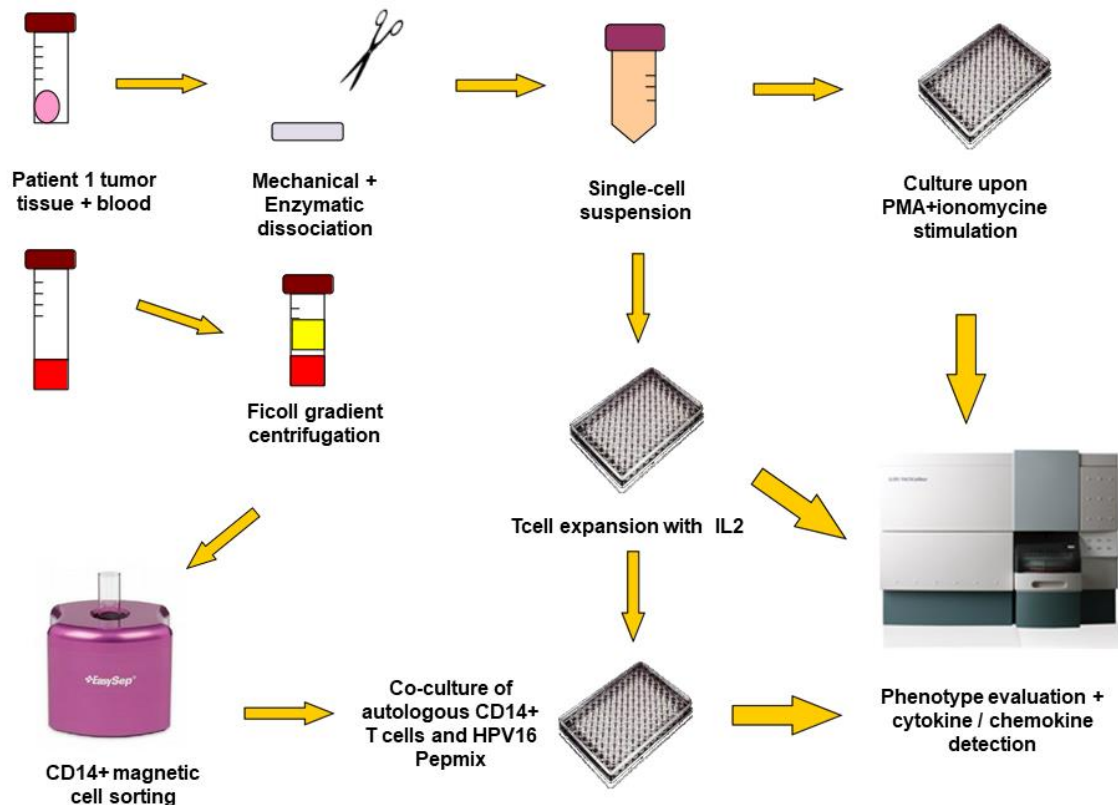
- TIL expansion

To obtain enough tumor-infiltrating T cells for functional experiments, we performed homeostatic *in vitro* expansion of tumor-derived T cells. Tumor-derived single cell suspensions were cultivated at concentration of  $3 \times 10^5$  lymphocytes/ml in 24-well plate for two weeks in RPMI 1640 with 10% human AB serum, penicillin-streptomycin, L-glutamine and 450 U of IL-2 (Proleukin, Prometheus Laboratories Inc.). Every 2 to 3 days, half of the old media was removed and refilled with a fresh medium supplemented with IL-2. After 2 weeks of homeostatic expansion, the population of expanded tumor infiltrating T cells was harvested.

- Detection of HPV16-specific T cells

We isolated CD14<sup>+</sup> monocytes from PBMC of the patients using Human CD14 Positive Selection Kit (Stemcell Technologies). The obtained monocytes were incubated with HPV16 E6 and E7 peptide pools at a concentration 5 µg/ml (JPT). Peptide-pulsed monocytes were washed in RPMI and added to expanded TILs at a ratio 1:10. Cells were co-cultivated for 6 h in the presence of Brefeldin A (BioLegend). After the incubation, cells were stained for

intracellular detection of  $IFN\gamma$  and  $TNF\alpha$ . The T cells that reacted by cytokine production to the specific stimulation provided by HPV peptide-loaded autologous monocytes, were considered as T cells specific to HPV antigens. As a positive control, artificial stimulation with PMA (50ng/ml) (Sigma Aldrich) and ionomycin (1ug/ml) (Sigma Aldrich) was used. Scheme of the experiment is below.



- Immune checkpoint molecule blocking

To evaluate the functional capacity and changes in immune checkpoint expression on expanded and fresh TILs, the cells were incubated with anti-PD-1 mAb (10 $\mu$ g/ml) (Nivolumab, Bristol-Myers-Squibb) and/or soluble TIM-3 (5  $\mu$ g/ml) (Recombinant Human TIM-3 protein, Abcam). The reactants were added separately or in combination to the TILs culture 42h before the cells were harvested and co-incubated with peptide-loaded autologous monocytes providing antigen-specific stimulation as described in the previous paragraph.

### 3.8.2 Study of tumor-infiltrating B cells in oropharyngeal cancer (Study 2)

- Detection of tumor-infiltrating Bregs

Tumor-derived single cell suspensions were incubated 5 and 24h with CpG ODN 2006 (5ug/ml) (Invivogen) and CD40L (1ug/ml) (R&D Systems) in the presence of PMA (50ng/ml) and ionomycin (1ug/ml) added at the same time. Brefeldin A (5ug/ml) (Biolegend) was added after 1h in case of 5h incubation and 5h since the beginning of stimulation in case of 24h incubation. After the incubation cells were intracellularly stained for IL-10 and analyzed using flow cytometry.

- Analysis of T cell functional capacity and viability

One half of the single-cell suspension yielded from the tumor specimens was labelled with CD19 MicroBeads and B cells were depleted using MACS LD column for magnetic cell separation (Miltenyi Biotech). The other half of the cells was pushed through the depletion column without labelling. The depleted and non-depleted cell suspensions were cultured at a concentration of  $6 \times 10^5$  cells per well in a 48-well plate in RPMI 1640 supplemented with 1% L-glutamine, 1% penicillin-streptomycin and 10% PHS. No other stimuli were added to the culture. After 6 days, viability and capacity to produce IL-2 and IFN $\gamma$  of CD8<sup>+</sup> and CD4<sup>+</sup> T cells was evaluated with flow cytometry using LIVE/DEAD™ Fixable Blue Dead Cell Stain Kit (Invitrogen) and appropriate fluorescent-labeled monoclonal antibodies.

### 3.8.3 Study of tumor-infiltrating plasmacytoid dendritic cells in head and neck cancer (Study 3)

- Analysis of inhibitory effect of HNSCC-derived supernatants and recombinant cytokines on IFN $\alpha$  production in pDCs

PBMC were isolated from blood of healthy donors with standard Ficoll-Paque density gradient centrifugation (GE Healthcare) described above. Plasmacytoid DCs were magnetically separated using CD304 (BDCA-4/Neuropilin-1) MicroBead Kit (Miltenyi Biotech). Enriched pDCs were seeded in 96-well U plate at a concentration of  $2.5 \times 10^5$ /ml and co-cultivated with supernatants derived from HPV<sup>-</sup> or HPV<sup>+</sup> tumors upon CpG ODN 2216 (5ug/ml) stimulation (Invivogen). After 24h of incubation supernatants were collected and IFN $\alpha$  levels were

measured with ELISA kit (PBL Assay Science). As a control, healthy donor blood-derived pDCs were stimulated with CpG ODN 2216 (5ug/ml) with addition of IL-6, IL-10, TNF $\alpha$  or their combinations at concentrations of 5 to 10 ng/ml (Biolegend). In part of the samples, neutralizing antibodies against IL-6, IL-10 and TNF $\alpha$  (BioLegend) were added to the cultures at a concentration of 10  $\mu$ g/ml. After 24h of incubation supernatants were collected and IFN $\alpha$  levels were measured with ELISA kit (PBL Assay Science). The reference value of IFN $\alpha$  production was estimated upon CpG stimulation in complete RPMI 1640 only.

- Effect of HNSCC-derived supernatants on Tregs expansion

Healthy-blood derived pDCs were seeded in a 96-well U-bottom plate at a concentration of  $5 \times 10^5$  pDCs/well and co-incubated with or without HPV<sup>+</sup> or HPV<sup>-</sup> HNSCC-derived culture supernatants overnight. Following incubation, pDCs were washed and magnetically isolated blood-derived autologous CD4<sup>+</sup> T cells were added at a ratio of 5:1 to pDCs. After 5 days of incubation, the proportion of CD4<sup>+</sup>CD25<sup>hi</sup>FoxP3<sup>+</sup> Tregs in the culture was analyzed using flow cytometry. The reference value was defined as the proportion of Tregs in co-cultures of CD4<sup>+</sup> T cells and pDCs cultivated in complete RPMI only.

### 3.9 Statistical analysis and graph editing

Statistical analyses were performed with Statistica® 10.0 software (StatSoft) and Graphpad Prism 8 (GraphPad Software). Statistical significance of all the results was considered when  $p < 0.05$ .

Verification of parametric distribution of the data was performed with Kolmogorov-Smirnov test for normality. Levene test was used for homogeneity of variances. Depending on the data distribution, comparison of groups was performed with t-test or Mann-Whitney U test for two groups and ANOVA or Kruskal-Wallis ANOVA for multiple groups. The correlation studies were tested using Pearson's chi-square test. Log rank test was used for analyses of immune cell prognostic value on patient survival. Univariate and multivariate analyses of prognostic factors were performed with Cox proportional hazard model.

All the graphs were created in GraphPad Prism 7 and GraphPad Prism 8. Final editing and arrangements of graphics were made in Adobe Photoshop.

## 4. Results

### 4.1 Study of HPV-specific tumor-infiltrating T cells in oropharyngeal cancer (Study 1)

(modified from Hladíková et al. 2018)

#### Overview

The study was focused on the detection of HPV-specific tumor-infiltrating T cells in native samples of OPSCC. Further, a functional state of T cells that are able to react to aforementioned HPV antigens was evaluated according to the expression of important immune checkpoints on their surface. We were able to detect HPV-specific T cells in 73.1 % of HPV<sup>+</sup> samples but none in HPV<sup>-</sup> tumors. Moreover, T cells able to react by IFN $\gamma$  and TNF $\alpha$  production upon specific stimulation by HPV peptides were mostly TIM-3 negative. TIM-3, but not PD-1 expression, proved to be the possible crucial marker of T-cell dysfunction even after blockade of TIM-3 and PD-1 pathways. Only the blockade of both of these pathways led to an increase of pro-inflammatory cytokine production by tumor-infiltrating T cells. Also, we observed increase in TIM-3 expression after selective PD-1 blockade in freshly isolated TILs. This upregulation of TIM-3 was decreased when specific stimulation by HPV peptides was used. The detailed results are described below.

- Detection of HPV-specific T cells

After fresh tumor tissue processing and homeostatic expansion of yielded T cells (according to the techniques described in Materials and Methods section) we had 31 tumor samples ready for testing of reactivity to HPV 16 antigens, using autologous CD14<sup>+</sup> monocytes loaded with E6 and E7 peptide pools as antigen presenting cells. We were able to detect CD8<sup>+</sup> T cells responding to the specific antigen stimulation by production of IFN $\gamma$  in 73.1% of HPV<sup>+</sup> OPSCC samples (Fig. 1A). TNF $\alpha$ -producing HPV-specific CD8<sup>+</sup> T cells were found in 40% of HPV<sup>+</sup> samples (Fig. 1B). Importantly, HPV-specific T cells were not detected in HPV<sup>-</sup> tumor samples.

**Figure 1**

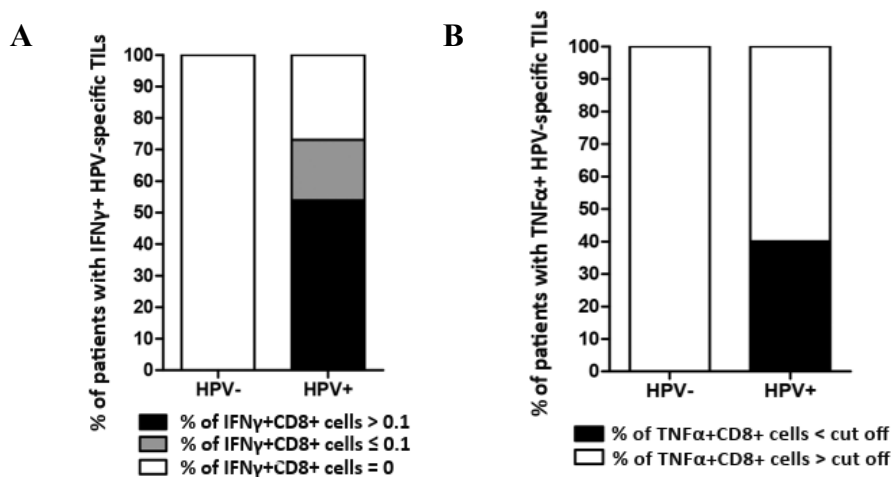


Figure 1. Proportions of HPV16 E6/E7 specific TILs derived from tumor tissues of OPSCC patients ( $n = 31$ ). Columns show proportions of tumor samples positive for HPV-specific IFN $\gamma^+$  (A) and TNF $\alpha^+$  (B) CD8 $^+$  T cells.

- Expression of checkpoint molecules PD-1 and TIM-3 according to IFN $\gamma$  and TNF $\alpha$  production by HPV-stimulated T cells

PD-1 and TIM-3 are well defined and important immune checkpoint receptors that were reported to define functionally exhausted immune cells. Using flow cytometer analysis, we evaluated expression of these markers on T cells stimulated with HPV peptides, as mentioned above. Surprisingly, the CD8 $^+$  T cell populations with the highest IFN $\gamma$  response were PD-1 $^+$ TIM-3 $^-$  and PD-1 $^-$ TIM-3 $^-$  (55.1 $\pm$ 11.0% and 29.7 $\pm$ 13.6% from all IFN $\gamma$  producing cells, respectively) (Fig. 2A, B). When we used a different approach to separate populations in flow cytometry dot plots we found consistent results showing that the highest proportion of IFN $\gamma$  cells was among the PD-1 $^+$ TIM-3 $^-$  subpopulation (9.3 $\pm$ 14.4% of PD-1 $^+$ TIM-3 $^-$ CD8 $^+$  T cells) (Fig 2E). Similar results were observed in TNF $\alpha$ -producing CD8 $^+$  T cells (Fig. 2C, D). PD-1 $^+$ TIM-3 $^-$  CD8 $^+$  T cells showed the highest proportion of TNF $\alpha$  positive cells (29.2 $\pm$ 17.4% of PD-1 $^+$ TIM-3 $^-$ CD8 $^+$  T cells) (Fig 2F). Generally, impaired ability to respond to the specific stimulation by HPV antigens was observed in TIM-3 expressing T cells but not in PD-1 $^+$  populations.

**Figure 2**

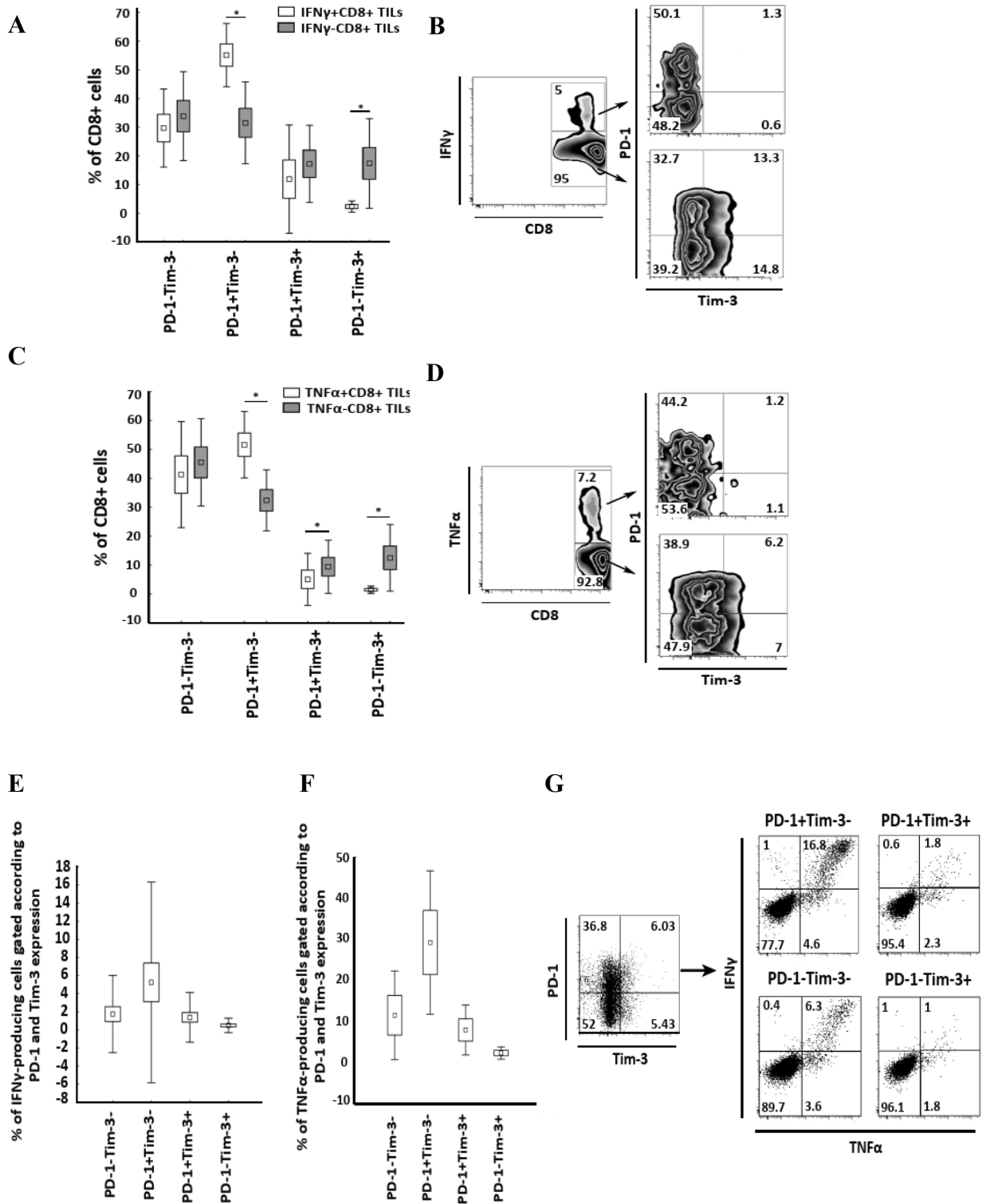


Figure 2. (A, C) Boxes show differences in proportions of IFN $\gamma$ <sup>+</sup> and IFN $\gamma$ <sup>-</sup> CD8<sup>+</sup> T cells (A) and TNF $\alpha$ <sup>+</sup> and TNF $\alpha$ <sup>-</sup> CD8<sup>+</sup> T cells (C) according to PD-1 and TIM-3 expression after

stimulation with HPV16 E6/E7. The boundaries of the boxes indicate the SEM, the squares in the boxes represent the mean. Whiskers indicate the SD. (B, D) Dot plots are gated on  $CD3^+CD8^+$  cells and show PD-1 and TIM-3 expression on  $CD8^+$  T cells according to production of  $IFN\gamma$  (B) and TNF $\alpha$  (D) in a representative patient. (E, F) Box plots show proportions of  $IFN\gamma$ -producing (E) and TNF $\alpha$ -producing (F)  $CD8^+$  T cells in populations gated according to PD-1 and TIM-3 expression. The boundaries of the boxes indicate the SEM, the squares in the boxes represent the mean. Whiskers indicate the SD. (G) Dot plots are gated on  $CD3^+CD8^+$  cells and show proportions of  $IFN\gamma$  and TNF $\alpha$ -producing cells according to PD-1 and TIM-3 expression in a representative patient. \* $p < 0.05$

- Immune checkpoint blocking studies and the effect of homeostatic expansion on tumor-infiltrating T cell phenotype

To support the result indicating important role of TIM-3 expression on  $CD8^+$  T cell activation, we performed blocking of PD-1/PD-L1 and TIM-3 pathways. For the PD-1 blocking studies we used commercially approved anti-PD-1 antibody nivolumab. To impair the TIM-3 signaling we used soluble TIM-3 (sTIM-3), as an artificial receptor that should consume all the TIM-3 ligands available in the suspension. After 48h of incubation of expanded TILs and nivolumab, we observed only small increase in  $IFN\gamma$  production upon specific stimulation. However, when soluble TIM-3 was added to the culture there was a 36% increase in  $CD8^+$  T cell  $IFN\gamma$  response (Fig. 3A). Nevertheless, against expectations, we did not see any effect of PD-1 blockade on upregulation of TIM-3 expression. In order to see whether this result could be a “side-effect“ of homeostatic expansion of tumor-infiltrating T cells, we performed the same experiments with freshly isolated cells. In the fresh samples we detected the hypothesized result and observed an increase in TIM-3 (+ 10% proportional change in TIM-3 expression) expression on HPV peptide-stimulated TILs after the anti-PD-1 treatment (Fig 3B). Importantly, when we applied nivolumab treatment on non-stimulated freshly isolated TILs, there was a much higher increase in TIM-3 expression (+ 60% proportional change in TIM3 expression) (Fig. 3B), an indication that the specific stimulation of T cells might reduce regulatory increase in expression of other checkpoint molecules, following PD-1 blockade.

**Figure 3**

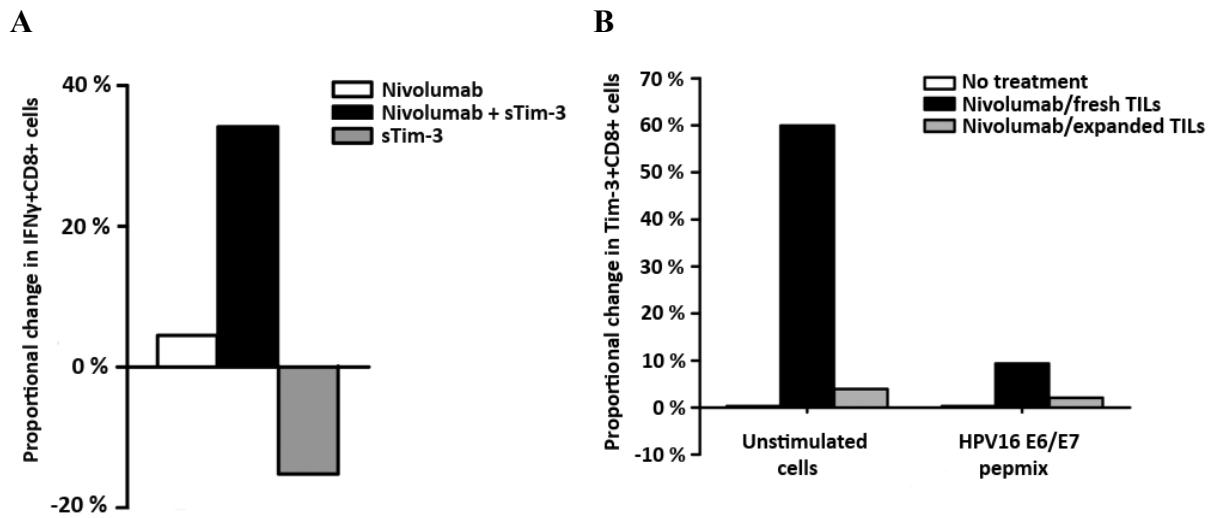


*Figure 3. The effect of PD-1 and/or TIM-3 blockade on IFN $\gamma$ -production and TIM-3 expression in HPV16-specific CD8<sup>+</sup> T cells. (A) Columns represent the percentual increase/decrease in proportions of IFN $\gamma$ -producing cells induced by anti-PD-1 mAb Nivolumab and soluble TIM-3 ( $n = 4$ ). The change was counted from the baseline represented by HPV16 E6/E7 stimulated TILs. (B) Columns represent the percentual increase in proportions of TIM-3-producing cells induced by anti-PD-1 mAb Nivolumab in freshly isolated ( $n = 4$ ) or two weeks expanded ( $n = 4$ ) cells. The change was counted from the baseline represented by unstimulated TILs without any treatment.*

- Effect of homeostatic expansion on tumor-infiltrating T cell phenotype

Based on the results observed during PD-1 and TIM-3 blocking studies, we further characterized the phenotype of OPSCC TILs expanded for 2 weeks in a medium supplemented with IL-2, and compared the results to freshly isolated TILs. In expanded cultures we detected significant changes in immune checkpoint molecule expression on both CD4<sup>+</sup> and CD8<sup>+</sup> T cells. The homeostatic expansion caused an increase of functionally impaired PD-1<sup>-</sup> TIM-3<sup>+</sup> and PD-1<sup>+</sup> TIM-3<sup>+</sup> populations and decrease of prevailing PD-1<sup>+</sup> TIM-3<sup>-</sup> cells in HPV<sup>-</sup> samples (Fig. 4A). The result was statistically significant for HPV<sup>-</sup> samples, but similar effect was observed also in HPV<sup>+</sup> cell cultures, however, the prevailing population was PD-1<sup>-</sup> TIM-3<sup>-</sup>. We observed no alterations of CD4<sup>+</sup> CD25<sup>high</sup> FoxP3<sup>+</sup> Treg proportions depending on the homeostatic expansion (Fig 4). Moreover, to test whether the observed impact of homeostatic expansion is specific to OPSCC, we made the same analysis using another HPV-associated malignancy,

which is cervical cancer. We did not observe the increase of TIM-3<sup>+</sup> cells nor decrease of PD-1<sup>+</sup> cell in CD8<sup>+</sup> population (Fig. 5A), but the effect was seen in CD4<sup>+</sup> T lymphocytes (Fig. 5B). In the healthy donor PBMCs we observed both the increase of PD-1 and TIM-3 expressing populations, but the increase was more pronounced in CD4<sup>+</sup> cells (Fig. 5B).

**Figure 4**

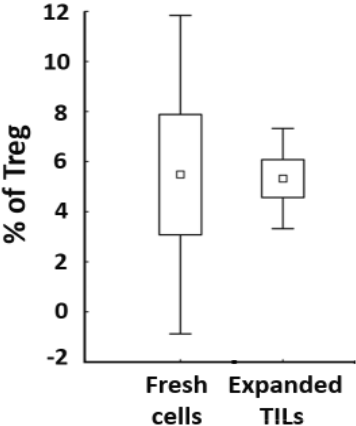
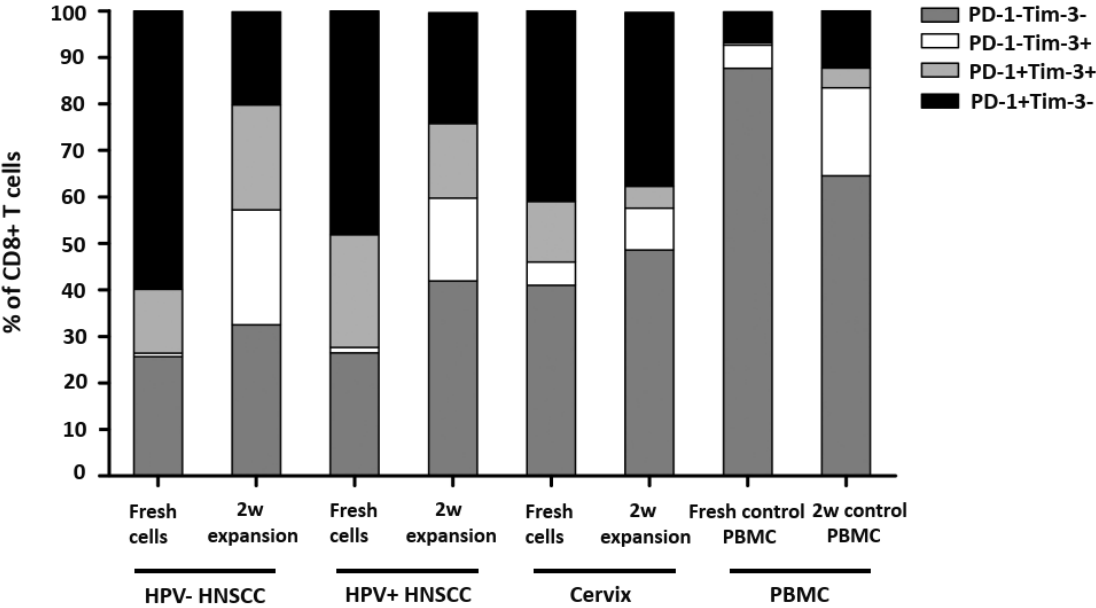


*Figure 4. Box-plots represent proportions of Tregs in fresh tumor cell suspensions and in TIL cultures after homeostatic expansion*

**Figure 5**

**A**



**B**

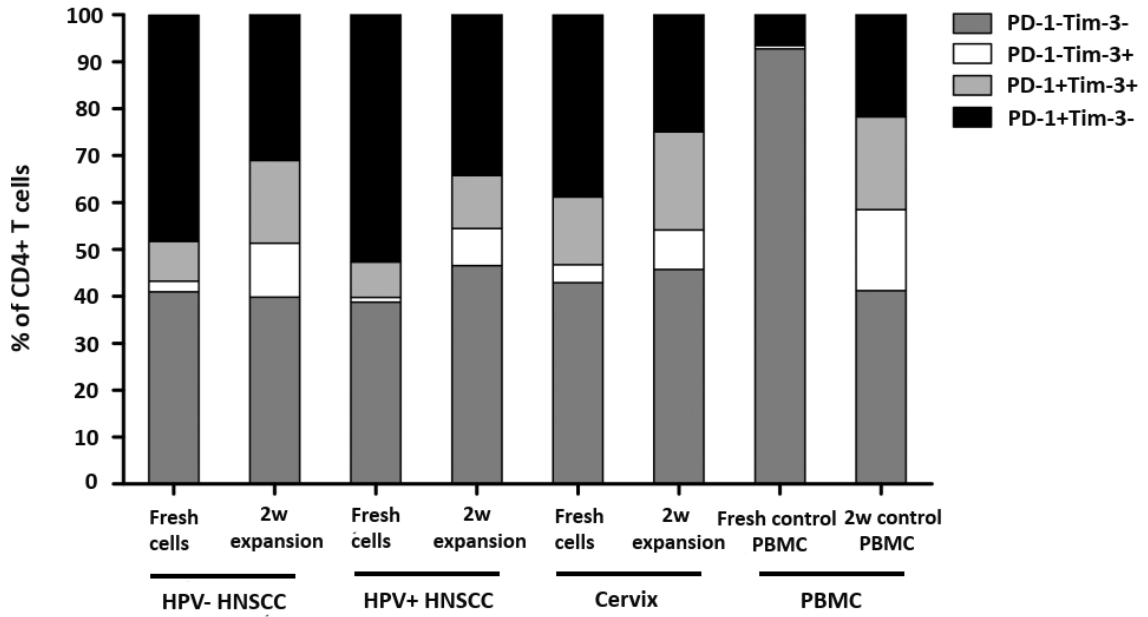


Figure 5. Columns show percentual distribution of CD8<sup>+</sup> (A) and CD4<sup>+</sup> (B) T cells derived from described tissues, according to PD-1 TIM-3 expression

For evaluation of other checkpoint molecules in OPSCC TILs, we tested mRNA expression levels of TIGIT, CTLA4, BTLA, LAG-3, PD-L1, PD-1 and TIM3. We observed significant positive correlation of TIGIT, CTLA-4, LAG-3, PD-L1 and TIM-3 with mRNA levels of PD-1 ( $r=0.62$ ;  $r=0.57$ ;  $r=0.78$ ;  $r=0.62$ ;  $r=0.45$ , respectively;  $p<0.05$  (Fig. 6).

**Figure 6**

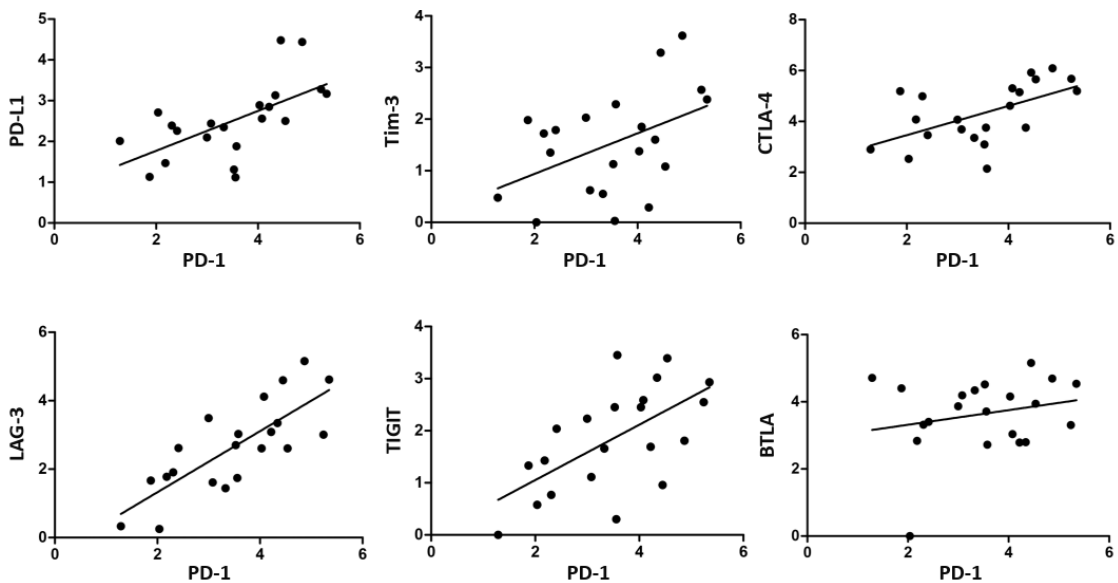
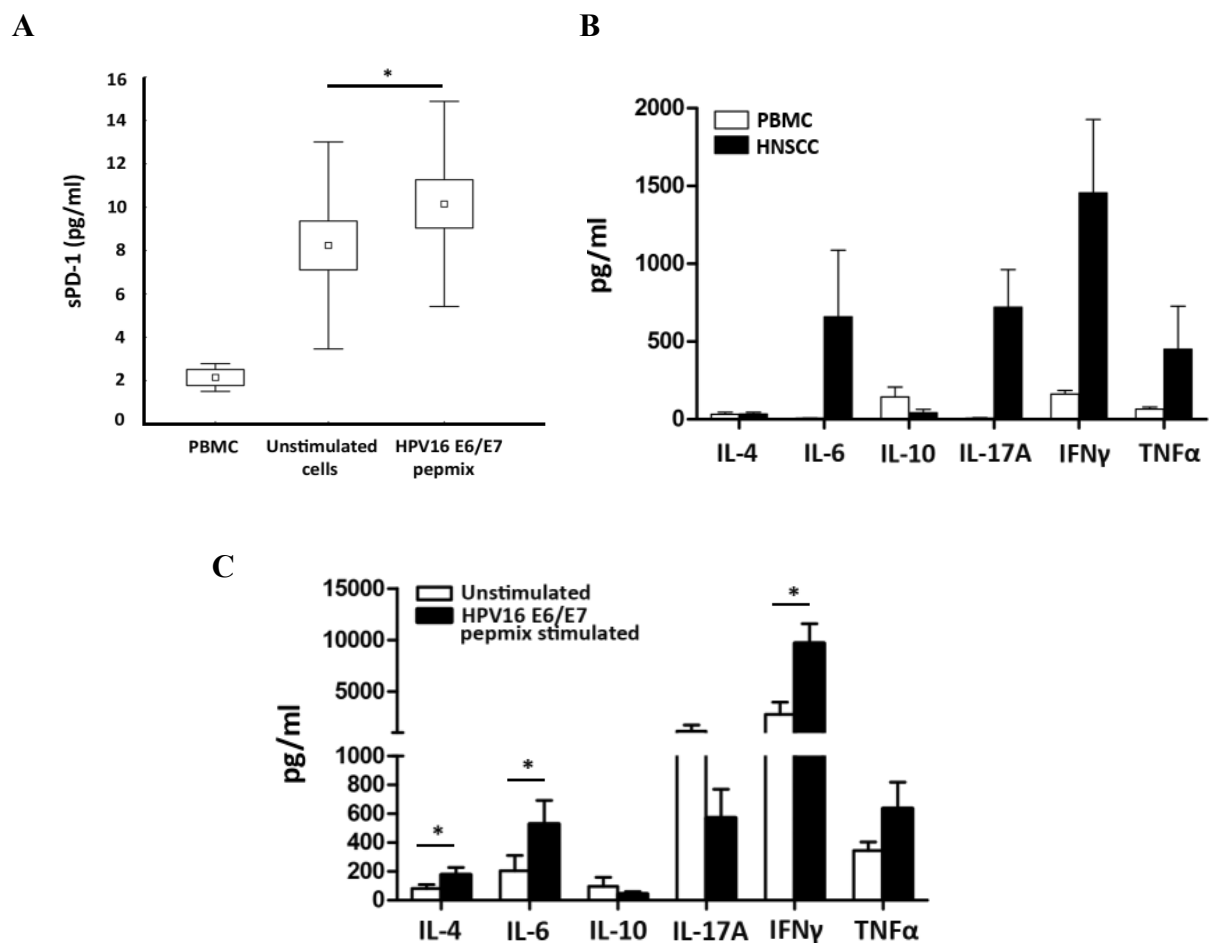


Figure 6. The correlation between mRNA levels of PD-1 (x-axis) and selected immune checkpoint molecules (y-axis) in expanded TILs. Linear trendlines are shown.

- Cytokine levels in supernatants of expanded TILs

Because the cytokines and other soluble components in the TME are known to be important factors that were reported to influence expression of immune checkpoints, we evaluated the levels of free adenosine, free fatty acids, soluble PD-1 (sPD-1) and cytokines IL-4, IL-6, IL-10, IL-17A, IFN $\gamma$ , TNF $\alpha$  in TIL cell culture supernatants. We did not measure any considerable levels of free-adenosine or free fatty acids levels, but we observed higher amounts of sPD-1, IL-6, IL-17A, IFN $\gamma$  and TNF $\alpha$  in TIL cultures compared to healthy donor PBMC-derived supernatants (Fig 7 A, B). In addition, the sPD-1, IL-4, IL-6, IFN $\gamma$  and TNF $\alpha$  concentrations were further enhanced upon specific stimulation by HPV16 E6/E7 pepmixes (Fig. 7C).

Figure 7



*Figure 7. Cytokine profile and soluble PD-1 (sPD-1) concentration in culture supernatants of tumor derived TILs and PBMCs after two weeks of homeostatic expansion. (A) Boxes show spontaneous release of sPD-1 or release of sPD-1 upon HPV16 E6/E7 stimulation. The boundaries of the boxes indicate the SEM, and the squares in the boxes represent the mean. Whiskers indicate the SD. (B) Columns show the mean spontaneous cytokine production. (C) White columns represent the mean spontaneous cytokine production; black columns represent the mean cytokine production upon HPV16 E6/E7 stimulation. All error bars indicate SEM. \*p < 0.05*

## 4.2 Study of tumor-infiltrating B cells in oropharyngeal cancer (Study 2)

(modified from Hladíková et al. 2019)

### Overview

The aim of the study was to evaluate a prognostic value and functional capacity of TIL-Bs in OPSCC. Using immunohistochemical staining of CD20<sup>+</sup> cells we found a strong positive prognostic value of TIL-Bs no matter the HPV status of the tumor. Moreover, for the first time we described small non-organized aggregates of CD20<sup>+</sup> B cells/CD8<sup>+</sup> T cells with even stronger positive prognostic value compared to tumor infiltrating B cells and T cells alone. The main phenotype of TIL-Bs was a memory subtype in samples showing both high (> 0,5% B cells from all measured cells) and low B cell infiltration. However, B cells from B<sup>hi</sup> oropharyngeal samples expressed higher levels of co-stimulatory molecules, suggesting their role in antigen presentation and T cell stimulation. Moreover, when we depleted CD19<sup>+</sup> cells from tumor-derived suspensions, the T cell survival was significantly decreased compared to bulk samples, presuming the essential role of B cells for effector T cell sustainability in the tumor tissue. The detailed results are described below.

- Densities of CD20<sup>+</sup> B cells and CD8<sup>+</sup> T cells in OPSCC samples according to HPV status  
We performed TaqMan analysis of transcriptional signature of immune response related genes in HPV<sup>+</sup> and HPV<sup>-</sup> OPSCC samples. Interestingly, we observed significantly higher expression levels of CD19, HLA-DOB, CR2, MS4A1, TNSFRSF17 and BLK, genes associated with B lymphocytes (Fig. 1A). In view of this result we evaluated levels of CD20<sup>+</sup> cells, CD8<sup>+</sup> cells and DC-LAMP<sup>+</sup> cells in 72 OPSCC tissue sections by immunohistochemistry. As expected, we observed higher densities of CD20<sup>+</sup> and CD8<sup>+</sup> cells in both tumor nests and tumor stroma in HPV<sup>+</sup> samples (Fig. 1B). Moreover, we noticed interesting positional relation of CD20<sup>+</sup> and CD8<sup>+</sup> cells. We described aggregates of these cells with clear membrane cell-to-cell contacts in both the tumor nests and stroma (Fig 1C, D). Densities of these cell aggregates were significantly higher in HPV<sup>+</sup> samples compared to HPV<sup>-</sup> sections (Fig 1F). On the contrary, we were able to detect well defined tertiary lymphoid structures (TLS) with germinal centers, a previously reported positive prognostic factor in breast and lung cancer and recently in HNSCC, in only 29.8% and 25% of HPV<sup>+</sup> and HPV<sup>-</sup> samples, respectively (Fig. 1E). Additionally, there was no difference concerning DC-LAMP staining in relation to HPV status.

**Figure 1**

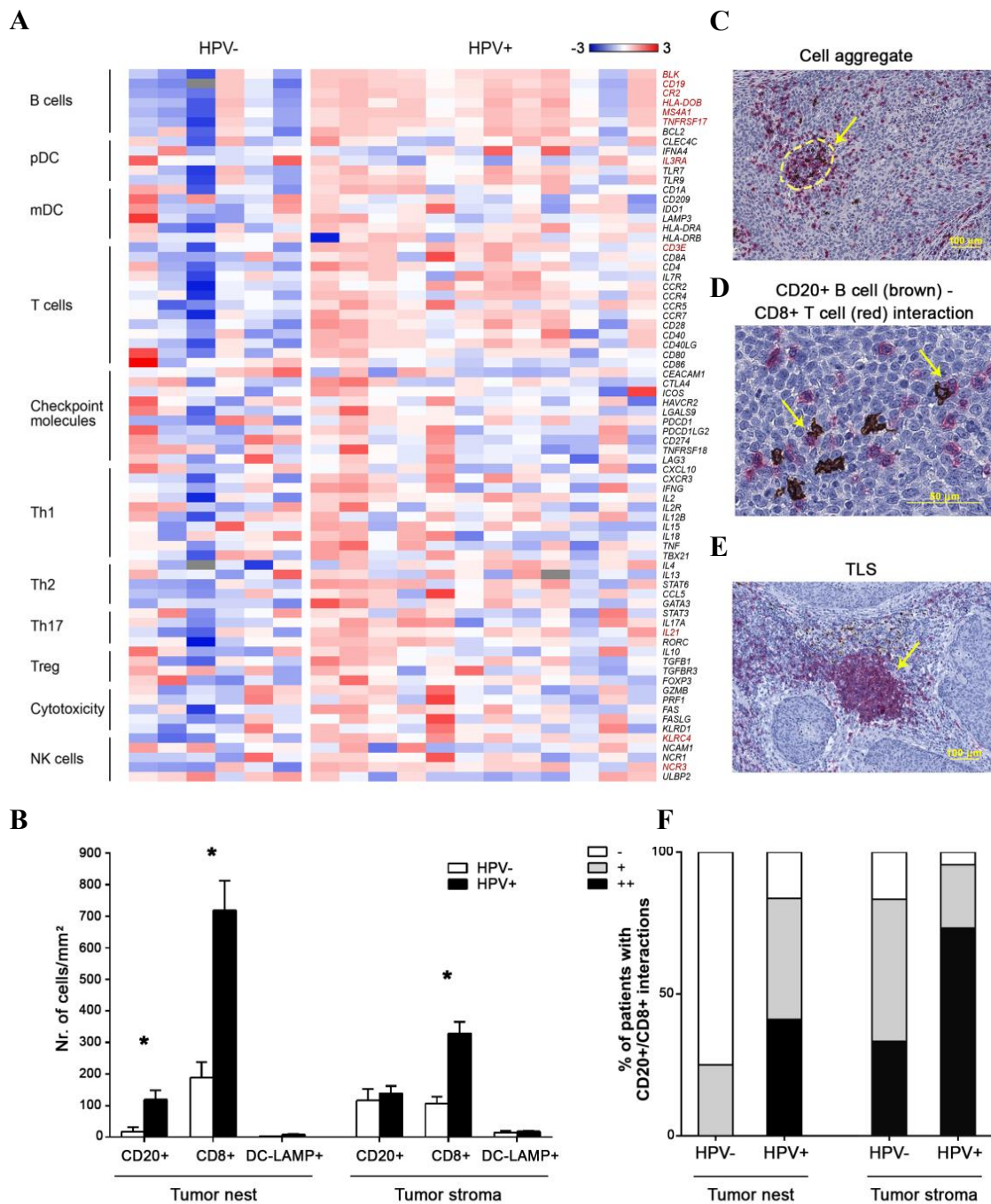


*Figure 1: Different proportions of tumor-infiltrating leukocytes in patients with oropharyngeal squamous cell carcinoma (OPSCC) in relation to the HPV status. (A) The heat-map shows z-scores of relative mRNA expression of selected genes in HPV<sup>-</sup> (n = 6) and HPV<sup>+</sup> (n = 12) tumor samples. Genes with significantly different expression are marked in red. (B) Columns*

represent the mean (+SEM) densities of CD20<sup>+</sup> B cells, CD8<sup>+</sup> T cells and DC-LAMP<sup>+</sup> dendritic cells in tumor nests and tumor stroma of FFPE sections of OPSCC patients from Cohort 1 (n = 72). (C) Example of stained non-organized CD20<sup>+</sup> B cell (brown)/CD8<sup>+</sup> T cell (red) aggregate. (D) Representative example of CD20<sup>+</sup> B cell (brown) – CD8<sup>+</sup> T cell membrane interactions. (E) Example of TLS. (F) Columns report proportions of patients where B cell/ T cell interactions were detected. Results are shown both for the tumor nest and the tumor stroma of OPSCC tissue sections (- interactions not detected; + interactions detected in 1 – 5 visual fields; ++ interactions detected in > 5 visual fields). \* p < 0.05 (Mann-Whitney U test).

- Prognostic role of CD20<sup>+</sup> B cells, CD8<sup>+</sup> T cells and CD20<sup>+</sup> B cell/CD8<sup>+</sup> T cell interactions in OPSCC patients

We evaluated the prognostic role of tumor nest and tumor stroma-infiltrating CD20<sup>+</sup> B cells, CD8<sup>+</sup> T cells and CD20<sup>+</sup> B cell/CD8<sup>+</sup> T cell interactions in patients with OPSCC using immunohistochemistry on FFPE sections. For that purpose, we divided our patient cohort using median value of positively stained cells per 1 mm<sup>2</sup> of the tumor nest or the tumor stroma area. As expected, based on the previous studies, the higher infiltration of CD8<sup>+</sup> T cells corresponded with better overall survival (OS) (p= 0,013) (Fig 2B). Additionally, we found that higher abundance of TIL-Bs was associated with improved OS (p<0.001)(Fig 2A). Importantly, the presence of CD20<sup>+</sup> B cell/CD8<sup>+</sup> T cell cell-to-cell interactions showed to be the strongest prognostic factor, both in case of intratumoral and stromal tissue (p = 0.001 and p = 0.009, respectively) (Fig 2C). The result was highlighted by the finding that the prognostic role of the detected cell-to-cell interactions showed better stratification of the patients than the parallel occurrence of B cells and T cells (Fig. 2D).

Figure 2

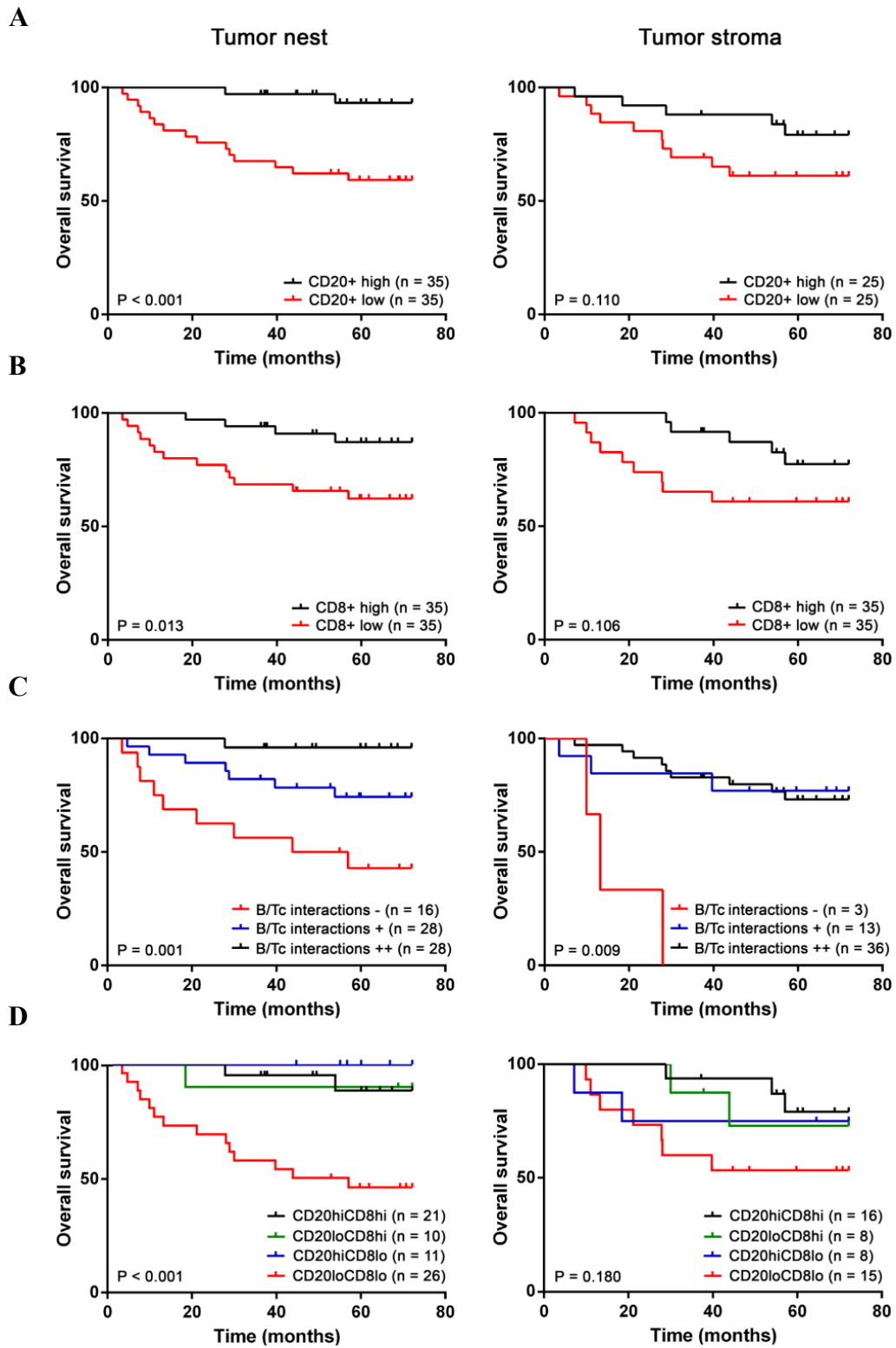


Figure 2: Prognostic role of tumor-infiltrating CD20<sup>+</sup> B cells (A), CD8<sup>+</sup> T cells (B), CD20<sup>+</sup>B cell/CD8<sup>+</sup> T cell (B/Tc) interactions (C) and combination of CD20<sup>+</sup> B cells and CD8<sup>+</sup> T cells (D) in patients with OPSCC (n = 70). OS of patients based on the densities of the indicated cells in the tumor nests (left) and in the tumor stroma (right) is expressed by Kaplan-Meier curves. Log-rank test was used for p value calculation.

The positive prognostic role of selected variables was confirmed using univariate Cox regression and multivariate Cox proportional hazard mode. The univariate analysis also showed statistical significance of generally accepted negative risk factors such as stage IV (p = 0.004), extranodal extension (p < 0.001), keratinizing histological subtype (p = 0.006), advanced tumor size (p = 0.042) and HPV negativity (p = 0.006) (Tab. 1). The multivariate analysis defined following risk factors as independent (Table 2): high abundance of CD20<sup>+</sup> B cells in tumor nests (p = 0.044, HR = 0.97, 95% CI = 0.93 – 0.99), high abundance of stromal B cell/CD8<sup>+</sup> T cell interactions (p = 0.019, HR = 0.10, 95% CI = 0.02 – 0.69) and extranodal extension (p = 0.004, HR = 5.25, 95% CI = 1.68 – 16.38). HPV negativity and densities of B cell/CD8<sup>+</sup> T cell interactions in the tumor nests were not statistically significant in the multivariate analysis, nevertheless, there was a strong trend (p = 0.063, HR = 0.29, 95% CI = 0.08 – 1.06 and p = 0.068, HR = 0.11, 95% CI = 0.01 – 1.17; respectively). The 5-year OS of patients in Cohort 1 was 75.7%, the median OS was 5.44 years (0.29 – 14.40).

**Table 1. Prognostic OS parameters, univariate analysis**

Variable	Class	Hazard Ratio	95% Confidence Interval	P value
<b>Sex</b>	Female	1		
	Male	1.14	0.37-0.5	0.816
<b>Stage</b>	I	1		
	II	2.78	0.78-9.87	0.113
	III	3.51	0.71-17.4	0.124
	IV	7.78	1.92-31.5	<b>0.004</b>
<b>LN ratio</b>		2.72	0.44-16.89	0.283
<b>Extranodal extension</b>	No	1		
	Yes	6.55	2.46-17.41	<b>&lt;0.001</b>
<b>Perineural spread</b>	No	1		
	Yes	2.10	0.67-6.47	0.194
<b>Resection margin</b>	R0	1		
	R1	1.56	0.57-4.29	0.389
<b>Concomitant chemotherapy</b>	No	1		
	Yes	1.63	0.62-4.28	0.323

SCC typing	NK	1		
	NK-M	2.31	0.78-6.90	0.131
	K	5.64	1.64-19.41	<b>0.006</b>
Tumor size		1.02	1.00-1.06	<b>0.042</b>
HPV status	Negative	1		
	Positive	0.23	0.08-0.66	<b>0.006</b>
Smoking history	Non Smoker	1		
	Ex smoker	0.42	0.13-1.42	0.165
	Smoker	0.63	0.20-1.91	0.412
Tertiary lymphoid structures	No	1		
	Yes	1.15	0.40-3.27	0.789
CD20+ B cell density tumor nest		0.96	0.93-0.99	<b>0.015</b>
CD20+ B cell density tumor stroma		1		
CD8+ T cell density tumor nest		0.99	0.99-1.00	<b>0.013</b>
CD8+ T cell density tumor stroma		0.99	0.99-1.00	0.231
DC density tumor nests		0.95	0.88-1.03	0.207
DC density tumor stroma		0.98	0.95-1.02	0.328
B cell/T cell clusters tumor nest	-	1		
	+	0.35	0.13-0.95	<b>0.040</b>
	++	0.05	0.01-0.41	<b>0.005</b>
B cell/T cell clusters tumor stroma	-	1		
	+	0.07	0.01-0.41	<b>0.003</b>
	++	0.08	0.02-0.33	<b>&lt;0.001</b>

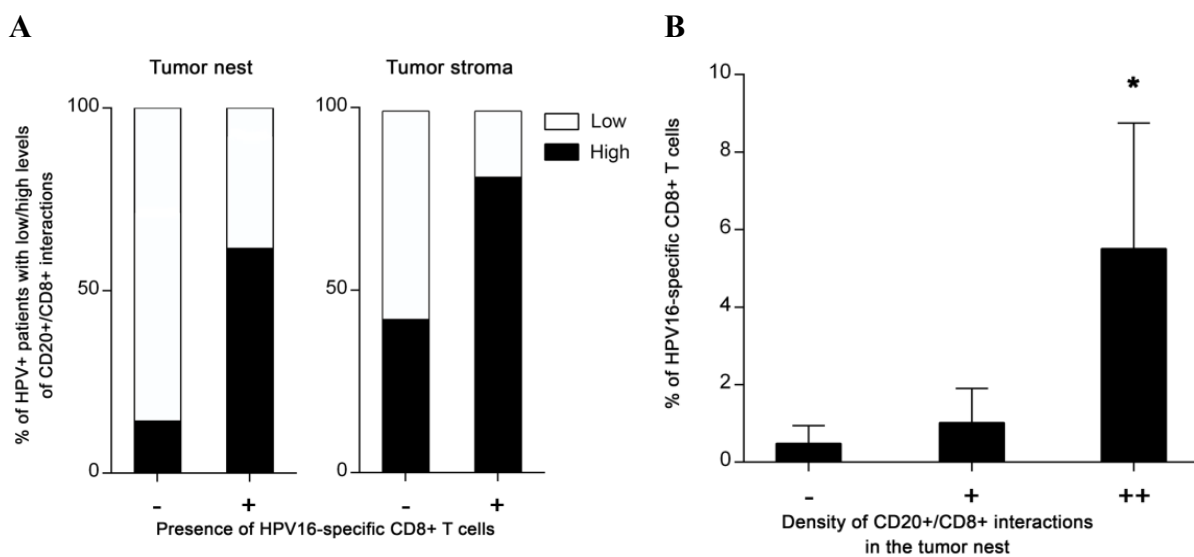
Table 2. Prognostic OS parameters, Multivariate analysis

Variable	Class	Hazard Ratio	95% Confidence Interval	P value
Extranodal extension	No	1		
	Yes	5.25	1.68-16.38	<b>0.004</b>
Tumor size		0.99	0.96-1.02	0.592
HPV status	Negative	1		
	Positive	0.29	0.08-1.06	0.063
CD20+ B cell density tumor nest		0.97	0.94-1.00	<b>0.044</b>
CD8+ T cell density tumor nest		1.00	1.00-1.00	0.581
B cell/T cell clusters tumor nest	-	1		
	+	0.59	0.13-2.65	0.491
	++	0.11	0.01-1.17	0.068
B cell/T cell clusters tumor stroma	-	1		
	+	0.10	0.02-0.69	<b>0.019</b>
	++	0.24	0.05-1.19	0.081

- Positive correlation of HPV16 E6/E7-specific CD8<sup>+</sup> tumor-infiltrating T-cells with CD20<sup>+</sup> B cell/CD8<sup>+</sup> T cell interactions in HPV<sup>+</sup> tumors

In our previous study we were able to detect HPV-specific T cells infiltrating the HPV<sup>+</sup> OPSCC in 73.1% of samples. Therefore, we wanted to evaluate whether the interactions between CD20<sup>+</sup> B cells and CD8<sup>+</sup> T cells could be associated with the specific anti-HPV T cell response. We prepared FFPE tumor sections from the patient tumor samples previously evaluated for the presence of HPV16-specific CD8<sup>+</sup> T cells (Cohort 2, see Materials and Methods). In these FFPE sections we identified proportions of B cell/CD8<sup>+</sup> T cell interactions and correlated the results with HPV-specific T cells detected in the matched native samples. Only 14.3% of patients without HPV16 E6/E7-specific CD8<sup>+</sup> T cell had CD20<sup>+</sup> B cell/CD8<sup>+</sup> T cell interactions in tumor nests. In the tumor stroma, CD20<sup>+</sup> B cell/CD8<sup>+</sup> T cell interactions were detected in 42.8% of samples (Fig. 3A). On the contrary, we found the interactions in tumor nests in 61.5% of patients with HPV16 E6/E7-specific CD8<sup>+</sup> T cells and in the tumor stroma even in 81.8% of samples (Fig. 3A). Importantly, we described a significant positive correlation between CD20<sup>+</sup> B cell/CD8<sup>+</sup> T cells interaction density in tumor nests and proportions of HPV16 E6/E7-specific CD8<sup>+</sup> T cells (Fig. 3B), but there was no statistically significant correlation between the HPV16 E6/E7-specific CD8<sup>+</sup> T cell and the density of tumor infiltrating CD20<sup>+</sup> B cells or CD8<sup>+</sup> T cells alone (Fig. 3C).

**Figure 3**



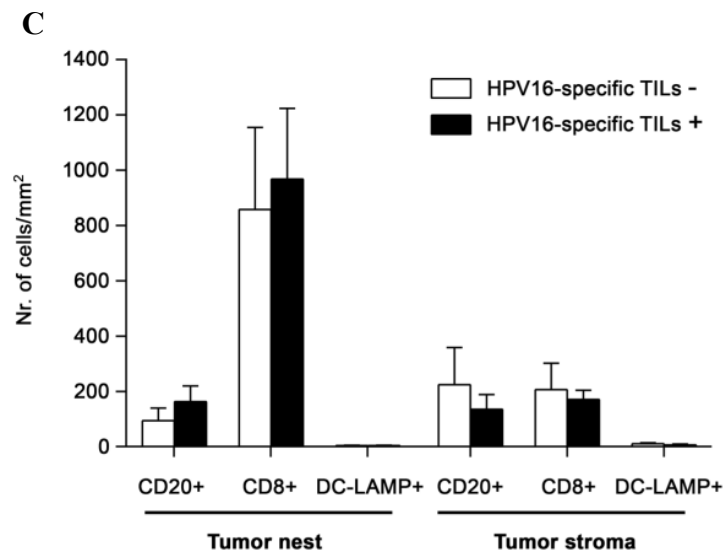
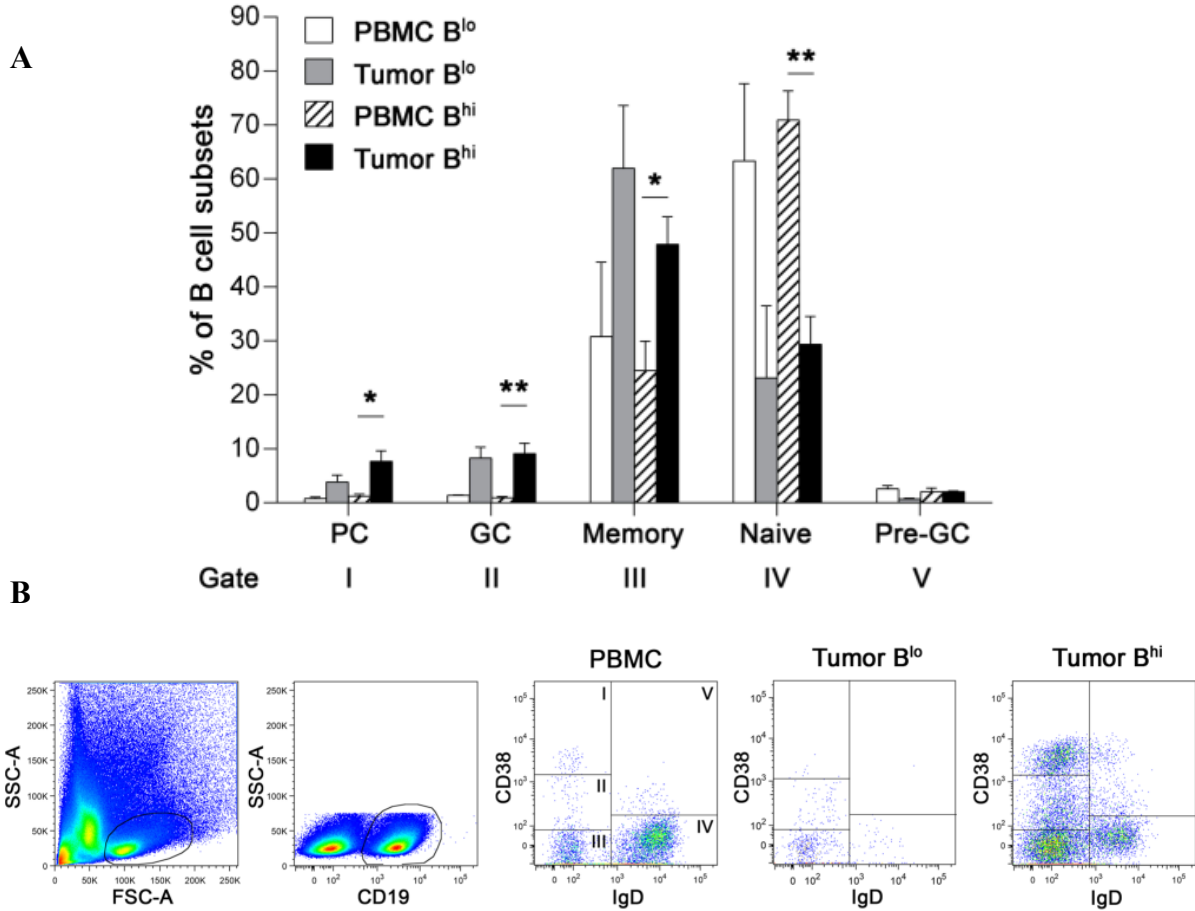


Figure 3: Relationship of CD20<sup>+</sup> B cell/CD8<sup>+</sup> T cell aggregates with HPV 16 E6/E7-specific CD8<sup>+</sup> T cells. (A) Columns show frequencies of patients with low (interactions detectable in 0 – 5 visual fields) and high (interactions detectable in > 5 visual fields) abundance of B cell/CD8<sup>+</sup> T cell interactions according to tumor-infiltrating HPV 16 E6/E7-specific CD8<sup>+</sup> T cells presence (B) Columns represent the mean (+ SEM) proportions of tumor-infiltrating HPV 16 E6/E7-specific CD8<sup>+</sup> T cells with respect to the B cell/CD8<sup>+</sup> T cell interactions in the tumor nests. (C) Columns represent the mean (+ SEM) densities of CD20<sup>+</sup> B cells, CD8<sup>+</sup> T cells and DC-LAMP<sup>+</sup> dendritic cells in tumor nests and tumor stroma of patients with respect HPV16-specific T cells detection. \*  $p < 0.05$  (Pearson's chi-square test and Mann-Whitney U test).

- Phenotyping of tumor-infiltrating B cells in OPSCC patients samples

According to the significant prognostic value of tumor-infiltrating CD20<sup>+</sup> B cells and their interactions with CD8<sup>+</sup> T cells, we performed phenotypic analysis of the B cells from native tumor tissue samples. We divided CD19<sup>+</sup> TIL-Bs into 5 subtypes based on the expression of IgD and CD38 (Fig. 4B). The subtypes were defined as follows: IgD<sup>-</sup>CD38<sup>high</sup> plasma cells, IgD<sup>-</sup>CD38<sup>intermediate</sup> germinal center B cells, IgD<sup>-</sup>CD38<sup>-</sup> memory B cells, IgD<sup>+</sup>CD38<sup>-</sup> naive B cells and IgD<sup>+</sup>CD38<sup>+</sup> pre-germinal center B cells. The samples were also separated into two groups based on the B cell proportions, B<sup>lo</sup> vs. B<sup>hi</sup>, to evaluate the difference between immunologically “hot“ and “cold“ tumors. B<sup>lo</sup> samples had less than 0,5% of B cells of total cell count (B<sup>lo</sup>: mean = 0.11 ± 0.05%; B<sup>hi</sup>: mean = 4.22 ± 5.96%). There was no difference in proportions of B cell subpopulations between the B<sup>lo</sup> and B<sup>hi</sup> tumor samples (Fig. 4A). The main subtype found in the samples were the memory B cells.

**Figure 4**

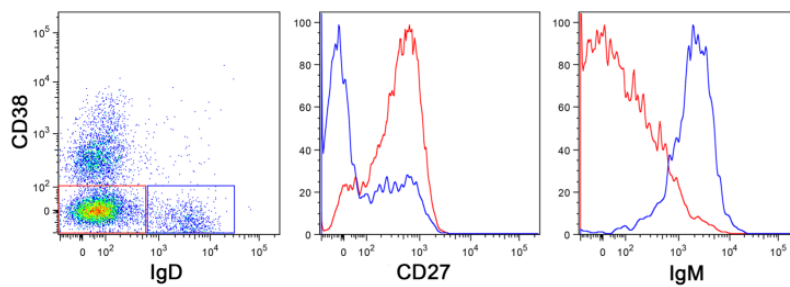


*Figure 4. Flow cytometric analysis of TIL-Bs and PBMCs-derived B cells divided in  $B^{lo}$  and  $B^{hi}$  samples. (A) Mean (+ SEM) frequency of B cell subpopulations among total  $CD19^+$  cells. (A) Gating strategy and results in representative dot plots of the selected tissues.  $IgD^-CD38^{++}$ , plasma cells;  $IgD^-CD38^+$ , germinal center B cells;  $IgD^-CD38^-$ , memory B cells;  $IgD^+CD38^-$ , naive B cells;  $IgD^+CD38^+$ , pre-germinal center B cells. \*  $p < 0.05$*

Further, we assessed expression of CD27 and IgM on tumor infiltrating memory B cells. The high expression of CD27 and low expression of IgM together with the absence of IgD in both  $B^{lo}$  and  $B^{hi}$  samples signifies classical memory, predominantly class-switched, phenotype (Fig. 5A). Moreover, we observed a significant difference in the expression of proliferation marker Ki67, that was markedly higher in  $B^{hi}$  compared to  $B^{lo}$  samples (Fig. 5B).

**Figure 5**

**A**



**B**

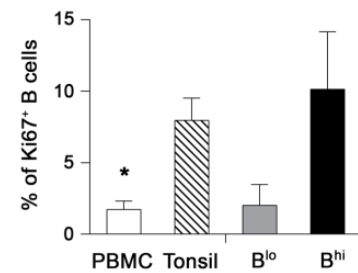


*Figure 5. (A) Dot plot show TIL-B expression of CD38 and IgD. The histograms compare IgD low (red line) and IgD high (blue line) subpopulations in respect to CD27 and IgM expression. (B) Columns represent proportions of Ki67 positive B cells in B<sup>lo</sup> and B<sup>hi</sup> OPSCC and control tissues. \*  $p < 0.05$*

- **Detection of Bregs in OPSCC**

Specific subpopulations of B cells were reported to have also immunosuppressive functions. Currently the only reliable marker Bregs are characterized with is the production of IL-10. In order to estimate proportions of Bregs in our samples (Cohort 3, see Materials and Methods section) we stimulated tumor-derived cells suspensions for 5 and 24h with CpG ODN 2006, CD40L, PMA and ionomycin, with addition of brefeldin A. The IL-10 production was assessed using flow cytometer. Tumor tissue samples were also compared to matched blood-derived PBMCs and control healthy tonsillar tissue. After 5h of stimulation we found higher proportions of Bregs in tumor tissue than in matched peripheral-blood derived B cells and control tonsils ( $0.98 \pm 0.78\%$  vs.  $0.46 \pm 0.12\%$  vs.  $0.41 \pm 0.09$ , respectively). After 24h stimulation the differences changed and we observed significantly lower proportions of Bregs in tumor tissue compared to matched-blood B cells, and similar numbers compared to healthy tonsillar tissue ( $2.74 \pm 0.53\%$  vs.  $8.01 \pm 1.75\%$  vs.  $2.16 \pm 1.51\%$ , respectively;  $p = 0.039$ ). Breg progenitors were reported to be able to develop into IL-10 producing Bregs when undergoing long TLR activation, which means we probably detected both Bregs and Breg progenitors after 24 h of *in vitro* cultivation. In addition to the phenotype of Bregs, the IL-10 producing Bregs were mainly CD5<sup>+</sup>CD24<sup>high</sup>. Because of the limited cell count in B<sup>lo</sup> samples, the experiments were performed only with B<sup>hi</sup> tumors.

- Potential antigen-presenting role of the tumor-infiltrating B cells

TIL-Bs are known to have capabilities of antigen presenting cells. In view of these observations we evaluated expression of costimulatory molecules on TIL-Bs that might elucidate the importance of B cell/CD8<sup>+</sup> T cell interactions. The expression levels of CD40, CD86, HLA-ABC and HLA-DR were significantly higher in TIL-Bs derived from B<sup>hi</sup> OPSCC samples compared to B<sup>lo</sup> samples. Moreover, there were significantly higher levels of CD40, CD86 and HLA-DR in TIL-Bs of B<sup>hi</sup> tumors, but not from B<sup>lo</sup> samples, compared to matched PBMCs-derived B cells.

**Figure 6**

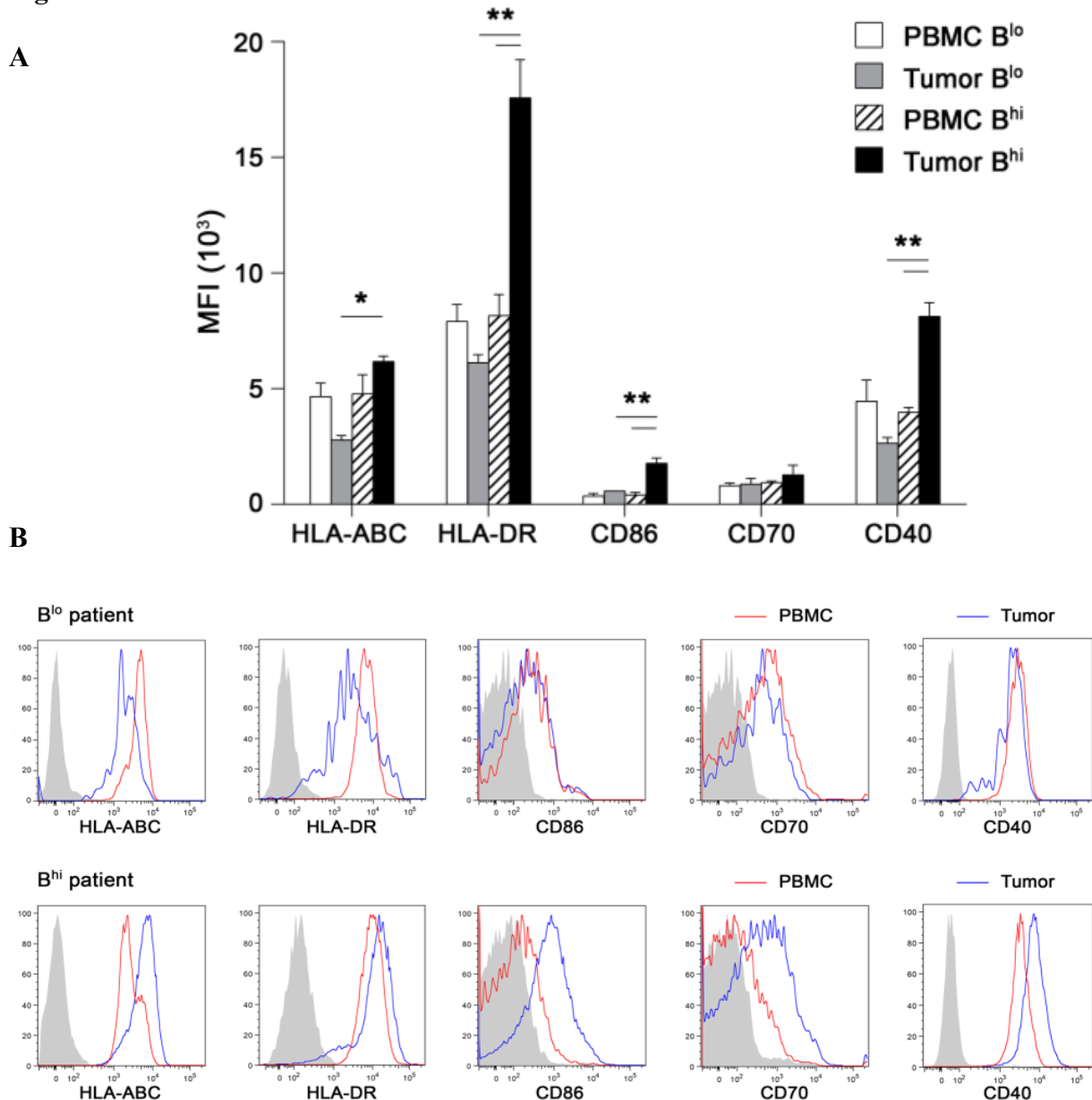


Figure 6. Columns represent mean (+ SEM) of the mean fluorescence intensity (MFI) of selected B cell surface markers associated with antigen-presentation evaluated on total CD19<sup>+</sup> B cells. (B) Histograms of a representative expression of B cell surface markers in B<sup>lo</sup> (upper line) and B<sup>hi</sup> (lower line) patient. Gray-filled areas show isotype-matched controls, red line represents peripheral blood B cells and blue line represents TIL-Bs of the same patient

- Expression of IL-2 and costimulatory molecules in HNSCC samples according to B cell infiltration, extracted from TCGA databases

To be able to assess a wide range of co-stimulatory molecules expressed in HNSCC samples, we used data from freely accessible TCGA databases. The expression was estimated in HNSCC B<sup>lo</sup> and B<sup>hi</sup> subgroups, selected according to the median expression of CD19. The B<sup>hi</sup> samples showed significantly higher expression of almost all the costimulatory molecules, except of BCL2L1, TNFSF9 and CD86 (Fig. 7).

Figure 7

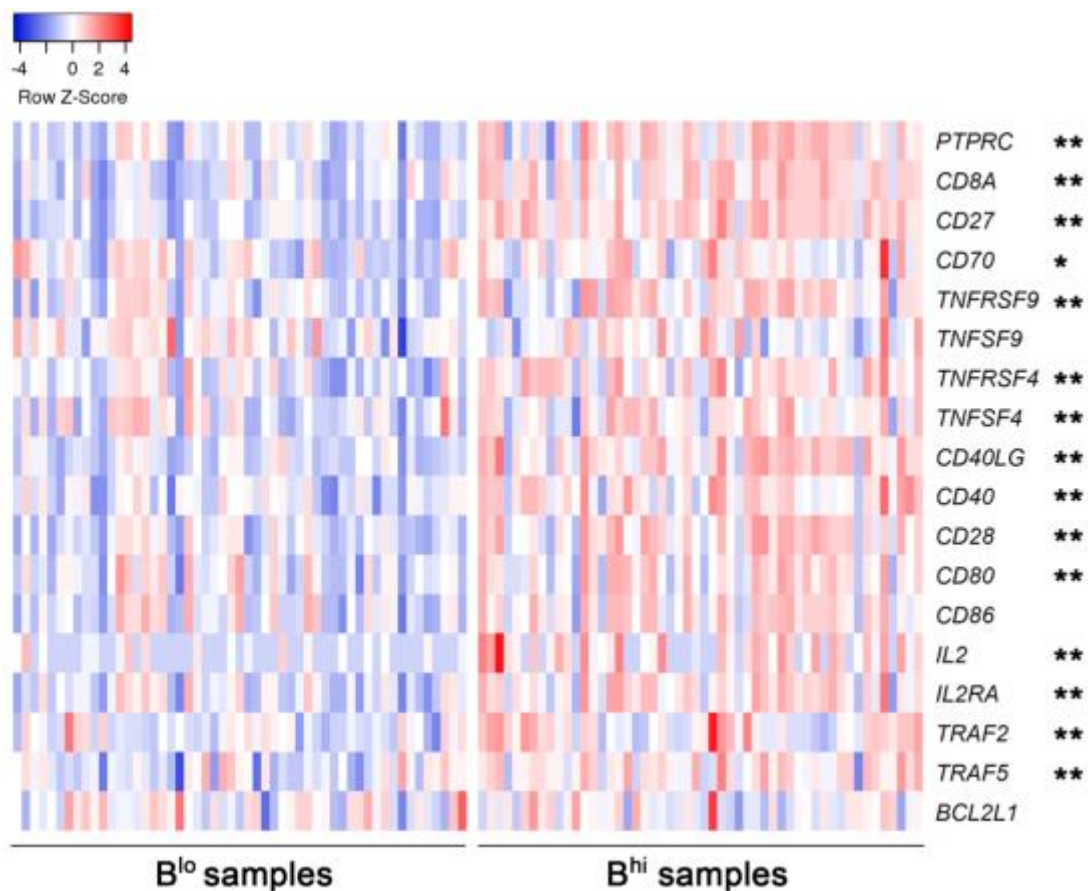


Figure 7. The heat-map expresses z-scores of relative mRNA expression of indicated genes within  $B^{lo}$  ( $n = 53$ ) and  $B^{hi}$  ( $n = 52$ ) samples extracted from TCGA databases.

- Evaluation of tumor-infiltrating B cell effect on tumor-infiltrating T cell survival

Besides the possible important antigen-presenting role of B cells that could partially explain the positive prognostic role of B cell/CD8<sup>+</sup> T cell interactions, we further examined the role of TIL-Bs on T cell survival and cytokine production. Therefore, we incubated the whole tumor-derived cell suspensions from  $B^{hi}$  samples and samples depleted from CD19<sup>+</sup> cells for 6 days. After that we assessed the viability and cytokine production of CD4<sup>+</sup> and CD8<sup>+</sup> T cells ( $n = 4$ ). The viability of both CD4<sup>+</sup> T cells and CD8<sup>+</sup> T cells was lower at day 6 in the depleted suspensions when compared to the whole, non-depleted samples ( $15.1 \pm 7.8\%$  vs.  $11.0 \pm 4.5\%$  for CD4<sup>+</sup> T cells;  $p = 0.068$  and  $22.4 \pm 10.6\%$  vs.  $14.4 \pm 8.4\%$  for CD8<sup>+</sup> T cells;  $p = 0.068$ ) (Fig. 8 A, B, C). However, we did not find any effect of B cell depletion on T cell functionality concerning production of IL-2 and IFN $\gamma$ .

Figure 8

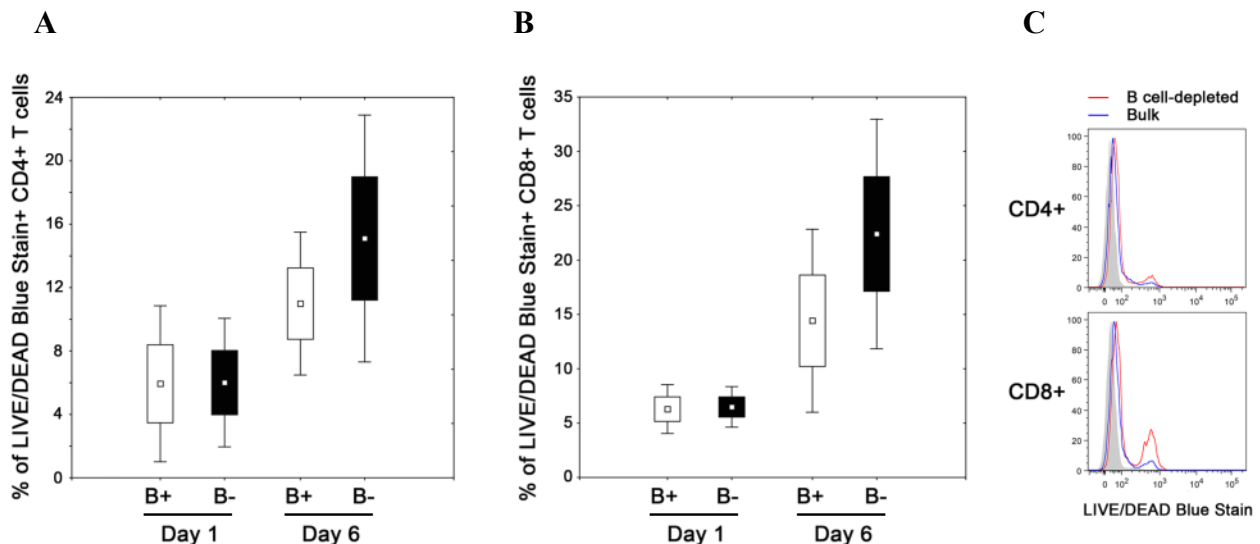


Figure 8. Proportions of dead cells in cultures of the whole and B cell-depleted tumor-derived single cell suspensions. (A, B) Graphs show the mean proportion of dead CD4<sup>+</sup> and CD8<sup>+</sup> T cells in whole (B+) and B cell-depleted (B-) tumor-derived cell suspension after 1 and 6 days

of cultivation. (C) Histograms of a representative patient show differences in the LIVE/DEAD Blue Stain positivity on day 6 of cultivation.

- Expression of IL-2, IL-2R, CD27, CD40L and BCL2L1 on CD8<sup>+</sup> TILs infiltrating B<sup>hi</sup> tumors

To explain the decreased survival of CD8<sup>+</sup> TILs in suspension depleted from B cells, we determined the expression of molecules that play important role in T cell stimulation, growth and apoptosis. We compared CD8<sup>+</sup> T cells from tumor tissue and peripheral blood of B<sup>hi</sup> and B<sup>lo</sup> OPSCC patients. Our results show significantly higher levels of IL-2 and IL-2R in tumor-derived CD8<sup>+</sup> T cells in comparison to peripheral blood samples (Fig. 9).

**Figure 9**

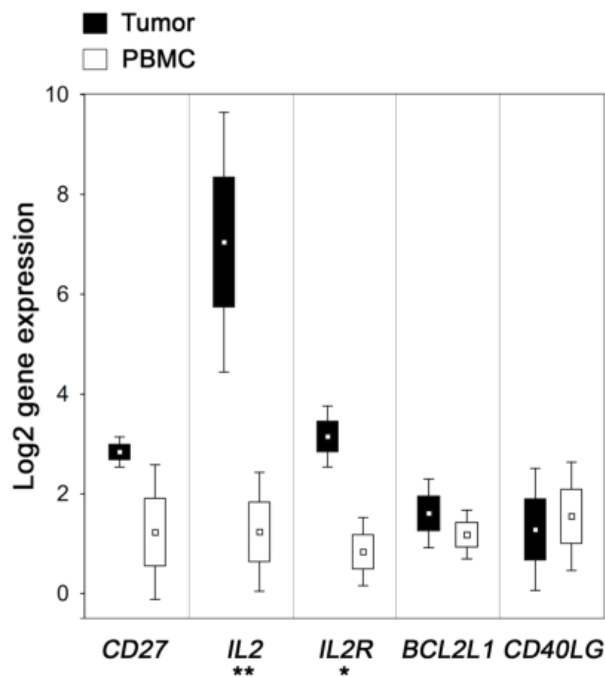


Figure 9. Box plots show the mean expression of selected genes in tumor tissues and matched PBMCs of B<sup>hi</sup> OPSCC patients (n = 4). Whiskers indicate the SD. The boundaries of the box indicate SEM and the squares in the box represent the mean.

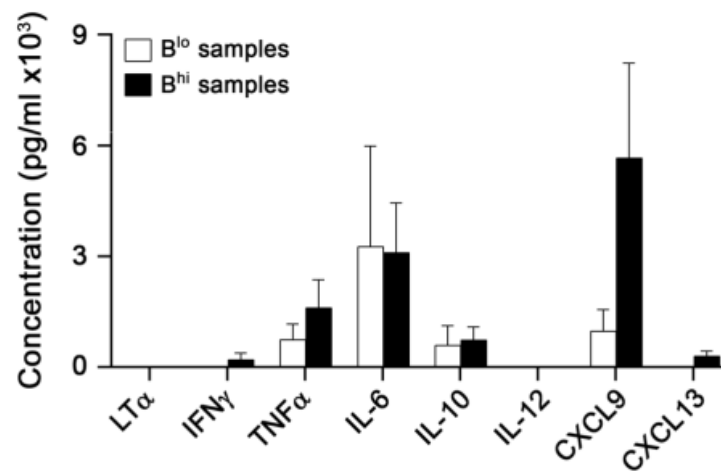
- B cell cytokine production in the tumor microenvironment

To evaluate the selective contribution of TIL-Bs to cytokine and chemokine environment of OPSCC that could be one of the reasons for better T cell survival, we compared the spontaneous cytokine and chemokine production in B<sup>lo</sup> samples, B<sup>hi</sup> samples and B<sup>hi</sup> samples magnetically

depleted of CD19<sup>+</sup> cells. The only significant difference was found in the production of CXCL9 that was much higher in B<sup>hi</sup> samples and correspondingly markedly lower in CD19-depleted suspensions, compared to non-depleted ones ( $579.6 \pm 262.9$  vs.  $1238.8 \pm 290.6$  pg/ml, respectively;  $p = 0.025$ ) (Fig. 10 A, B). CXCL9 was reported to play an important role in T cell chemoattraction and our result suggests that TIL-Bs might be the important source of this chemokine in OPSCC.

**Figure 10**

**A**



**B**

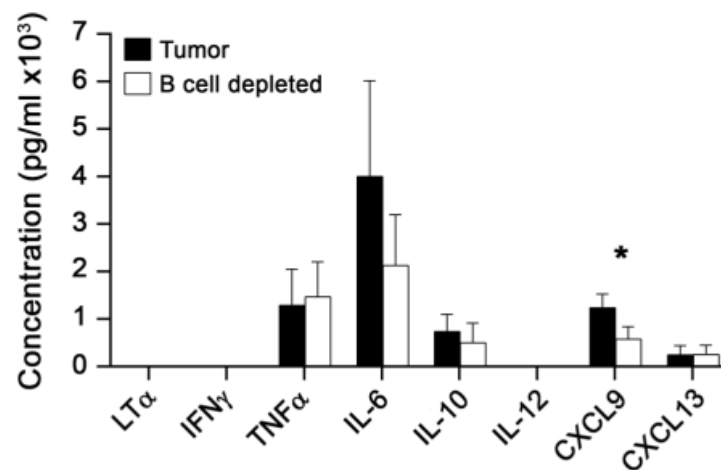


*Figure 10. Columns show mean (+SEM) spontaneous cytokine/chemokine production in cell culture supernatants of B<sup>lo</sup> and B<sup>hi</sup> samples (A) and a difference between B<sup>hi</sup> samples and B<sup>hi</sup> samples depleted from CD19<sup>+</sup> cells. \*  $p < 0.05$*

### 4.3 Study of tumor-infiltrating plasmacytoid dendritic cells in head and neck cancer

#### (Study 3)

(modified from Koucký et al. 2021)

#### Overview

In this study we analyzed phenotype and functional capacity of pDCs infiltrating HNSCC with respect to HPV status of the tumor, using native tumor tissue. We found similar proportions of pDCs in HPV<sup>+</sup> and HPV<sup>-</sup> tumors; however, the pDCs in HPV<sup>+</sup> tumors were able to produce higher amounts of IFN $\alpha$  in response to TLR7 and TLR9 stimulation. Further, we identified different composition of cytokine environment as the main factor affecting pDC functional capacity. Specifically, high levels of IL-10 and TNF $\alpha$  in culture supernatants derived from HPV<sup>-</sup> tumor cell suspensions were shown to suppress the IFN $\alpha$  production in pDCs. Moreover, proportions of pDCs in the tumor tissue of HPV<sup>-</sup>, but not HPV<sup>+</sup> tumors, correlated to Tregs proportions. Indeed, pDCs were shown to be able to induce Tregs under the influence of the TME. The detailed results are described below.

- Proportions of tumor-infiltrating pDCs in HPV<sup>-</sup> and HPV<sup>+</sup> HNSCC

We prepared single cell suspensions from 32 samples of HPV<sup>+</sup> HNSCC, 44 samples of HPV<sup>-</sup> HNSCC, 9 samples of healthy tonsils and 6 samples of macroscopically cancer-free peritumoral mucosa. Using flow cytometric analysis we identified pDCs as CD45<sup>+</sup>Lin<sup>-</sup>CD4<sup>+</sup>CD123<sup>+</sup>BDCA-2<sup>+</sup> cells (Fig. 1C). The proportions of pDCs in HPV<sup>+</sup> and HPV<sup>-</sup> HNSCC were similar when gated on both total cells (0.13 $\pm$ 0.23% and 0.11 $\pm$ 0.14%, respectively) and CD45<sup>+</sup> cells (0.19 $\pm$ 0.26% and 0.24 $\pm$ 0.26% ) (Fig. 1A). The proportions of tumor-infiltrating pDCs did not differ from peritumoral mucosa and healthy palatine tonsil tissue and we did not find any correlation to clinical and histo-pathological characteristics of the patients.

**Figure 1**

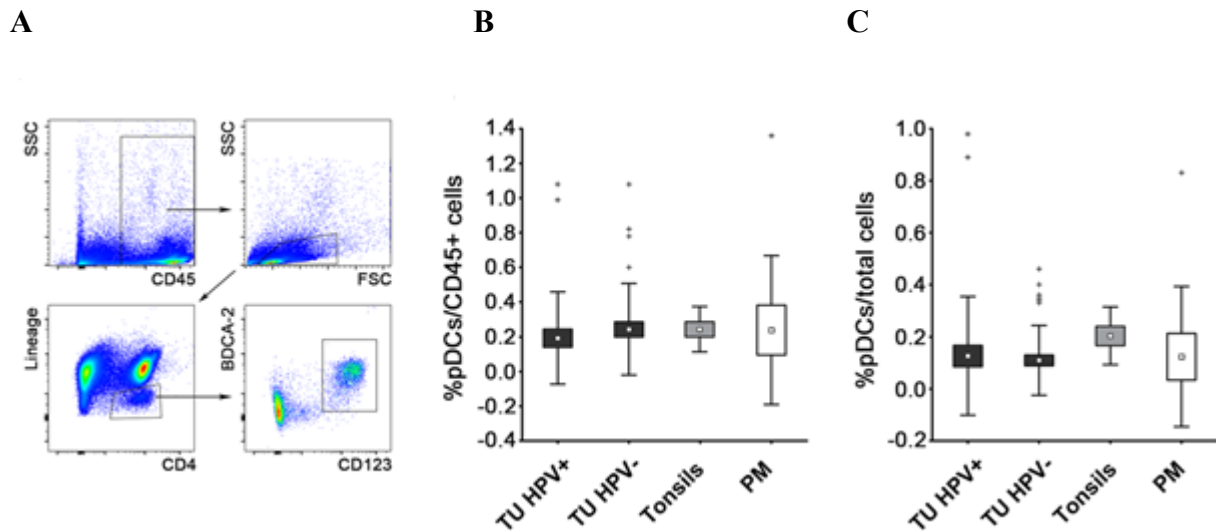


*Figure 1. Flow cytometric analysis of pDC proportions in native tumor tissue of HPV<sup>+</sup> HNSCC samples (n=32), HPV<sup>-</sup> HNSCC samples (n=44), aged-matched tonsils from healthy donors (n=9), and macroscopically tumor-free peritumoral mucosa (PM, n=9). (A) Dot plots show the gating strategy in a representative HPV<sup>+</sup> tumor sample. Box-plots show pDC proportions when gated on CD45<sup>+</sup> cells (B) and total cells (C).*

- Different responsiveness between pDCs infiltrating HPV<sup>+</sup> or HPV<sup>-</sup> tumors upon stimulation by TLR7 and TLR9 agonists

Plasmacytoid DCs are the main producers of IFN $\alpha$  in the human body. Therefore, IFN $\alpha$  production is widely used as a marker of pDC functional capabilities. We assessed the pDC capacity to produce IFN $\alpha$  by stimulation of the whole tumor-derived cells suspension by TLR7 agonist, imiquimod, and TLR 9 agonist, CpG ODN 2216. We determined both the proportion of IFN $\alpha$  -producing pDCs with flow cytometer and the level of IFN $\alpha$  in cell culture supernatants using ELISA and Luminex. Based on the MFI, pDCs derived from HPV<sup>+</sup> tumors showed significantly higher IFN $\alpha$  production upon CpG stimulation ( $4137\pm 3346$  vs.  $7879\pm 4272$  for HPV<sup>-</sup> and HPV<sup>+</sup> samples, respectively) (Fig. 2B), albeit the proportions of IFN $\alpha$ -producing cells were similar ( $3.2\pm 5.4$  vs.  $3.0\pm 3.1\%$ ) (Fig. 2A). We confirmed the result by comparison of IFN $\alpha$  levels in tumor-derived cell culture supernatants after stimulation by CpG. Again, the levels of IFN $\alpha$  were significantly higher in HPV<sup>+</sup> samples ( $240.7\pm 380.8$  pg/ml for HPV<sup>-</sup> cultures vs.  $971.8\pm 1461$  pg/ml for HPV<sup>+</sup> cultures) (Fig. 2C). Moreover, we did not see any suppression of IFN $\alpha$  production in HPV<sup>+</sup> tumor samples compared to healthy tonsils ( $893\pm 1431$

pg/ml). We observed the similar trend upon imiquimod stimulation, nevertheless, the result did not reach statistical significance. The corresponding flow cytometry analysis did not identify any other cell population in our tumor derived cell suspensions that would produce IFN $\alpha$  upon chosen TLR stimulation, thus, we assume that pDCs are the only source of IFN $\alpha$  in our cell cultures. Additionally, when we compared survival of the HPV<sup>+</sup> patients according to the IFN $\alpha$  levels in cell culture supernatants, we found lower amounts of IFN $\alpha$  in samples from patients that deceased (Fig. 2D).

**Figure 2**

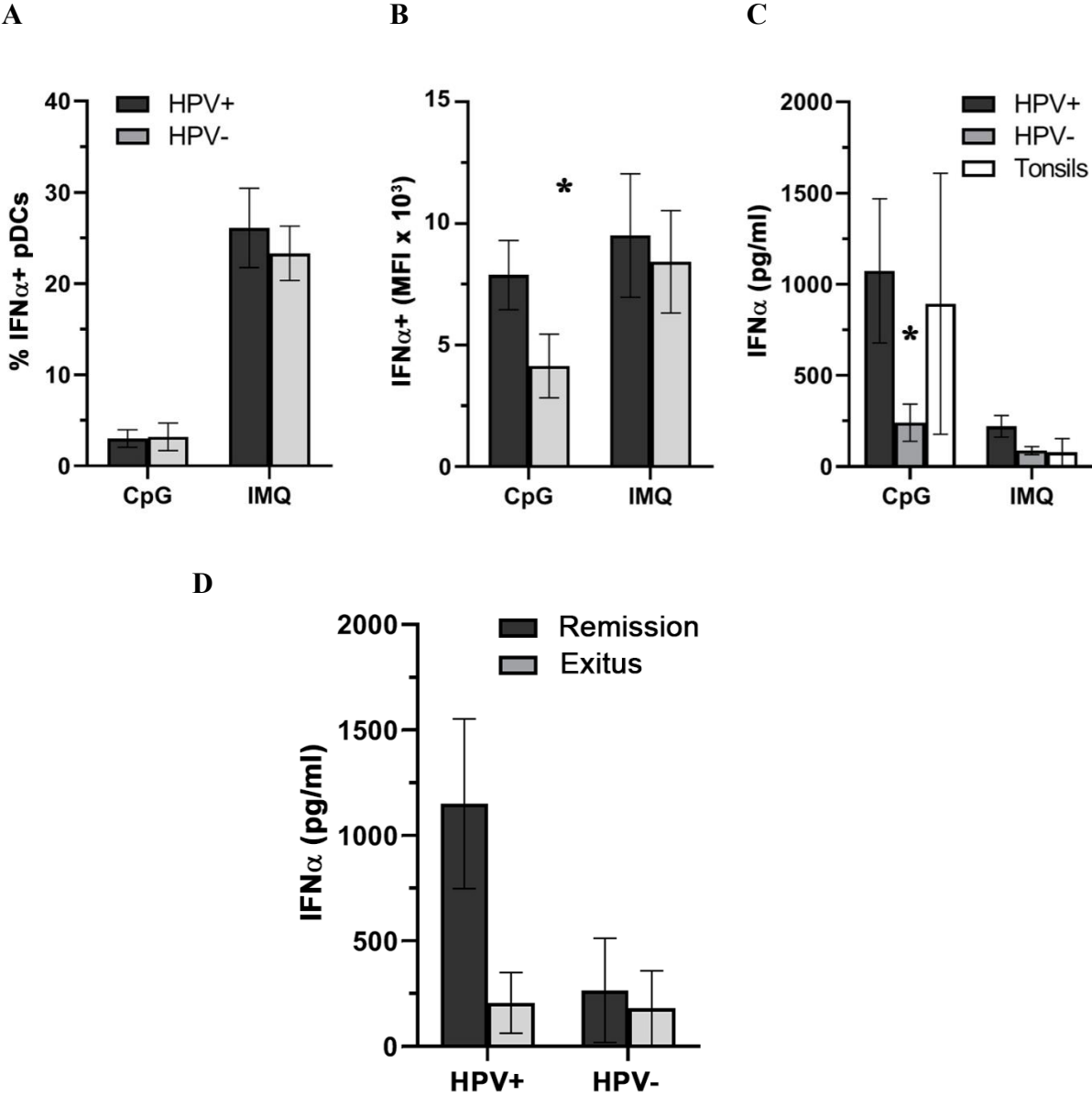


Figure 2. (A) Columns show the mean proportions of tumor-infiltrating pDCs producing IFN $\alpha$  upon stimulation with CpG ODN 2216 (CpG; 20  $\mu$ g/ml, 5 h) or imiquimod (IMQ; 5  $\mu$ g/ml, 5 h). (B) Graph shows the MFI of IFN $\alpha$ -producing pDCs upon stimulation with CpG or IMQ. (C) Columns represent the mean concentration of IFN $\alpha$  in cell culture supernatants derived from tumor tissue after 24 h stimulation with CpG or IMQ. Error bars indicate SEM. (D) Columns represent differences in CpG-induced IFN $\alpha$  production in supernatants obtained from HPV $^{+}$  and HPV $^{-}$  tumor samples according to the overall survival of patients.

- Expression profile of tumor-infiltrating pDCs in HNSCC

To find possible explanation of different functional capacity of pDCs in HNSCC subtypes, we evaluated expression levels of molecules that were reported to be involved in modulation of IFN $\alpha$  production by pDCs. Specifically, we assessed the expression of TLR7, TLR9, CD28, NKp44, Granzyme B, IDO, TIM-3 and TRAIL. Nevertheless, only NKp44 expression showed significant difference between HPV $^{+}$  and HPV $^{-}$  tumor-infiltrating pDCs. Crosslinking of NKp44 was previously described to inhibit IFN $\alpha$  production by pDCs. Although we found significantly higher expression of NKp44 on pDCs derived from HPV $^{+}$  samples (22.9 $\pm$ 14% vs. 16.2 $\pm$ 11.4%) (Fig. 3A), the proportion of cytokine producing cells were similar both in NKp44 $^{+}$  and NKp44 $^{-}$  pDCs (26.9% and 25.1%, respectively) (Fig. 3B). The proportions of active cells in relation to NKp44 expression were also similar when grouped on HPV $^{+}$  and HPV $^{-}$  tumors (Fig. 3B).

**Figure 3**

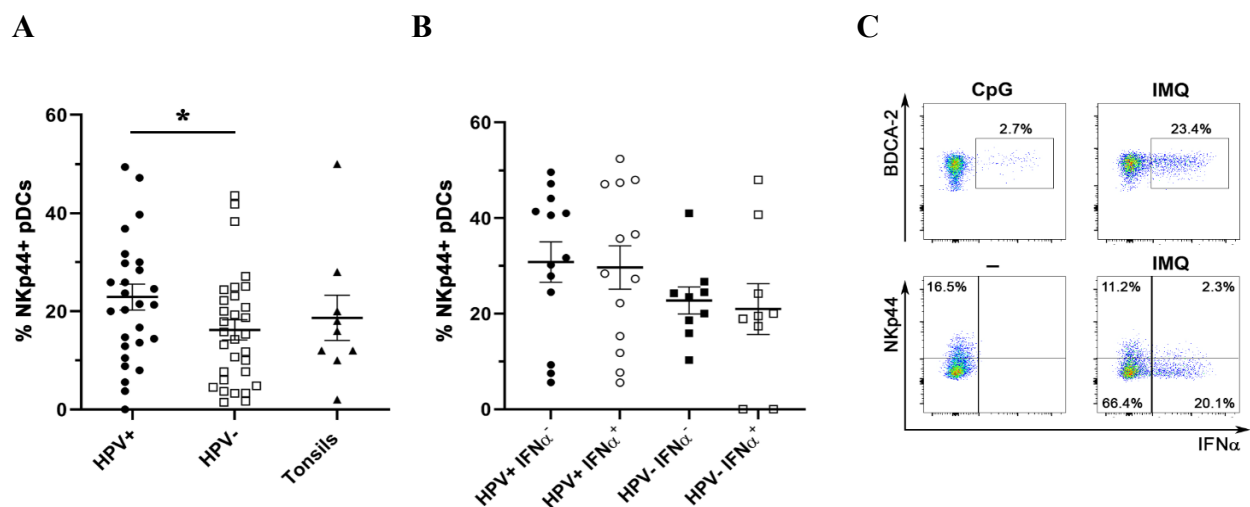


Figure 3. (A) Dot plot show proportions of NKp44 $^{+}$  pDCs derived from HPV $^{+}$  HNSCC (n=28), HPV $^{-}$  HNSCC (n=31) and aged-matched control tonsils (n=9) (B) Dot plot showing

proportions of IMQ-stimulated IFN $\alpha$ <sup>+</sup> pDCs derived from HPV<sup>+</sup> HNSCC (n=13) and HPV<sup>-</sup> HNSCC (n=9) in relation to NKp44 expression. Each symbol represents a patient, the horizontal line represents the average, and error bars indicate SEM. (C) Gating of a representative patient showing the production of IFN $\alpha$  and expression of NKp44.

- Effect of HNSCC-derived supernatants on healthy donor blood-derived pDCs

To clarify the differences in IFN $\alpha$  production by pDCs in HPV<sup>+</sup> and HPV<sup>-</sup> tumors, we focused on the evaluation of the cytokine environment in these tumor groups. We isolated pDCs from blood of 4 healthy donors and incubated them with 12 HPV<sup>+</sup> and 12 HPV<sup>-</sup> HNSCC-derived cell culture supernatants. After 24h of culture, IFN $\alpha$  levels were significantly lower in samples incubated with HPV<sup>-</sup> tumor-derived cell culture supernatants compared to HPV<sup>+</sup> samples, suggesting important role of cytokine milieu in pDC activity (Fig. 4A). To identify the specific components in the cytokine environment responsible for the phenomenon, we assessed the levels of IFN $\gamma$ , TNF $\alpha$ , IL-3, IL-4, IL-6, IL-10, IL-12, IL-17A and HMGB1 in culture supernatants of both HPV<sup>+</sup> and HPV<sup>-</sup> samples. The amounts of IL-6, IL-10 and TNF $\alpha$  were significantly higher in HPV<sup>-</sup> tumor-derived cell culture supernatants in comparison to HPV<sup>+</sup> samples (Fig. 4B).

**Figure 4**

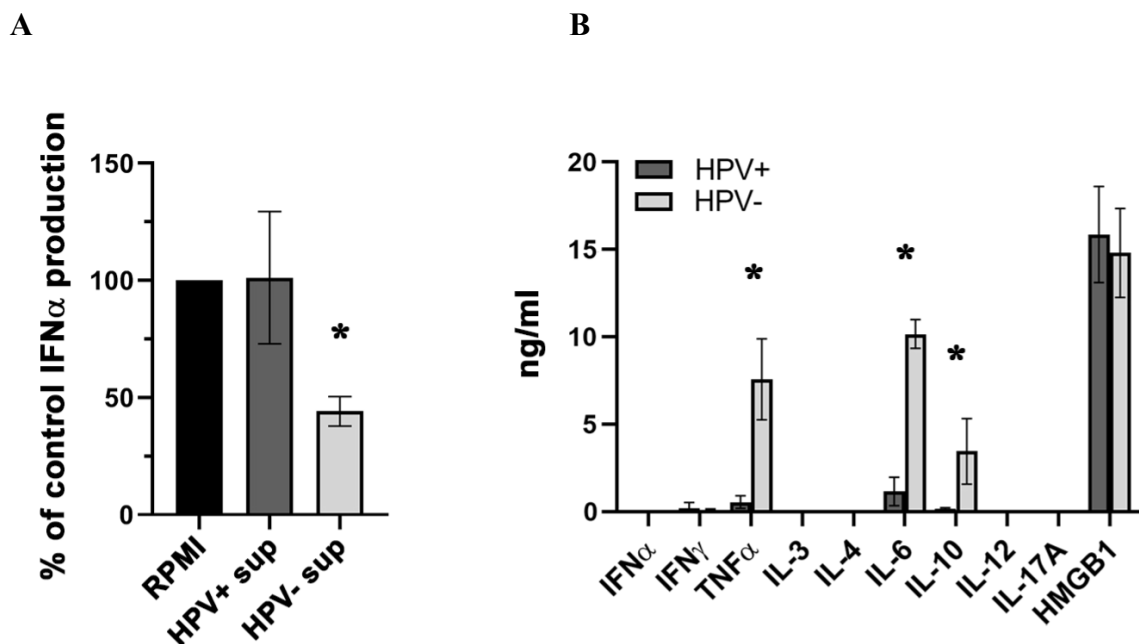


Figure 4. (A) pDCs were isolated from PBMCs of healthy donors (n=4) and incubated in the presence of both tumor supernatants (n=18) and CpG ODN 2216 (5 µg/ml). The used reference value is the production of IFN $\alpha$  upon CpG stimulation in complete RPMI medium only and was evaluated for each donor individually. Columns show the mean proportion of the reference production of IFN $\alpha$  ( $\pm$  SEM). (B) Columns show differences in amounts of selected cytokines analyzed in highly suppressive (>50%) HPV $^{-}$  derived supernatants (n = 5) and supernatants from non-suppressive HPV $^{+}$  samples (n = 5).

In addition, we assessed the expression of IL-10, TNF $\alpha$  and TGF $\beta$  on mRNA level. These cytokines were reported to have the most significant inhibitory effect on IFN $\alpha$  production in pDCs. In concordance with cell culture supernatant analysis, the relative mRNA expression of TNF $\alpha$  was significantly higher in HPV $^{-}$  samples. However, we found no difference in the expression levels of TGF $\beta$  between HPV $^{-}$  and HPV $^{+}$  cell suspensions (Fig. 5).

**Figure 5**

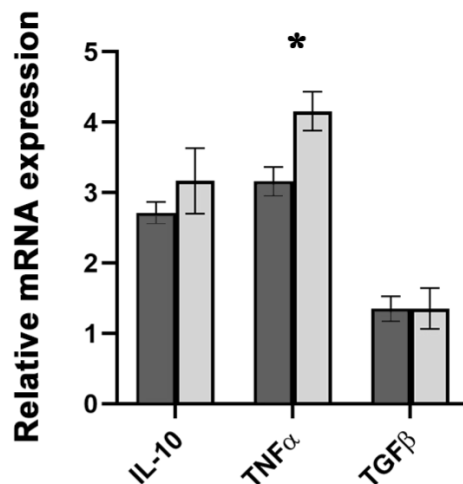


Figure 5. Columns show the mean ( $\pm$  SEM) relative mRNA expression of IL-10, TNF $\alpha$  and TGF $\beta$  in HPV $^{+}$  (n = 4) and HPV $^{-}$  (n = 6) HNSCC samples.

- Determination of the main inhibitors of IFN $\alpha$  production in the cytokine environment of HPV $^{-}$  HNSCC

After identification of the cytokines with significantly different levels in HPV $^{+}$  and HPV $^{-}$  supernatants, we tested the effect of IL-10, IL-6 and TNF $\alpha$  on healthy donor blood-derived pDCs. Recombinant cytokines were added to control blood-derived pDCs at concentrations

corresponding to the levels observed in the tumor derived supernatants and stimulated upon CpG ODN 2216. After 24h incubation, IFN $\alpha$  levels were analyzed. The strongest inhibitory effect was shown when all three cytokines were combined in one sample (Fig. 6).

**Figure 6**

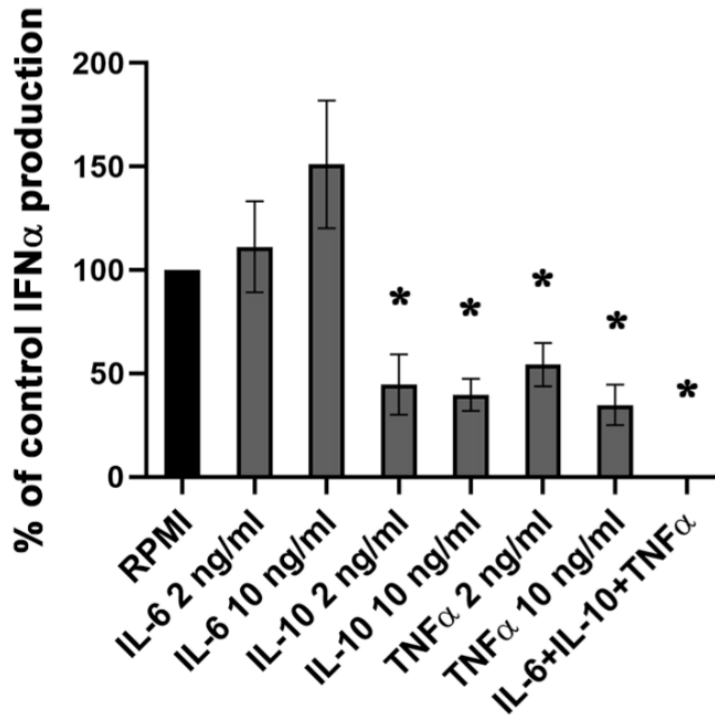
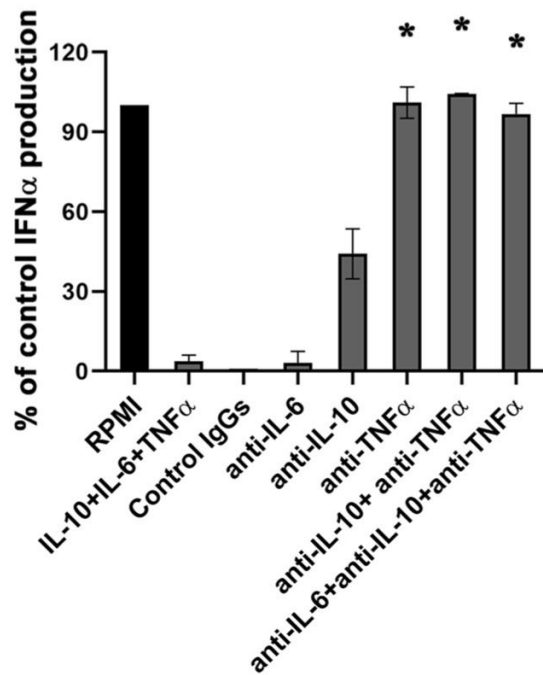


*Figure 6. Effect of the indicated recombinant cytokines on CpG ODN 2216-induced IFN $\alpha$  production in healthy control blood-derived pDCs. The reference value (100%) indicates the IFN $\alpha$  level after the addition of RPMI only. Columns represent the mean proportion of the reference production  $\pm$  SEM in three separate experiments performed with 8 different donors.*

For the confirmation of the observed inhibitory effect of IL10, TNF $\alpha$  and IL-6 we further co-cultivated healthy donor blood-derived pDCs with HPV<sup>-</sup> tumor-derived supernatants or IL6, IL-10 and TNF $\alpha$  with addition of corresponding neutralizing antibodies. The neutralization of TNF $\alpha$  restored pDC ability to produce IFN $\alpha$  to  $101 \pm 5.9\%$  in pDC cultures with recombinant cytokines and to  $82.8 \pm 13.5\%$  in pDC cultures with HPV<sup>-</sup> cell culture supernatants. Neutralization of IL-10 restored the IFN $\alpha$  production to  $44.2 \pm 9.4$  and  $47.3 \pm 19.9\%$ . We did not observe any synergistic effect after neutralization of more cytokines simultaneously (Fig. 7).

Figure 7

A



B

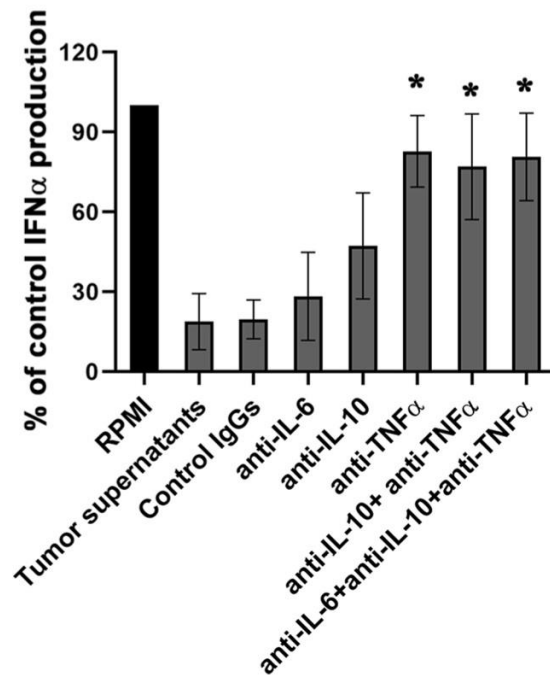


Figure 7. Columns show changes in IFN $\alpha$  production in pDC cultures with addition of recombinant IL-6, IL-10, TNF $\alpha$  according to the presence or absence of anti-IL-6, anti-IL-10 and anti-TNF $\alpha$  neutralizing antibodies (10  $\mu$ g/ml). (F) Columns show changes in IFN $\alpha$  production in pDC cultures with addition of HPV $^-$  derived cell culture supernatants according to the presence or absence of anti-IL-6, anti-IL-10 and anti-TNF $\alpha$  neutralizing antibodies (10  $\mu$ g/ml). \* $p$  < 0.05

- Identification of the IL-6, IL-10 and TNF $\alpha$ -producing cells in HPV $^-$  HNSCC samples

We evaluated expression of the cytokines identified as the main inhibitors of IFN $\alpha$  production by pDCs using immunohistochemistry staining of HNSCC HPV $^+$  and HPV $^-$  FFPE tissue sections (Fig. 8). Tumor cells seemed to be a very important source of the mentioned cytokines. IL-6, IL-10 and TNF $\alpha$  were detected in the tumor epithelium of 80%, 72.7% and 81.8% of HPV $^-$  samples, respectively. The proportions of HPV $^+$  samples expressing these cytokines in the tumor cells were markedly lower, namely 50%, 14.3% and 50%.

Figure 8

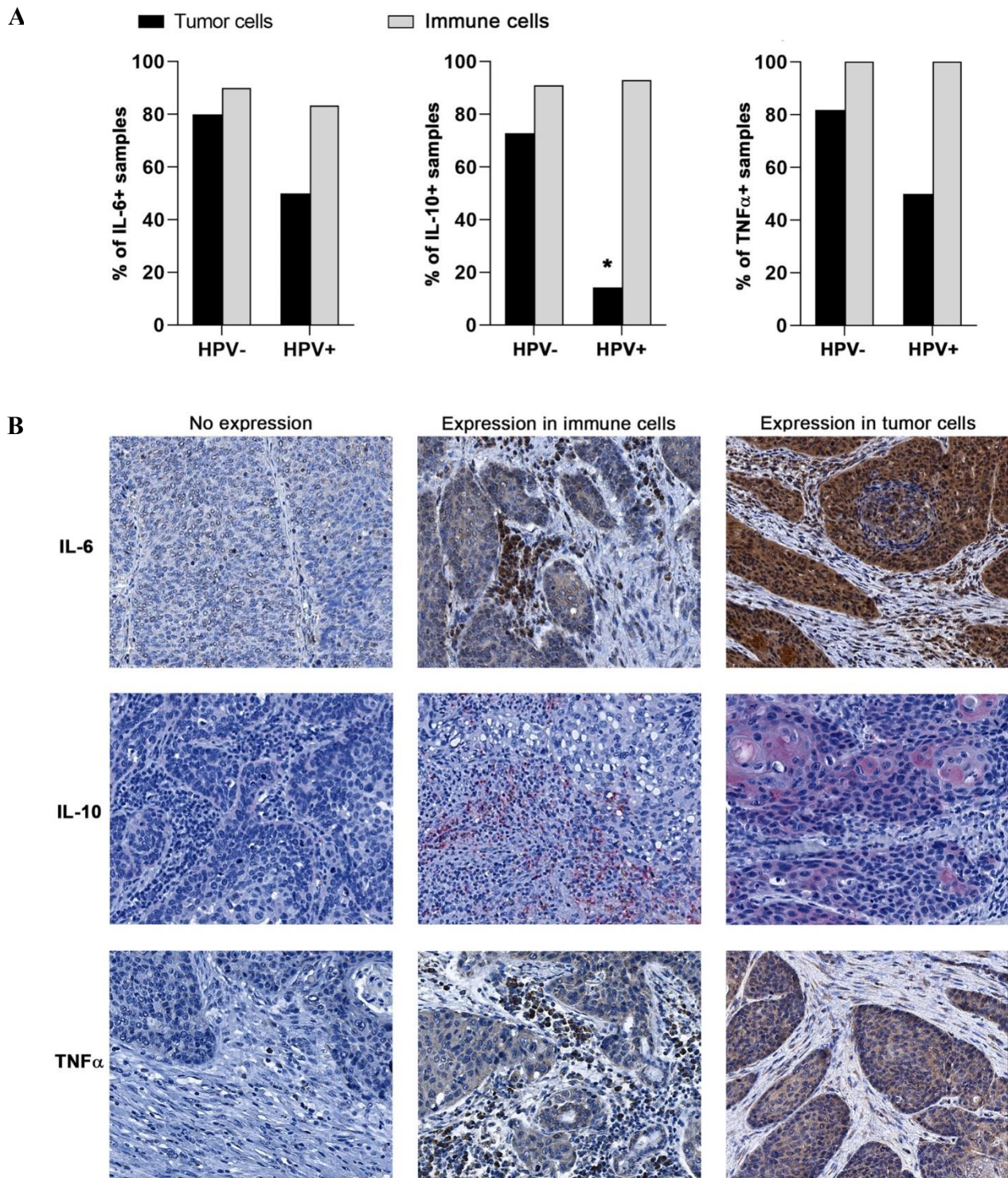
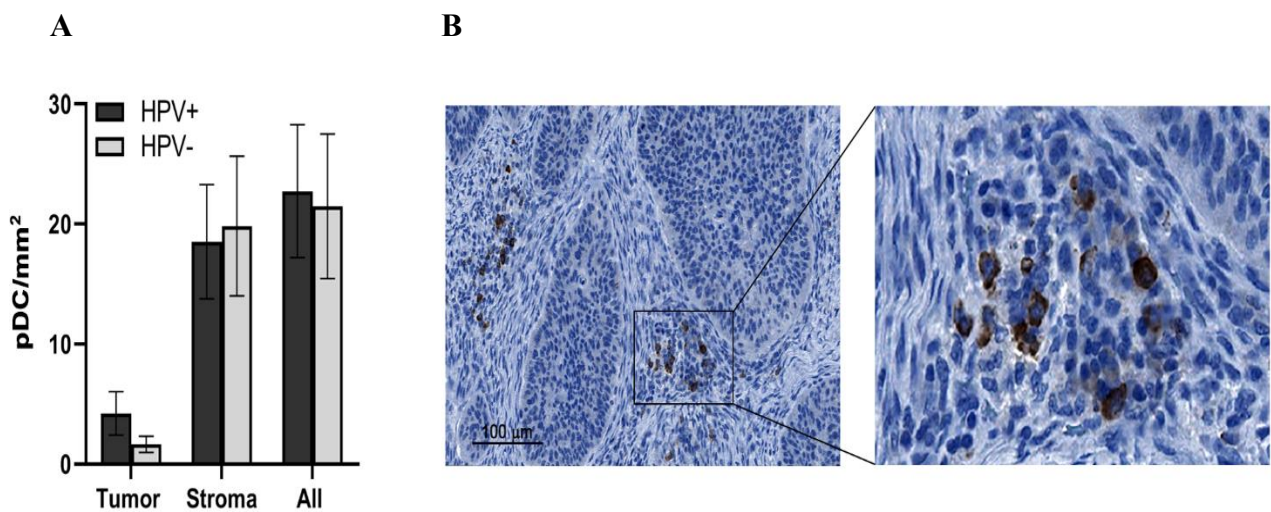


Figure 8. IL-6, IL-10 and TNF $\alpha$  production in tumor-infiltrating immune cells and tumor cells according to HPV status. (A) Columns show proportions of samples positively stained for IL-6, IL-10 or TNF $\alpha$  in immune and tumor cells. (B) Representative immunohistochemistry staining of IL-6, IL-10 and TNF $\alpha$ .

- Immunohistochemical analysis of pDC localization

Besides the analysis of pDC proportions in native tumor tissue we wanted to demonstrate tissue distribution of pDCs in HNSCC. We randomly selected 14 FFPE tissue sections of HPV<sup>+</sup> and 14 FFPE tissue section of HPV<sup>-</sup> patients and applied immunohistochemical staining using anti-BDCA-2 primary antibody. Concerning cell proportions, we confirmed our cytometric data, showing similar pDC counts in both HPV<sup>+</sup> and HPV<sup>-</sup> tumors (Fig. 9A). Moreover, we depicted that pDCs are preferentially localized in the tumor stroma in loose aggregates (Fig. 9B).

**Figure 9**



*Figure 9. (A) Columns show mean densities  $\pm$  SEM of pDCs in the tumor nests and stroma of HPV<sup>+</sup> and HPV<sup>-</sup> tumors. (B) Representative IHC staining of pDCs infiltrating HNSCC stroma using goat polyclonal anti-BDCA-2 antibody.*

- Co-localization and correlation of tumor-infiltrating Treg proportions with pDCs in HNSCC

Plasmacytoid DCs were many times reported as important inducers of Tregs that mediate their immunosuppressive effect. We optimized dual staining of BDCA-2<sup>+</sup> pDCs and FoxP3<sup>+</sup> Tregs and observed obvious colocalization of pDCs with Tregs in the tumor stroma, suggesting possible interactions between these immune cell groups. However, there was no statistically significant difference in Tregs proportions between HPV<sup>+</sup> and HPV<sup>-</sup> tumor samples (Fig. 10)

**Figure 10**

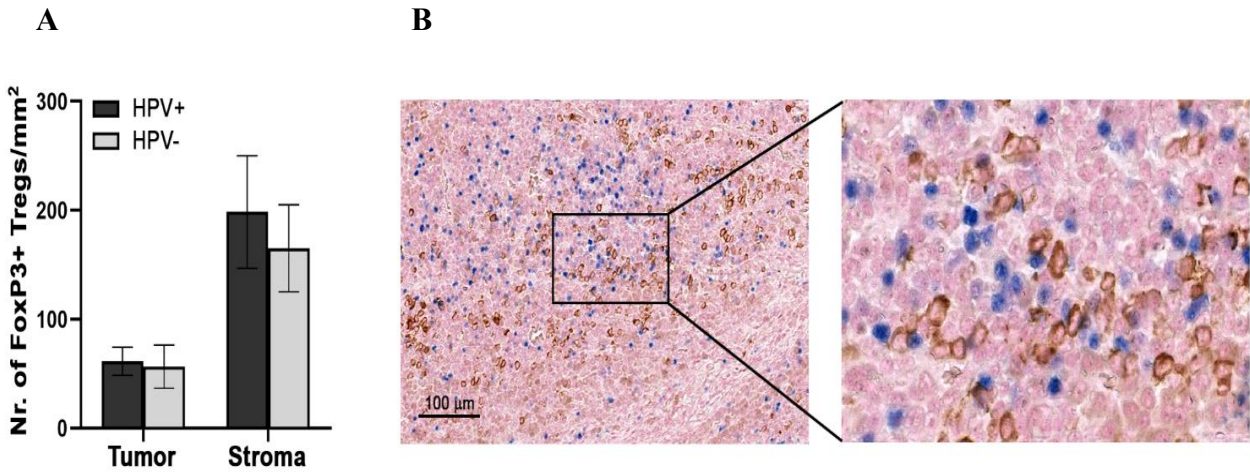


*Figure 10. (A) Columns represent the mean ( $\pm$  SEM) densities of FoxP3<sup>+</sup> cells in tumor nests and tumor stroma of immunohistochemically stained FFPE sections of HPV<sup>+</sup> (n=12) and HPV<sup>-</sup> (n=11) HNSCC. (B) Colocalization of FoxP3<sup>+</sup> Tregs (blue nuclei) and BDCA-2<sup>+</sup> pDCs (brown membranes) in the stroma of a representative HNSCC patient.*

To support the IHC results, we evaluated Tregs, defined as CD4<sup>+</sup>CD127<sup>-/lo</sup>CD25<sup>hi</sup>FoxP3<sup>+</sup>, in native tumor tissue samples using flow cytometer. Despite the same Treg proportions in HPV<sup>+</sup> and HPV<sup>-</sup> samples, corresponding to immunohistochemistry analysis, we demonstrated a strong positive correlation of pDCs and Treg proportions in HPV<sup>-</sup> tumor samples, but not in HPV<sup>+</sup> HNSCC (Fig. 11).

**Figure 11**

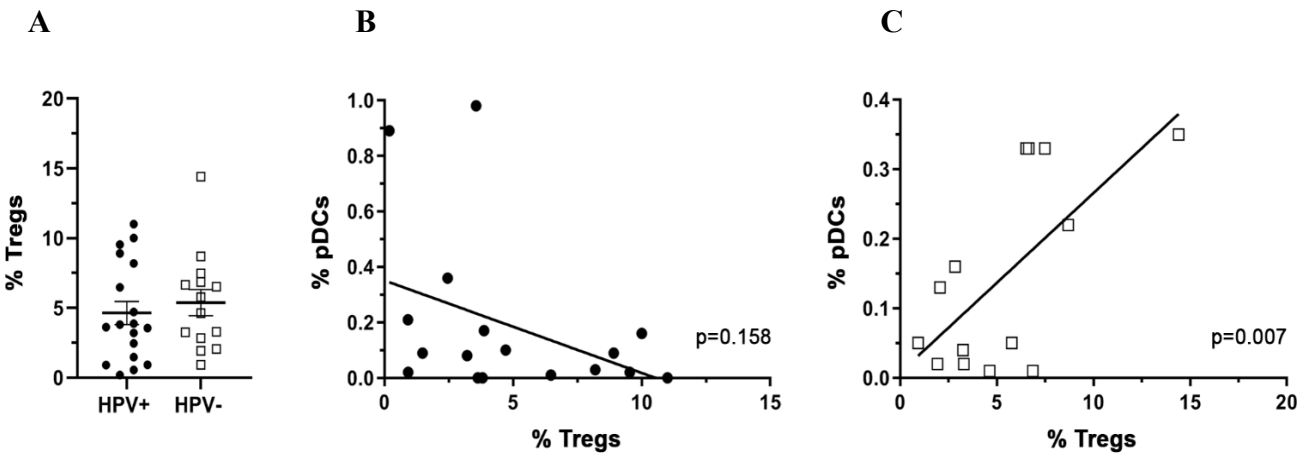


Figure 11. (C) Frequency of  $CD127^{lo}CD25^{hi}FoxP3^{+}CD4^{+}$  Tregs in  $HPV^{+}$  ( $n=18$ ) and  $HPV^{-}$  ( $n=14$ ) HNSCC patients using flow cytometry analysis. Each symbol represents a patient, the horizontal line represents the average, and error bars indicate SEM. (B, C) Correlation between Treg and pDC proportions in  $HPV^{+}$  (B) and  $HPV^{-}$  (C) HNSCC patients. Linear trendlines and  $p$  values are shown.

- Tumor-infiltrating pDC capability of Treg induction

Capability of pDCs to induce Treg expansion under the influence of HNSCC microenvironment was tested using cultivation of blood-derived pDCs from healthy donors with  $HPV^{+}$  and  $HPV^{-}$  HNSCC cell culture supernatants. Subsequently, supernatant-affected pDCs were co-cultured with magnetically separated blood-derived autologous  $CD4^{+}$  T cells. pDCs influenced by  $HPV^{-}$  HNSCC supernatants generated significantly higher numbers of Tregs compared to control pDCs and pDCs cultured with  $HPV^{+}$  HNSCC supernatants (Fig. 12).

**Figure 12**

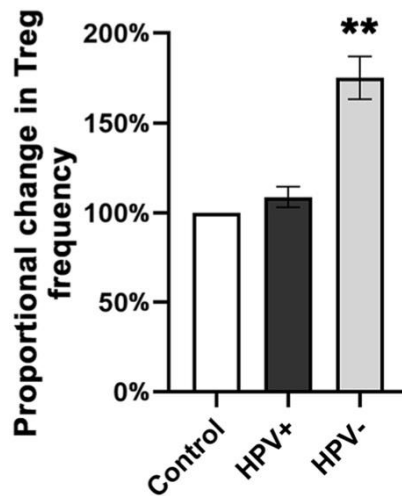


Figure 12. Columns show the average change in proportions of Tregs in pDC /  $CD4^{+}$  T cell co-cultures after cultivation of healthy donor pDCs with or without  $HPV^{+}$  ( $n = 7$ ; black column) and  $HPV^{-}$  ( $n = 7$ ; grey column) HNSCC-derived cell culture supernatants. Error bars represent SEM. \*\*  $p < 0.01$

## 5. Discussion

HNSCC is one of the major groups of malignant tumors affecting the global population. Current treatment protocols produce promising results in cases of limited disease; however, many patients are diagnosed in advanced stages with significantly decreased chances for complete recovery. Recently, modern immunotherapy was introduced for use in recurrent or metastatic HNSCC, with a reported response rate of 13–18% (Seiwert, 2016, Ferris, 2016, Bauml, 2017). The essential role of the immune response in the development and prognosis of malignant tumors was established and in-depth research of the TME may further improve the efficacy of tumor immunotherapy. HPV-induced HNSCCs especially have shown promising potential for application of immune-based treatments. This subgroup of HNSCCs has better prognosis and *in vitro* studies suggest that the immune response may be the decisive factor. Studies on the differences in composition of the TME and functional properties of immune elements between HPV<sup>-</sup> and HPV<sup>+</sup> HNSCCs may elucidate the key mechanisms of the anti-tumor immune response in HNSCC and possibly in other malignant tumors.

ICIs, the only approved immunotherapy in HNSCC, are a T cell-targeting treatment that unleashes the cytotoxic properties of effector T cells present in the TME. In Study 1, we showed that in 73.1% of HPV<sup>+</sup> OPSCC samples, CD8<sup>+</sup> T cells were able to react against HPV16 E6 and E7 by producing of IFN. In addition, CD8<sup>+</sup> T cells producing TNF $\alpha$  upon stimulation with HPV antigens were detected in 40% of samples. The results confirmed the findings of Heusinkveld et al. using larger sample cohort [Heusinkveld et al. 2012] . Similarly, Welters et al. detected HPV16-specific CD4<sup>+</sup> and CD8<sup>+</sup> T cells mostly producing IFN $\gamma$  and IL-17 in 64% of HPV-driven tumors [Welters et al. 2018]. Moreover, the authors reported a positive association between their abundance and lower stage and better overall patient survival, signifying the important role of the activated local immune response and potential for its artificial support [Welters et al. 2018]. We found that, upon stimulation with HPV oncoproteins, the IFN $\gamma$ -producing T cells were mostly PD-1<sup>+</sup> TIM-3<sup>-</sup> and PD-1<sup>-</sup> TIM3<sup>-</sup>, suggesting that TIM-3 is a better marker of T-cell exhaustion than PD-1 in OPSCC. Badoual et al. showed that an increased density of intratumoral T cells expressing PD-1 correlated with better prognosis, and PD-1 expression alone instead reflected a state of activation [Badoual et al. 2013]. To support this observation, the authors showed that expression of the activation markers HLA-DR and CD38 was higher in PD-1<sup>+</sup> T cells [Badoual et al. 2013]. Kim et al. also found prolonged OS in HNSCC patients with higher expression of PD-1 regardless of HPV positivity [Kim et al. 2016].

In line with our results, Fourcade et al. reported that TIM-3 expression on PD1<sup>+</sup> T cells represented marked the most dysfunctional subset in melanoma patients [Fourcade et al. 2010]. Moreover, Sakuishi et al. showed in the CT26 mouse model that a combined blockade of PD-1 and TIM-3 restored control of tumor growth [Sakuishi et al. 2010]. Shayan et al. reported a similar finding in an HPV<sup>+</sup> HNSCC mouse model [Shayan et al. 2017]. Therefore, we tested dynamic changes in TIM-3 expression and IFN $\gamma$  production in TILs following anti-PD-1 treatment with nivolumab. Consistent with previous reports, we observed a significant increase in the proportion of IFN $\gamma$ -producing T cells following blockade of both PD-1 and TIM-3 pathways compared with single-agent treatment. However, we did not register complementary TIM-3 overexpression in TILs expanded *ex vivo* following addition of nivolumab, a mechanism of adaptive resistance that was proposed by Shayan et al. We performed the experiments with freshly isolated TILs from HNSCCs and observed the expected overexpression of TIM-3, indicating that homeostatic expansion of TILs changed the dynamics of immune checkpoint molecule expression. Phenotyping the expanded TILs revealed a shift from the prevailing PD-1<sup>+</sup> Tim-3<sup>-</sup> subset to PD-1<sup>+</sup> Tim-3<sup>+</sup> and PD-1<sup>-</sup> Tim-3<sup>+</sup> subsets. This change was more evident in cultures derived from HPV<sup>-</sup> samples than from HPV<sup>+</sup> samples. To determine whether this finding was specific to OPSCC samples, we evaluated samples of cervical cancer, another HPV-induced malignancy. In the cervical cancer cells, we did not observe an increase in TIM-3<sup>+</sup> cells or decrease of PD-1<sup>+</sup> cells in the CD8<sup>+</sup> population. In the control PBMCs isolated from healthy donors, we observed an increase in both the PD-1<sup>-</sup> and TIM-3-expressing populations; however, this increase was more pronounced in the CD4<sup>+</sup> cells. Our results suggest that there is no generally applicable impact of homeostatic expansion of high levels of IL-2 on the expression of immune checkpoint molecules.

Importantly, the phenomenon of TIM-3 overexpression on fresh (non-expanded) TILs was markedly lower in cells that underwent stimulation by the HPV16 oncoproteins E6 and E7. The results strongly suggest that specific stimulation of tumor effector T cells using vaccination may circumvent adaptive TIM-3 overexpression and be a promising complementary treatment for combined immune checkpoint blockade. Currently, there are ongoing clinical trials (NCT03489343) testing the effect of an anti-TIM-3 antibody in various advanced solid tumors and lymphomas, including HNSCC. In 2019, Massarelli et al. reported the results of a non-randomized clinical trial testing a combination of nivolumab with a long-peptide HPV16 vaccine in patients with incurable HPV16<sup>+</sup> cancer (mostly OPSCC). The response rate was 33%, which markedly surpassed that of anti-PD-1 monotherapy [Massarelli et al. 2019]. Other

ongoing clinical trials tested an E6/E7-targeting vaccine with or without concurrent ICI (NCT04180215 and NCT03669718) and an E7-based mRNA vaccine in combination with an anti-CD40 antibody (NCT03418480) [Lechner et al. 2022].

Vaccination strategies using HPV16 antigens associated with cancer cell transformation may increase the number of HPV-specific T cells infiltrating tumor tissue; however, their persistence, survival, and effectiveness in the TME is directed by many other factors beside the expression of immune checkpoints. Recently, Wieland et al. detected intratumoral antigen-specific B cells producing HPV-specific IgG in samples from HPV<sup>+</sup> HNSCCs [Wieland et al. 2021]. The authors suggested that the HPV-specific antibodies might contribute to the generation and maintenance of HPV-specific T-cell responses. In Study 2, we thoroughly studied intratumoral B lymphocytes in HPV<sup>+</sup> and HPV<sup>-</sup> oropharyngeal cancer. We reported a significant correlation between the abundance of E6/E7 HPV-specific T cells and the cell-to-cell interactions B and T lymphocytes. Localization of B cells and their potential interactions with other leukocytes mainly occur in tertiary lymphoid structures (TLS) in the tumor stroma. TLS are islands of organized lymphoid tissue resembling secondary lymphoid organs that can develop in response to chronic inflammation or infection [Pitzalis et al. 2014]. In HNSCC, Li et al. reported the positive prognostic role of TLS in patients with oral squamous cell carcinoma [Li et al. 2020]. Ruffin et al. found that higher TLS frequency was observed in HPV-associated tumors [Ruffin et al. 2021]. The authors also observed a strong positive correlation between the density of TLS with germinal centers and the OS of HNSCC patients, regardless of HPV status. In contrast, we observed typical TLS with germinal centers only in 29.8% and 25% of HPV<sup>+</sup> and HPV<sup>-</sup> OPSCC samples, respectively, with no significant difference between the groups. Furthermore, we did not observe any effect of TLS on the OS of patients. However, we described small, well-defined cell aggregates of B cells and CD8<sup>+</sup> T cells with clear membrane interactions. We confirmed B/T-cell interactions, both in the tumor nests and tumor stroma, as a positive prognostic factor using univariate and multivariate survival analysis. The significance of this biomarker was even stronger than HPV status. Consistent with previous reports, we also confirmed higher intratumoral densities of B cells in HPV-associated tumors.

In accordance with other studies, we observed a positive correlation between high densities of intratumoral CD8<sup>+</sup> T cells and B cells and patient OS. Importantly, the presence of high densities of T/B-cell interactions were statistically stronger prognostic factors than T- and B-cell counts alone. Publications on the association of the abundance of intratumoral B cells and patient prognosis are contradictory. Pretschner et al. found no correlation between intratumoral

B cells in the primary tumor and survival of the patients in oro- and hypopharyngeal cancers [Pretscher et al. 2009]. In ovarian cancer, Lundgren et al. reported an association between CD20<sup>+</sup> cells and higher tumor stage and showed the negative prognostic impact of cells co-expressing CD20 and CD138 on the OS of the patients [Lundgren et al. 2016]. The differences might have been caused by insufficient phenotyping of the B-cell population, which could have revealed potentially different functionality of the B-cell subsets present in the TME. Therefore, we characterized the TIL-B phenotype by flow cytometry. We showed that, based on the expression of CD38 and IgD, TIL-B cells in HNSCC were mainly CD38<sup>+</sup>IgD<sup>-</sup> memory cells. Importantly, in B<sup>hi</sup> (>0.5% of total cell count) tumor samples, TIL-B expressed higher levels of CD40, CD86, HLA-ABC, and HLA-DR, indicating an activated phenotype. Furthermore, Ki-67, a marker of proliferation, was higher in B<sup>hi</sup> tumors compared to B<sup>lo</sup> samples. We also found a higher abundance of IL-10-producing Bregs in tumor samples compared with matched PBMCs and control tonsils. The results are in accordance with data from Lechner et al. and Zhou et al., who also found higher IL-10<sup>+</sup> Breg counts in tumor tissue of HNSCCs [Lechner et al. 2019, Zhou et al. 2016]. In summary, the results indicated that the better OS of patients with higher B-cell abundance might be caused by the different functional capacity of these cells.

The activated phenotype, co-localization of T and B cells, and the correlation of such interactions with the abundance of E6/E7 HPV-specific T cells suggest that B cells may serve as APCs that could support T cell-mediated immunity and prolong the survival of T cells in the tumor tissue. CD40, expressed in high levels on B cells from B<sup>hi</sup> samples, could interact with CD40L on T cells, resulting in “licensing” of B cells to become APCs. The activated APCs upregulate other co-stimulatory molecules that provide promoting signals to other T-cell receptors, such as CD27 and OX40, and enhance T cell-mediated antitumoral activity. In accordance with this hypothesis, we observed higher CD27 gene expression in tumor samples than in PBMCs. The CD27-CD70 pathway has often been reported to positively affect T-cell survival and clonal expansion both in an IL-2-dependent and independent manner [Carr et al. 2006, Peperzak et al. 2010]. We observed that depletion of B cells from tumor-derived cell cultures resulted in significantly decreased survival of both CD4<sup>+</sup> and CD8<sup>+</sup> T cells. Nevertheless, whether prolonged T-cell survival is caused mainly by direct T/B-cell interactions or by secreted B-cell products requires further evaluation. Our analysis of cytokine and chemokine production in cell cultures derived from B<sup>hi</sup> and B<sup>lo</sup> samples showed markedly higher levels of CXCL9, an important T-cell chemoattractant, in B<sup>hi</sup> samples. Furthermore, cell cultures depleted of B cells showed decreased levels of CXCL9, confirming B cells as an

important source of the chemokine. In conclusion, T cells might be partially attracted to the tumor site via the CXCL9 produced by B cells, and T-cell survival and activity might be supported by interactions with B cells through CD40/CD40L and CD27/CD70 pathways. Potential artificial augmentation of the B-cell mediated effects on T cells could intensify the antigen-specific antitumor immune response.

Although mDCs are responsible for the initiation of antigen-specific T-cell activity, we hypothesized that additional antigenic stimuli that might be presented by B cells to effector T cells could play a crucial role in sustaining the antitumor immune response. A smaller subgroup of DCs, pDCs, was also shown to support adaptive immunity both via production of type I IFN and through direct cell-to-cell contact. Tel et al. demonstrated the capability of pDCs to induce an antigen-specific T-cell response in patients with metastatic melanoma [Tel et al. 2013]. Moreover, pDCs were shown to elicit proliferation of naive and memory B cells through CD27-CD70 interaction [Shaw et al. 2010]. Despite the cited data, in malignant tumors, including HNSCC, the role of pDCs was reported to be mostly negative, supporting an immunosuppressive TME, as observed in melanoma and ovarian cancer [Jensen et al. 2012, Labidi-Galy et al. 2012]. Previous data from our research team showed a non-significant negative association of pDCs with the OS of HPV<sup>-</sup> HNSCC patients (not published). Based on the inconclusive findings and the essential role of pDCs in viral infections, we focused in more detail on the pDC functional state and prognostic role in HNSCC with regard to HPV status.

In Study 3, we found similar proportions of pDCs in HPV<sup>+</sup> and HPV<sup>-</sup> HNSCCs and no correlations between pDC density and the clinical and pathological characteristics of the patients. The finding is in contrast with those of Han et al., who reported a negative prognostic role of pDCs in a cohort of oral squamous cell carcinoma patients [Han et al. 2017]. Nevertheless, our cohort consisted of HNSCCs of various sublocations and a more specific identification of pDCs with BDCA-2 compared with CD123 staining only. Importantly, we observed a diminished capability of pDCs to produce IFN $\alpha$  upon TLR stimulation by imiquimod and CpG in HPV<sup>-</sup> tumors only. Interestingly, the proportions of pDCs that were able to produce IFN $\alpha$  were similar between HPV<sup>+</sup> samples, HPV<sup>-</sup> samples, and control tissue; however, the amount of IFN $\alpha$  differed significantly based on MFI values. We confirmed the result of decreased IFN $\alpha$  production in HPV<sup>-</sup> tumors by measuring IFN $\alpha$  levels in supernatants of CpG-stimulated tumor-derived single-cell suspensions. Reduced IFN $\alpha$  production by pDCs derived from HNSCC compared with blood-derived pDCs was also observed by Hartmann et al. [Hartmann et al. 2003]; however, healthy tonsillar tissue and peritumoral mucosa were used

as controls in our study following the finding that sample processing markedly influenced the capacity of pDCs to produce IFN $\alpha$  (not published).

To explain the difference in IFN $\alpha$  production by pDCs between HPV<sup>+</sup> and HPV<sup>-</sup> samples, we evaluated the expression of functional markers associated with IFN $\alpha$  secretion. We did not find any difference in expression of TLR7, TL9, CD28, TIM-3, TRAIL, IDO, or granzyme B on a protein level. The only marker with significantly increased expression on HPV<sup>+</sup> tumor-derived pDCs was NKp44. NKp44 was originally described as an activating receptor of NK cells. Fuchs et al. described that triggering NKp44 in a subset of tonsillar pDCs led to inhibition of IFN $\alpha$  production [Fuchs et al. 2005]. Paradoxically, we observed increased expression of NKp44 in pDCs infiltrating HPV<sup>+</sup> tumors and no difference in expression in relation to IFN $\alpha$  production. A possible explanation might be the higher abundance of CD8<sup>+</sup> in HPV<sup>+</sup> tumors because NKp44 expression was associated with the production of IL-3 by co-localized CD8<sup>+</sup> T cells [Fuchs et al. 2005].

We further tested the influence of the tumor cytokine microenvironment on pDC functional capacity. In accordance with our aforementioned results, only HPV<sup>-</sup> tumor-derived culture supernatants significantly inhibited IFN $\alpha$  production in blood-derived pDCs from healthy donors. Similar result were previously reported in relation to cervical, breast, ovarian cancer, and HNSCC, where IL-6, IL-10, HMGB-1, TNF $\alpha$  and TNF $\beta$  were identified as the main factors directly impairing pDC function [Labidi-Galy et al. 2011, Sisirak et al. 2013, Demoulin et al. 2015, Bruchhage et al. 2018]. In our study, we selected cytokines with the highest difference in levels between the most suppressive HPV<sup>-</sup> supernatants and non-suppressive HPV<sup>+</sup> supernatants, and we tested their direct effect on pDCs. IL-6, IL-10, and TNF $\alpha$  were present at significantly higher levels in HPV<sup>-</sup> supernatants. When the recombinant forms of the selected cytokines were applied to blood-derived pDCs from healthy donors at the concentrations detected in tumor supernatants, IL-10 and TNF $\alpha$  caused a significant decrease in IFN $\alpha$  secretion. Moreover, inhibition of IL-10 in culture supernatants via blocking antibody restored IFN $\alpha$  production to  $47.3 \pm 19.9\%$  and TNF $\alpha$  inhibition restored IFN $\alpha$  production by pDCs to  $82.8 \pm 13.5\%$ . No additive effect of combined inhibition was observed. The finding indicates that TNF $\alpha$  might be the main factor impairing IFN $\alpha$  production by pDCs in HNSCC. In view of these results, we tested the main source of IL-10 and TNF $\alpha$  in HNSCCs. Our immunohistochemical analysis showed tumor cells as the main source of the cytokines and, consistent with our data, we found TNF $\alpha$ <sup>+</sup> tumor cells in 81.8% of our HPV<sup>-</sup> samples compared

with 50% of our HPV<sup>+</sup> samples. Furthermore, IL-10<sup>+</sup> tumor cells were observed in 72.7% of our HPV<sup>-</sup> samples and only in 14.3% of HPV<sup>+</sup> tumors.

Reduced levels of IFN $\alpha$  that have a multimodal effect on the immune response might be only one of the mechanisms by which functionally impaired pDCs contribute to immunosuppression in the TME. The second most discussed mechanism of pDC-mediated immunosuppression is peripheral induction of Tregs, mainly through the ICOS/ICOS-L pathway [Conrad et al. 2012, Aspod et al. 2013]. Moreover, Tregs produce IL-10 that could intensify pDCs impairment, as demonstrated previously, and could potentially contribute to a vicious cycle of immunosuppression in the TME. In the current study, we did not observe any significant differences in Treg counts between HPV<sup>+</sup> and HPV<sup>-</sup> tumors. However, we found a significant positive correlation between pDC proportion and Tregs in HPV<sup>-</sup> but not in HPV<sup>+</sup> HNSCC. We observed clear co-localization of Tregs and pDCs using IHC staining. Correlation of Treg and pDC counts have been reported in thyroid cancer, gastric cancer, and glioma [Yu et al. 2013, Dey et al. 2015, Huang et al. 2014]. Interestingly, blood-derived pDCs from healthy donors exposed to HPV<sup>-</sup> tumor-derived supernatants were able to induce Treg expansion, whereas HPV<sup>+</sup> tumor-derived supernatants did not have this effect. Clearly, pDCs in the TME of HNSCCs have the potential to induce Tregs; however, the proportions of these Tregs relative to the whole Treg population and potential effects of blocking this effect requires further evaluation.

## 6. Conclusions

Following the approval of ICIs, immunotherapy has become a fourth pillar of cancer treatment. HNSCCs are a large group of tumors contributing significantly to worldwide cancer morbidity and mortality. Fortunately, based on current knowledge, HNSCC is a promising target for various immunotherapeutic approaches. Despite the success of ICIs, there remains a significant group of non-responders that require a different therapeutic approach. Complex study of the TME and insight into the processes that contribute to tumor-mediated evasion of the immune system has one of the highest priorities in the cancer-related research. Results presented in the thesis represent a small but significant piece of the puzzle and deepen the knowledge of the HNSCC immune microenvironment. We described the functional capacity of HPV-specific tumor-infiltrating T cells in HPV-induced OPSCC in relation to the expression of immune checkpoint molecules. Our findings support the combined use of ICIs in oropharyngeal cancer with therapeutic HPV vaccines. Indeed, combined immunotherapy is the main theme of current clinical trials. Although most of the focus in basic and clinical research is devoted to T cells, we evaluated the prognostic role and functional properties of other, less-studied TIL populations. We identified the positive prognostic role of TIL-Bs in oropharyngeal carcinoma and, more importantly, we were the first team to describe B/T-cell interactions that showed even stronger prognostic impact. We showed that B cells might affect T-cell survival and potentially their antitumor function. The results identified B cells as a valuable biomarker for patient stratification and as a promising target for future immunotherapy. Finally, we studied the differences of pDCs infiltrating HPV-related and nonrelated HNSCCs. We were the first team to publish the functional characteristics of pDCs in HNSCC, based on the HPV status of the disease. We showed that pDCs significantly supported immunosuppression in the TME of HPV<sup>-</sup> HNSCC and had preserved functional capacity in HPV<sup>+</sup> tumors. In conclusion, the thesis partially clarifies the important relationships and mechanisms in the TME of HNSCC; at the same time, the results emphasize the diversity and complexity of the immunological network. Further research on the cancer-immune system relationship is needed; nevertheless, the current data imply that widely effective and long-lasting cancer immunotherapy must target more than one of the immune system components by utilizing multiple approaches in combination.

## References

1. Peto, R., A.D. Lopez, J. Boreham, M. Thun and C. Heath, Jr., *Mortality from tobacco in developed countries: indirect estimation from national vital statistics*. Lancet, 1992. **339**(8804): p. 1268-78.
2. Guo, F., L.E. Cofie and A.B. Berenson, *Cervical Cancer Incidence in Young U.S. Females After Human Papillomavirus Vaccine Introduction*. Am J Prev Med, 2018. **55**(2): p. 197-204.
3. Gargano, J.W., I.U. Park, M.R. Griffin, L.M. Niccolai, M. Powell, et al., *Trends in High-grade Cervical Lesions and Cervical Cancer Screening in 5 States, 2008-2015*. Clin Infect Dis, 2019. **68**(8): p. 1282-1291.
4. Bray, F., J. Ferlay, I. Soerjomataram, R.L. Siegel, L.A. Torre, et al., *Global cancer statistics 2018: GLOBOCAN estimates of incidence and mortality worldwide for 36 cancers in 185 countries*. CA Cancer J Clin, 2018. **68**(6): p. 394-424.
5. Hashibe, M., P. Brennan, S.C. Chuang, S. Boccia, X. Castellsague, et al., *Interaction between tobacco and alcohol use and the risk of head and neck cancer: pooled analysis in the International Head and Neck Cancer Epidemiology Consortium*. Cancer Epidemiol Biomarkers Prev, 2009. **18**(2): p. 541-50.
6. Tomar, S.L., *Duration of cigarette smoking is a stronger risk factor than number smoked per day for head and neck cancer, and quitting dramatically lowers the risk*. The Journal of Evidence-Based Dental Practice, 2020. **20**(1).
7. Chen, A.M., L.M. Chen, A. Vaughan, R. Sreeraman, D.G. Farwell, et al., *Tobacco smoking during radiation therapy for head-and-neck cancer is associated with unfavorable outcome*. Int J Radiat Oncol Biol Phys, 2011. **79**(2): p. 414-9.
8. Marur, S., G. D'Souza, W.H. Westra and A.A. Forastiere, *HPV-associated head and neck cancer: a virus-related cancer epidemic*. Lancet Oncol, 2010. **11**(8): p. 781-9.
9. Chaturvedi, A.K., E.A. Engels, R.M. Pfeiffer, B.Y. Hernandez, W. Xiao, et al., *Human papillomavirus and rising oropharyngeal cancer incidence in the United States*. J Clin Oncol, 2011. **29**(32): p. 4294-301.
10. Gillison, M.L., A.K. Chaturvedi, W.F. Anderson and C. Fakhry, *Epidemiology of Human Papillomavirus-Positive Head and Neck Squamous Cell Carcinoma*. J Clin Oncol, 2015. **33**(29): p. 3235-42.
11. Ang, K.K., J. Harris, R. Wheeler, R. Weber, D.I. Rosenthal, et al., *Human papillomavirus and survival of patients with oropharyngeal cancer*. N Engl J Med, 2010. **363**(1): p. 24-35.
12. Licitra, L., F. Perrone, P. Bossi, S. Suardi, L. Mariani, et al., *High-risk human papillomavirus affects prognosis in patients with surgically treated oropharyngeal squamous cell carcinoma*. J Clin Oncol, 2006. **24**(36): p. 5630-6.
13. Fakhry, C., W.H. Westra, S. Li, A. Cmelak, J.A. Ridge, et al., *Improved survival of patients with human papillomavirus-positive head and neck squamous cell carcinoma in a prospective clinical trial*. J Natl Cancer Inst, 2008. **100**(4): p. 261-9.
14. James D. Brierley, M.K.G., Christian Wittekind, *TNM Classification of Malignant Tumours, 8th Edition*. 2017: Wiley-Blackwell.
15. Chow, L.Q.M., *Head and Neck Cancer. Reply*. N Engl J Med, 2020. **382**(20): p. e57.
16. Goldenberg, D., S. Begum, W.H. Westra, Z. Khan, J. Sciubba, et al., *Cystic lymph node metastasis in patients with head and neck cancer: An HPV-associated phenomenon*. Head Neck, 2008. **30**(7): p. 898-903.
17. Axelsson, L., J. Nyman, H. Haugen-Cange, M. Bove, L. Johansson, et al., *Prognostic factors for head and neck cancer of unknown primary including the impact of human papilloma virus infection*. J Otolaryngol Head Neck Surg, 2017. **46**(1): p. 45.
18. Motz, K., J.R. Qualliotine, E. Rettig, J.D. Richmon, D.W. Eisele, et al., *Changes in Unknown Primary Squamous Cell Carcinoma of the Head and Neck at Initial Presentation in the Era of Human Papillomavirus*. JAMA Otolaryngol Head Neck Surg, 2016. **142**(3): p. 223-8.

19. David, J.M., A.S. Ho, M. Luu, E.J. Yoshida, S. Kim, et al., *Treatment at high-volume facilities and academic centers is independently associated with improved survival in patients with locally advanced head and neck cancer*. *Cancer*, 2017. **123**(20): p. 3933-3942.
20. Jones, A.S., D.E. Phillips, T.R. Helliwell and N.J. Roland, *Occult node metastases in head and neck squamous carcinoma*. *Eur Arch Otorhinolaryngol*, 1993. **250**(8): p. 446-9.
21. Vermorken, J.B., R. Mesia, F. Rivera, E. Remenar, A. Kawecki, et al., *Platinum-based chemotherapy plus cetuximab in head and neck cancer*. *N Engl J Med*, 2008. **359**(11): p. 1116-27.
22. Ferris, R.L., G. Blumenschein, Jr., J. Fayette, J. Guigay, A.D. Colevas, et al., *Nivolumab for Recurrent Squamous-Cell Carcinoma of the Head and Neck*. *N Engl J Med*, 2016. **375**(19): p. 1856-1867.
23. Cohen, E.E.W., D. Soulieres, C. Le Tourneau, J. Dinis, L. Licitra, et al., *Pembrolizumab versus methotrexate, docetaxel, or cetuximab for recurrent or metastatic head-and-neck squamous cell carcinoma (KEYNOTE-040): a randomised, open-label, phase 3 study*. *Lancet*, 2019. **393**(10167): p. 156-167.
24. Mehanna, H., M. Robinson, A. Hartley, A. Kong, B. Foran, et al., *Radiotherapy plus cisplatin or cetuximab in low-risk human papillomavirus-positive oropharyngeal cancer (De-ESCALaTE HPV): an open-label randomised controlled phase 3 trial*. *Lancet*, 2019. **393**(10166): p. 51-60.
25. Gillison, M.L., A.M. Trotti, J. Harris, A. Eisbruch, P.M. Harari, et al., *Radiotherapy plus cetuximab or cisplatin in human papillomavirus-positive oropharyngeal cancer (NRG Oncology RTOG 1016): a randomised, multicentre, non-inferiority trial*. *Lancet*, 2019. **393**(10166): p. 40-50.
26. Schiffman, M., J. Doorbar, N. Wentzensen, S. de Sanjose, C. Fakhry, et al., *Carcinogenic human papillomavirus infection*. *Nat Rev Dis Primers*, 2016. **2**: p. 16086.
27. de Martel, C., M. Plummer, J. Vignat and S. Franceschi, *Worldwide burden of cancer attributable to HPV by site, country and HPV type*. *Int J Cancer*, 2017. **141**(4): p. 664-670.
28. Bouvard, V., R. Baan, K. Straif, Y. Grosse, B. Secretan, et al., *A review of human carcinogens-Part B: biological agents*. *Lancet Oncol*, 2009. **10**(4): p. 321-2.
29. Herfs, M., Y. Yamamoto, A. Laury, X. Wang, M.R. Nucci, et al., *A discrete population of squamocolumnar junction cells implicated in the pathogenesis of cervical cancer*. *Proc Natl Acad Sci U S A*, 2012. **109**(26): p. 10516-21.
30. Bruni, L., M. Diaz, X. Castellsague, E. Ferrer, F.X. Bosch, et al., *Cervical human papillomavirus prevalence in 5 continents: meta-analysis of 1 million women with normal cytological findings*. *J Infect Dis*, 2010. **202**(12): p. 1789-99.
31. McQuillan, G., D. Kruszon-Moran, L.E. Markowitz, E.R. Unger and R. Paulose-Ram, *Prevalence of HPV in Adults Aged 18-69: United States, 2011-2014*. *NCHS Data Brief*, 2017(280): p. 1-8.
32. Kreimer, A.R., A. Villa, A.G. Nyitray, M. Abrahamsen, M. Papenfuss, et al., *The epidemiology of oral HPV infection among a multinational sample of healthy men*. *Cancer Epidemiol Biomarkers Prev*, 2011. **20**(1): p. 172-82.
33. Tam, S., S. Fu, L. Xu, K.J. Krause, D.R. Lairson, et al., *The epidemiology of oral human papillomavirus infection in healthy populations: A systematic review and meta-analysis*. *Oral Oncol*, 2018. **82**: p. 91-99.
34. Malerova, S., A. Hejtmankova, E. Hamsikova, M. Salakova, J. Smahelova, et al., *Prevalence and Risk Factors for Oral HPV in Healthy Population, in Central Europe*. *Anticancer Res*, 2020. **40**(3): p. 1597-1604.
35. Pierce Campbell, C.M., A.R. Kreimer, H.Y. Lin, W. Fulp, M.T. O'Keefe, et al., *Long-term persistence of oral human papillomavirus type 16: the HPV Infection in Men (HIM) study*. *Cancer Prev Res (Phila)*, 2015. **8**(3): p. 190-6.
36. Mollers, M., J. Boot Hein, J. Vriend Henrike, J. King Audrey, V.F. van den Broek Ingrid, et al., *Prevalence, incidence and persistence of genital HPV infections in a large cohort of sexually active young women in the Netherlands*. *Vaccine*, 2013. **31**(2): p. 394-401.
37. Kero, K., J. Rautava, K. Syrjanen, J. Willberg, S. Grenman, et al., *Smoking increases oral HPV persistence among men: 7-year follow-up study*. *Eur J Clin Microbiol Infect Dis*, 2014. **33**(1): p. 123-33.

38. D'Souza, G., C. Fakhry, E.A. Sugar, E.C. Seaberg, K. Weber, et al., *Six-month natural history of oral versus cervical human papillomavirus infection*. *Int J Cancer*, 2007. **121**(1): p. 143-50.
39. Mordechai, R.A., S. Steinberg, L. Apel-Sarid, E. Shaoul, S.Z. Rozen, et al., *Detection of high-risk human papillomavirus in the tonsils of galilee region adults and young adults undergoing tonsillectomy*. *Eur Arch Otorhinolaryngol*, 2019. **276**(10): p. 2865-2871.
40. Palmer, E., R.G. Newcombe, A.C. Green, C. Kelly, O. Noel Gill, et al., *Human papillomavirus infection is rare in nonmalignant tonsil tissue in the UK: implications for tonsil cancer precursor lesions*. *Int J Cancer*, 2014. **135**(10): p. 2437-43.
41. Rieth, K.K.S., S.R. Gill, A.A. Lott-Limbach, M.A. Merkley, N. Botero, et al., *Prevalence of High-Risk Human Papillomavirus in Tonsil Tissue in Healthy Adults and Colocalization in Biofilm of Tonsillar Crypts*. *JAMA Otolaryngol Head Neck Surg*, 2018. **144**(3): p. 231-237.
42. Lechner, M., J. Liu, L. Masterson and T.R. Fenton, *HPV-associated oropharyngeal cancer: epidemiology, molecular biology and clinical management*. *Nat Rev Clin Oncol*, 2022.
43. McBride, A.A. and A. Warburton, *The role of integration in oncogenic progression of HPV-associated cancers*. *PLoS Pathog*, 2017. **13**(4): p. e1006211.
44. Schwartz, S., *Papillomavirus transcripts and posttranscriptional regulation*. *Virology*, 2013. **445**(1-2): p. 187-96.
45. Doorbar, J., W. Quint, L. Banks, I.G. Bravo, M. Stoler, et al., *The biology and life-cycle of human papillomaviruses*. *Vaccine*, 2012. **30** **Suppl 5**: p. F55-70.
46. Thomas, M., D. Pim and L. Banks, *The role of the E6-p53 interaction in the molecular pathogenesis of HPV*. *Oncogene*, 1999. **18**(53): p. 7690-700.
47. Boyer, S.N., D.E. Wazer and V. Band, *E7 protein of human papilloma virus-16 induces degradation of retinoblastoma protein through the ubiquitin-proteasome pathway*. *Cancer Res*, 1996. **56**(20): p. 4620-4.
48. Estevao, D., N.R. Costa, R.M. Gil da Costa and R. Medeiros, *Hallmarks of HPV carcinogenesis: The role of E6, E7 and E5 oncoproteins in cellular malignancy*. *Biochim Biophys Acta Gene Regul Mech*, 2019. **1862**(2): p. 153-162.
49. Panczyszyn, A., E. Boniewska-Bernacka and G. Glab, *Telomeres and Telomerase During Human Papillomavirus-Induced Carcinogenesis*. *Mol Diagn Ther*, 2018. **22**(4): p. 421-430.
50. Jiang, P. and Y. Yue, *Human papillomavirus oncoproteins and apoptosis (Review)*. *Exp Ther Med*, 2014. **7**(1): p. 3-7.
51. Alexandrov, L.B., S. Nik-Zainal, D.C. Wedge, S.A. Aparicio, S. Behjati, et al., *Signatures of mutational processes in human cancer*. *Nature*, 2013. **500**(7463): p. 415-21.
52. Seiwert, T.Y., Z. Zuo, M.K. Keck, A. Khattri, C.S. Pedamallu, et al., *Integrative and comparative genomic analysis of HPV-positive and HPV-negative head and neck squamous cell carcinomas*. *Clin Cancer Res*, 2015. **21**(3): p. 632-41.
53. Leemans, C.R., B.J. Braakhuis and R.H. Brakenhoff, *The molecular biology of head and neck cancer*. *Nat Rev Cancer*, 2011. **11**(1): p. 9-22.
54. Kiessling, S.Y., M.A. Broglie, A. Soltermann, G.F. Huber and S.J. Stoeckli, *Comparison of PI3K Pathway in HPV-Associated Oropharyngeal Cancer With and Without Tobacco Exposure*. *Laryngoscope Investig Otolaryngol*, 2018. **3**(4): p. 283-289.
55. Steenbergen, R.D., P.J. Snijders, D.A. Heideman and C.J. Meijer, *Clinical implications of (epi)genetic changes in HPV-induced cervical precancerous lesions*. *Nat Rev Cancer*, 2014. **14**(6): p. 395-405.
56. Ronco, G., J. Dillner, K.M. Elfstrom, S. Tunesi, P.J. Snijders, et al., *Efficacy of HPV-based screening for prevention of invasive cervical cancer: follow-up of four European randomised controlled trials*. *Lancet*, 2014. **383**(9916): p. 524-32.
57. Prigge, E.S., M. Arbyn, M. von Knebel Doeberitz and M. Reuschenbach, *Diagnostic accuracy of p16(INK4a) immunohistochemistry in oropharyngeal squamous cell carcinomas: A systematic review and meta-analysis*. *Int J Cancer*, 2017. **140**(5): p. 1186-1198.
58. Lewis, J.S., Jr., B. Beadle, J.A. Bishop, R.D. Chernock, C. Colasacco, et al., *Human Papillomavirus Testing in Head and Neck Carcinomas: Guideline From the College of American Pathologists*. *Arch Pathol Lab Med*, 2018. **142**(5): p. 559-597.

59. Romagosa, C., S. Simonetti, L. Lopez-Vicente, A. Mazo, M.E. Lleonart, et al., *p16(Ink4a) overexpression in cancer: a tumor suppressor gene associated with senescence and high-grade tumors*. *Oncogene*, 2011. **30**(18): p. 2087-97.
60. Albers, A.E., X. Qian, A.M. Kaufmann and A. Coordes, *Meta analysis: HPV and p16 pattern determines survival in patients with HNSCC and identifies potential new biologic subtype*. *Sci Rep*, 2017. **7**(1): p. 16715.
61. Pfister, D.G., S. Spencer, D. Adelstein, D. Adkins, Y. Anzai, et al., *Head and Neck Cancers, Version 2.2020, NCCN Clinical Practice Guidelines in Oncology*. *J Natl Compr Canc Netw*, 2020. **18**(7): p. 873-898.
62. Burnet, F.M., *Cancer a biological approach*. *Br Med J*, 1957. **1**: p. 841-7.
63. Dunn, G.P., A.T. Bruce, H. Ikeda, L.J. Old and R.D. Schreiber, *Cancer immunoediting: from immunosurveillance to tumor escape*. *Nat Immunol*, 2002. **3**(11): p. 991-8.
64. Hanahan, D. and R.A. Weinberg, *Hallmarks of cancer: the next generation*. *Cell*, 2011. **144**(5): p. 646-74.
65. Hiam-Galvez, K.J., B.M. Allen and M.H. Spitzer, *Systemic immunity in cancer*. *Nat Rev Cancer*, 2021. **21**(6): p. 345-359.
66. Almand, B., J.I. Clark, E. Nikitina, J. van Beynen, N.R. English, et al., *Increased production of immature myeloid cells in cancer patients: a mechanism of immunosuppression in cancer*. *J Immunol*, 2001. **166**(1): p. 678-89.
67. Lang, S., K. Bruderek, C. Kaspar, B. Hoing, O. Kanaan, et al., *Clinical Relevance and Suppressive Capacity of Human Myeloid-Derived Suppressor Cell Subsets*. *Clin Cancer Res*, 2018. **24**(19): p. 4834-4844.
68. Hoffmann, T.K., J. Muller-Berghaus, R.L. Ferris, J.T. Johnson, W.J. Storkus, et al., *Alterations in the frequency of dendritic cell subsets in the peripheral circulation of patients with squamous cell carcinomas of the head and neck*. *Clin Cancer Res*, 2002. **8**(6): p. 1787-93.
69. O'Higgins, C., F.J. Ward and R. Abu Eid, *Deciphering the Role of Regulatory CD4 T Cells in Oral and Oropharyngeal Cancer: A Systematic Review*. *Front Oncol*, 2018. **8**: p. 442.
70. Ahmadzadeh, M., A. Pasetto, L. Jia, D.C. Deniger, S. Stevanovic, et al., *Tumor-infiltrating human CD4(+) regulatory T cells display a distinct TCR repertoire and exhibit tumor and neoantigen reactivity*. *Sci Immunol*, 2019. **4**(31).
71. Kawai, O., G. Ishii, K. Kubota, Y. Murata, Y. Naito, et al., *Predominant infiltration of macrophages and CD8(+) T Cells in cancer nests is a significant predictor of survival in stage IV nonsmall cell lung cancer*. *Cancer*, 2008. **113**(6): p. 1387-95.
72. Al-Saleh, K., N. Abd El-Aziz, A. Ali, W. Abozeed, A. Abd El-Warith, et al., *Predictive and prognostic significance of CD8(+) tumor-infiltrating lymphocytes in patients with luminal B/HER 2 negative breast cancer treated with neoadjuvant chemotherapy*. *Oncol Lett*, 2017. **14**(1): p. 337-344.
73. Sato, E., S.H. Olson, J. Ahn, B. Bundy, H. Nishikawa, et al., *Intraepithelial CD8+ tumor-infiltrating lymphocytes and a high CD8+/regulatory T cell ratio are associated with favorable prognosis in ovarian cancer*. *Proc Natl Acad Sci U S A*, 2005. **102**(51): p. 18538-43.
74. Galon, J. and A. Lanzi, *Immunoscore and its introduction in clinical practice*. *Q J Nucl Med Mol Imaging*, 2020. **64**(2): p. 152-161.
75. Maleki Vareki, S., *High and low mutational burden tumors versus immunologically hot and cold tumors and response to immune checkpoint inhibitors*. *J Immunother Cancer*, 2018. **6**(1): p. 157.
76. Nathanson, T., A. Ahuja, A. Rubinsteyn, B.A. Aksoy, M.D. Hellmann, et al., *Somatic Mutations and Neoepitope Homology in Melanomas Treated with CTLA-4 Blockade*. *Cancer Immunol Res*, 2017. **5**(1): p. 84-91.
77. Partlova, S., J. Boucek, K. Kloudova, E. Lukesova, M. Zabrodsky, et al., *Distinct patterns of intratumoral immune cell infiltrates in patients with HPV-associated compared to non-virally induced head and neck squamous cell carcinoma*. *Oncoimmunology*, 2015. **4**(1): p. e965570.
78. Takahashi, H., K. Sakakura, T. Kudo, M. Toyoda, K. Kaira, et al., *Cancer-associated fibroblasts promote an immunosuppressive microenvironment through the induction and accumulation of protumoral macrophages*. *Oncotarget*, 2017. **8**(5): p. 8633-8647.

79. Joshi, R.S., S.S. Kanugula, S. Sudhir, M.P. Pereira, S. Jain, et al., *The Role of Cancer-Associated Fibroblasts in Tumor Progression*. *Cancers (Basel)*, 2021. **13**(6).
80. Berndt, A., P. Richter, H. Kosmehl and M. Franz, *Tenascin-C and carcinoma cell invasion in oral and urinary bladder cancer*. *Cell Adh Migr*, 2015. **9**(1-2): p. 105-11.
81. Mhaweche, P., P. Dulguerov, M. Assaly, C. Ares and A.S. Allal, *EB-D fibronectin expression in squamous cell carcinoma of the head and neck*. *Oral Oncol*, 2005. **41**(1): p. 82-8.
82. Plzak, J., J. Boucek, V. Bandurova, M. Kolar, M. Hradilova, et al., *The Head and Neck Squamous Cell Carcinoma Microenvironment as a Potential Target for Cancer Therapy*. *Cancers (Basel)*, 2019. **11**(4).
83. Wu, M.H., H.C. Hong, T.M. Hong, W.F. Chiang, Y.T. Jin, et al., *Targeting galectin-1 in carcinoma-associated fibroblasts inhibits oral squamous cell carcinoma metastasis by downregulating MCP-1/CCL2 expression*. *Clin Cancer Res*, 2011. **17**(6): p. 1306-16.
84. Honjo, Y., H. Inohara, S. Akahani, T. Yoshii, Y. Takenaka, et al., *Expression of cytoplasmic galectin-3 as a prognostic marker in tongue carcinoma*. *Clin Cancer Res*, 2000. **6**(12): p. 4635-40.
85. Tokmak, S., D. Arik, O. Pinarbasli, M.K. Gurbuz and M.F. Acikalın, *Evaluation and Prognostic Significance of Galectin-3 Expression in Oral Squamous Cell Carcinoma*. *Ear Nose Throat J*, 2021. **100**(5\_suppl): p. 578S-583S.
86. Sparano, A., D.M. Lathers, N. Achille, G.J. Petruzzelli and M.R. Young, *Modulation of Th1 and Th2 cytokine profiles and their association with advanced head and neck squamous cell carcinoma*. *Otolaryngol Head Neck Surg*, 2004. **131**(5): p. 573-6.
87. Lathers, D.M., N.J. Achille and M.R. Young, *Incomplete Th2 skewing of cytokines in plasma of patients with squamous cell carcinoma of the head and neck*. *Hum Immunol*, 2003. **64**(12): p. 1160-6.
88. Duffy, S.A., J.M. Taylor, J.E. Terrell, M. Islam, Y. Li, et al., *Interleukin-6 predicts recurrence and survival among head and neck cancer patients*. *Cancer*, 2008. **113**(4): p. 750-7.
89. Jebreel, A., D. Mistry, D. Loke, G. Dunn, V. Hough, et al., *Investigation of interleukin 10, 12 and 18 levels in patients with head and neck cancer*. *J Laryngol Otol*, 2007. **121**(3): p. 246-52.
90. Balermipas, P., F. Rodel, C. Rodel, M. Krause, A. Linge, et al., *CD8+ tumour-infiltrating lymphocytes in relation to HPV status and clinical outcome in patients with head and neck cancer after postoperative chemoradiotherapy: A multicentre study of the German cancer consortium radiation oncology group (DKTK-ROG)*. *Int J Cancer*, 2016. **138**(1): p. 171-81.
91. Nasman, A., M. Romanitan, C. Nordfors, N. Grun, H. Johansson, et al., *Tumor infiltrating CD8+ and Foxp3+ lymphocytes correlate to clinical outcome and human papillomavirus (HPV) status in tonsillar cancer*. *PLoS One*, 2012. **7**(6): p. e38711.
92. Solomon, B., R.J. Young, M. Bressel, D. Urban, S. Hendry, et al., *Prognostic Significance of PD-L1(+) and CD8(+) Immune Cells in HPV(+) Oropharyngeal Squamous Cell Carcinoma*. *Cancer Immunol Res*, 2018. **6**(3): p. 295-304.
93. Chen, X., B. Yan, H. Lou, Z. Shen, F. Tong, et al., *Immunological network analysis in HPV associated head and neck squamous cancer and implications for disease prognosis*. *Mol Immunol*, 2018. **96**: p. 28-36.
94. Gameiro, S.F., F. Ghasemi, J.W. Barrett, J. Koropatnick, A.C. Nichols, et al., *Treatment-naive HPV+ head and neck cancers display a T-cell-inflamed phenotype distinct from their HPV-counterparts that has implications for immunotherapy*. *Oncoimmunology*, 2018. **7**(10): p. e1498439.
95. Ward, M.J., S.M. Thirdborough, T. Mellows, C. Riley, S. Harris, et al., *Tumour-infiltrating lymphocytes predict for outcome in HPV-positive oropharyngeal cancer*. *Br J Cancer*, 2014. **110**(2): p. 489-500.
96. Welters, M.J.P., W. Ma, S. Santegoets, R. Goedemans, I. Ehsan, et al., *Intratumoral HPV16-Specific T Cells Constitute a Type I-Oriented Tumor Microenvironment to Improve Survival in HPV16-Driven Oropharyngeal Cancer*. *Clin Cancer Res*, 2018. **24**(3): p. 634-647.
97. Heusinkveld, M., R. Goedemans, R.J. Briet, H. Gelderblom, J.W. Nortier, et al., *Systemic and local human papillomavirus 16-specific T-cell immunity in patients with head and neck cancer*. *Int J Cancer*, 2012. **131**(2): p. E74-85.

98. Hanna, G.J., P. Lizotte, M. Cavanaugh, F.C. Kuo, P. Shivdasani, et al., *Frameshift events predict anti-PD-1/L1 response in head and neck cancer*. JCI Insight, 2018. **3**(4).
99. Wolf, G.T., D.B. Chepeha, E. Bellile, A. Nguyen, D. Thomas, et al., *Tumor infiltrating lymphocytes (TIL) and prognosis in oral cavity squamous carcinoma: a preliminary study*. Oral Oncol, 2015. **51**(1): p. 90-5.
100. Cillo, A.R., C.H.L. Kurten, T. Tabib, Z. Qi, S. Onkar, et al., *Immune Landscape of Viral- and Carcinogen-Driven Head and Neck Cancer*. Immunity, 2020. **52**(1): p. 183-199 e9.
101. Wondergem, N.E., I.H. Nauta, T. Muijlwijk, C.R. Leemans and R. van de Ven, *The Immune Microenvironment in Head and Neck Squamous Cell Carcinoma: on Subsets and Subsites*. Curr Oncol Rep, 2020. **22**(8): p. 81.
102. Togashi, Y., K. Shitara and H. Nishikawa, *Regulatory T cells in cancer immunosuppression - implications for anticancer therapy*. Nat Rev Clin Oncol, 2019. **16**(6): p. 356-371.
103. Munn, D.H. and A.L. Mellor, *Indoleamine 2,3-dioxygenase and tumor-induced tolerance*. J Clin Invest, 2007. **117**(5): p. 1147-54.
104. Hori, S., T. Nomura and S. Sakaguchi, *Control of regulatory T cell development by the transcription factor Foxp3*. Science, 2003. **299**(5609): p. 1057-61.
105. Sun, J., D.N. Tang, T. Fu and P. Sharma, *Identification of human regulatory T cells in the setting of T-cell activation and anti-CTLA-4 immunotherapy on the basis of expression of latency-associated peptide*. Cancer Discov, 2012. **2**(2): p. 122-30.
106. Bron, L., C. Jandus, S. Andrejevic-Blant, D.E. Speiser, P. Monnier, et al., *Prognostic value of arginase-II expression and regulatory T-cell infiltration in head and neck squamous cell carcinoma*. Int J Cancer, 2013. **132**(3): p. E85-93.
107. Seminerio, I., G. Descamps, S. Dupont, L. de Marrez, J.A. Laigle, et al., *Infiltration of FoxP3+ Regulatory T Cells is a Strong and Independent Prognostic Factor in Head and Neck Squamous Cell Carcinoma*. Cancers (Basel), 2019. **11**(2).
108. Liang, Y.J., H.C. Liu, Y.X. Su, T.H. Zhang, M. Chu, et al., *Foxp3 expressed by tongue squamous cell carcinoma cells correlates with clinicopathologic features and overall survival in tongue squamous cell carcinoma patients*. Oral Oncol, 2011. **47**(7): p. 566-70.
109. Chen, W.Y., C.T. Wu, C.W. Wang, K.H. Lan, H.K. Liang, et al., *Prognostic significance of tumor-infiltrating lymphocytes in patients with operable tongue cancer*. Radiat Oncol, 2018. **13**(1): p. 157.
110. Feng, Z., D. Bethmann, M. Kappler, C. Ballesteros-Merino, A. Eckert, et al., *Multiparametric immune profiling in HPV- oral squamous cell cancer*. JCI Insight, 2017. **2**(14).
111. Zajac, A.J., J.N. Blattman, K. Murali-Krishna, D.J. Sourdive, M. Suresh, et al., *Viral immune evasion due to persistence of activated T cells without effector function*. J Exp Med, 1998. **188**(12): p. 2205-13.
112. Wherry, E.J., *T cell exhaustion*. Nat Immunol, 2011. **12**(6): p. 492-9.
113. Wang, J., T. Yoshida, F. Nakaki, H. Hiai, T. Okazaki, et al., *Establishment of NOD-Pdcd1-/- mice as an efficient animal model of type I diabetes*. Proc Natl Acad Sci U S A, 2005. **102**(33): p. 11823-8.
114. Veigas, F., Y.D. Mahmoud, J. Merlo, A. Rinflerch, G.A. Rabinovich, et al., *Immune Checkpoints Pathways in Head and Neck Squamous Cell Carcinoma*. Cancers (Basel), 2021. **13**(5).
115. Karpathiou, G., F. Casteillo, J.B. Giroult, F. Forest, P. Fournel, et al., *Prognostic impact of immune microenvironment in laryngeal and pharyngeal squamous cell carcinoma: Immune cell subtypes, immuno-suppressive pathways and clinicopathologic characteristics*. Oncotarget, 2017. **8**(12): p. 19310-19322.
116. Yang, W.F., M.C.M. Wong, P.J. Thomson, K.Y. Li and Y.X. Su, *The prognostic role of PD-L1 expression for survival in head and neck squamous cell carcinoma: A systematic review and meta-analysis*. Oral Oncol, 2018. **86**: p. 81-90.
117. Badoual, C., S. Hans, N. Merillon, C. Van Ryswick, P. Ravel, et al., *PD-1-expressing tumor-infiltrating T cells are a favorable prognostic biomarker in HPV-associated head and neck cancer*. Cancer Res, 2013. **73**(1): p. 128-38.

118. Oweida, A., M.K. Hararah, A. Phan, D. Binder, S. Bhatia, et al., *Resistance to Radiotherapy and PD-L1 Blockade Is Mediated by TIM-3 Upregulation and Regulatory T-Cell Infiltration*. Clin Cancer Res, 2018. **24**(21): p. 5368-5380.
119. Shayan, G., R. Srivastava, J. Li, N. Schmitt, L.P. Kane, et al., *Adaptive resistance to anti-PD1 therapy by Tim-3 upregulation is mediated by the PI3K-Akt pathway in head and neck cancer*. Oncoimmunology, 2017. **6**(1): p. e1261779.
120. Du, W., M. Yang, A. Turner, C. Xu, R.L. Ferris, et al., *TIM-3 as a Target for Cancer Immunotherapy and Mechanisms of Action*. Int J Mol Sci, 2017. **18**(3).
121. Yang, R., L. Sun, C.F. Li, Y.H. Wang, J. Yao, et al., *Galectin-9 interacts with PD-1 and TIM-3 to regulate T cell death and is a target for cancer immunotherapy*. Nat Commun, 2021. **12**(1): p. 832.
122. Yang, F., Z. Zeng, J. Li, X. Ren and F. Wei, *TIM-3 and CEACAM1 are Prognostic Factors in Head and Neck Squamous Cell Carcinoma*. Front Mol Biosci, 2021. **8**: p. 619765.
123. Griss, J., W. Bauer, C. Wagner, M. Simon, M. Chen, et al., *B cells sustain inflammation and predict response to immune checkpoint blockade in human melanoma*. Nat Commun, 2019. **10**(1): p. 4186.
124. Tsou, P., H. Katayama, E.J. Ostrin and S.M. Hanash, *The Emerging Role of B Cells in Tumor Immunity*. Cancer Res, 2016. **76**(19): p. 5597-5601.
125. Fridman, W.H., F. Petitprez, M. Meylan, T.W. Chen, C.M. Sun, et al., *B cells and cancer: To B or not to B?* J Exp Med, 2021. **218**(1).
126. Murakami, Y., H. Saito, S. Shimizu, Y. Kono, Y. Shishido, et al., *Increased regulatory B cells are involved in immune evasion in patients with gastric cancer*. Sci Rep, 2019. **9**(1): p. 13083.
127. Shao, Y., C.M. Lo, C.C. Ling, X.B. Liu, K.T. Ng, et al., *Regulatory B cells accelerate hepatocellular carcinoma progression via CD40/CD154 signaling pathway*. Cancer Lett, 2014. **355**(2): p. 264-72.
128. Lechner, A., H.A. Schlosser, M. Thelen, K. Wennhold, S.I. Rothschild, et al., *Tumor-associated B cells and humoral immune response in head and neck squamous cell carcinoma*. Oncoimmunology, 2019. **8**(3): p. 1535293.
129. Russell, S., T. Angell, M. Lechner, D. Liebertz, A. Correa, et al., *Immune cell infiltration patterns and survival in head and neck squamous cell carcinoma*. Head Neck Oncol, 2013. **5**(3): p. 24.
130. Distel, L.V., R. Fickenscher, K. Dietel, A. Hung, H. Iro, et al., *Tumour infiltrating lymphocytes in squamous cell carcinoma of the oro- and hypopharynx: prognostic impact may depend on type of treatment and stage of disease*. Oral Oncol, 2009. **45**(10): p. e167-74.
131. Zhou, X., Y.X. Su, X.M. Lao, Y.J. Liang and G.Q. Liao, *CD19(+)IL-10(+) regulatory B cells affect survival of tongue squamous cell carcinoma patients and induce resting CD4(+) T cells to CD4(+)Foxp3(+) regulatory T cells*. Oral Oncol, 2016. **53**: p. 27-35.
132. Wculek, S.K., F.J. Cueto, A.M. Mujal, I. Melero, M.F. Krummel, et al., *Dendritic cells in cancer immunology and immunotherapy*. Nat Rev Immunol, 2020. **20**(1): p. 7-24.
133. Reichert, T.E., C. Scheuer, R. Day, W. Wagner and T.L. Whiteside, *The number of intratumoral dendritic cells and zeta-chain expression in T cells as prognostic and survival biomarkers in patients with oral carcinoma*. Cancer, 2001. **91**(11): p. 2136-47.
134. Goldman, S.A., E. Baker, R.J. Weyant, M.R. Clarke, J.N. Myers, et al., *Peritumoral CD1a-positive dendritic cells are associated with improved survival in patients with tongue carcinoma*. Arch Otolaryngol Head Neck Surg, 1998. **124**(6): p. 641-6.
135. O'Donnell, R.K., R. Mick, M. Feldman, S. Hino, Y. Wang, et al., *Distribution of dendritic cell subtypes in primary oral squamous cell carcinoma is inconsistent with a functional response*. Cancer Lett, 2007. **255**(1): p. 145-52.
136. Koucky, V., J. Boucek and A. Fialova, *Immunology of Plasmacytoid Dendritic Cells in Solid Tumors: A Brief Review*. Cancers (Basel), 2019. **11**(4).
137. Sisirak, V., J. Faget, M. Gobert, N. Goutagny, N. Vey, et al., *Impaired IFN-alpha production by plasmacytoid dendritic cells favors regulatory T-cell expansion that may contribute to breast cancer progression*. Cancer Res, 2012. **72**(20): p. 5188-97.

138. Labidi-Galy, S.I., V. Sisirak, P. Meeus, M. Gobert, I. Treilleux, et al., *Quantitative and functional alterations of plasmacytoid dendritic cells contribute to immune tolerance in ovarian cancer*. *Cancer Res*, 2011. **71**(16): p. 5423-34.
139. Chen, W., X. Liang, A.J. Peterson, D.H. Munn and B.R. Blazar, *The indoleamine 2,3-dioxygenase pathway is essential for human plasmacytoid dendritic cell-induced adaptive T regulatory cell generation*. *J Immunol*, 2008. **181**(8): p. 5396-404.
140. Wu, J., S. Li, Y. Yang, S. Zhu, M. Zhang, et al., *TLR-activated plasmacytoid dendritic cells inhibit breast cancer cell growth in vitro and in vivo*. *Oncotarget*, 2017. **8**(7): p. 11708-11718.
141. Hartmann, E., B. Wollenberg, S. Rothenfusser, M. Wagner, D. Wellisch, et al., *Identification and functional analysis of tumor-infiltrating plasmacytoid dendritic cells in head and neck cancer*. *Cancer Res*, 2003. **63**(19): p. 6478-87.
142. Han, N., Z. Zhang, S. Liu, A. Ow, M. Ruan, et al., *Increased tumor-infiltrating plasmacytoid dendritic cells predicts poor prognosis in oral squamous cell carcinoma*. *Arch Oral Biol*, 2017. **78**: p. 129-134.
143. Martinez, F.O. and S. Gordon, *The M1 and M2 paradigm of macrophage activation: time for reassessment*. *F1000Prime Rep*, 2014. **6**: p. 13.
144. Zhou, J., Z. Tang, S. Gao, C. Li, Y. Feng, et al., *Tumor-Associated Macrophages: Recent Insights and Therapies*. *Front Oncol*, 2020. **10**: p. 188.
145. Saloura, V., E. Izumchenko, Z. Zuo, R. Bao, M. Korzinkin, et al., *Immune profiles in primary squamous cell carcinoma of the head and neck*. *Oral Oncol*, 2019. **96**: p. 77-88.
146. Cooper, M.A., T.A. Fehniger and M.A. Caligiuri, *The biology of human natural killer-cell subsets*. *Trends Immunol*, 2001. **22**(11): p. 633-40.
147. Wagner, S., C. Wittekindt, M. Reuschenbach, B. Hennig, M. Thevarajah, et al., *CD56-positive lymphocyte infiltration in relation to human papillomavirus association and prognostic significance in oropharyngeal squamous cell carcinoma*. *Int J Cancer*, 2016. **138**(9): p. 2263-73.
148. Mandal, R., Y. Senbabaoglu, A. Desrichard, J.J. Havel, M.G. Dalin, et al., *The head and neck cancer immune landscape and its immunotherapeutic implications*. *JCI Insight*, 2016. **1**(17): p. e89829.
149. Dumitru, C.A., A. Bankfalvi, X. Gu, W.E. Eberhardt, R. Zeidler, et al., *Neutrophils Activate Tumoral CORTACTIN to Enhance Progression of Oropharynx Carcinoma*. *Front Immunol*, 2013. **4**: p. 33.
150. Evrard, D., M. Hourseau, A. Couvelard, V. Paradis, H. Gauthier, et al., *PD-L1 expression in the microenvironment and the response to checkpoint inhibitors in head and neck squamous cell carcinoma*. *Oncoimmunology*, 2020. **9**(1): p. 1844403.
151. Ferris, R.L., R. Haddad, C. Even, M. Tahara, M. Dvorkin, et al., *Durvalumab with or without tremelimumab in patients with recurrent or metastatic head and neck squamous cell carcinoma: EAGLE, a randomized, open-label phase III study*. *Ann Oncol*, 2020. **31**(7): p. 942-950.
152. Siu, L.L., C. Even, R. Mesia, E. Remenar, A. Daste, et al., *Safety and Efficacy of Durvalumab With or Without Tremelimumab in Patients With PD-L1-Low/Negative Recurrent or Metastatic HNSCC: The Phase 2 CONDOR Randomized Clinical Trial*. *JAMA Oncol*, 2019. **5**(2): p. 195-203.
153. Cheng, G., H. Dong, C. Yang, Y. Liu, Y. Wu, et al., *A review on the advances and challenges of immunotherapy for head and neck cancer*. *Cancer Cell Int*, 2021. **21**(1): p. 406.
154. Massarelli, E., W. William, F. Johnson, M. Kies, R. Ferrarotto, et al., *Combining Immune Checkpoint Blockade and Tumor-Specific Vaccine for Patients With Incurable Human Papillomavirus 16-Related Cancer: A Phase 2 Clinical Trial*. *JAMA Oncol*, 2019. **5**(1): p. 67-73.
155. Kim, H.R., S.J. Ha, M.H. Hong, S.J. Heo, Y.W. Koh, et al., *PD-L1 expression on immune cells, but not on tumor cells, is a favorable prognostic factor for head and neck cancer patients*. *Sci Rep*, 2016. **6**: p. 36956.
156. Fourcade, J., Z. Sun, M. Benallaoua, P. Guillaume, I.F. Luescher, et al., *Upregulation of Tim-3 and PD-1 expression is associated with tumor antigen-specific CD8+ T cell dysfunction in melanoma patients*. *J Exp Med*, 2010. **207**(10): p. 2175-86.

157. Sakuishi, K., L. Apetoh, J.M. Sullivan, B.R. Blazar, V.K. Kuchroo, et al., *Targeting Tim-3 and PD-1 pathways to reverse T cell exhaustion and restore anti-tumor immunity*. J Exp Med, 2010. **207**(10): p. 2187-94.
158. Wieland, A., M.R. Patel, M.A. Cardenas, C.S. Eberhardt, W.H. Hudson, et al., *Defining HPV-specific B cell responses in patients with head and neck cancer*. Nature, 2021. **597**(7875): p. 274-278.
159. Pitzalis, C., G.W. Jones, M. Bombardieri and S.A. Jones, *Ectopic lymphoid-like structures in infection, cancer and autoimmunity*. Nat Rev Immunol, 2014. **14**(7): p. 447-62.
160. Li, Q., X. Liu, D. Wang, Y. Wang, H. Lu, et al., *Prognostic value of tertiary lymphoid structure and tumour infiltrating lymphocytes in oral squamous cell carcinoma*. Int J Oral Sci, 2020. **12**(1): p. 24.
161. Ruffin, A.T., A.R. Cillo, T. Tabib, A. Liu, S. Onkar, et al., *B cell signatures and tertiary lymphoid structures contribute to outcome in head and neck squamous cell carcinoma*. Nat Commun, 2021. **12**(1): p. 3349.
162. Pretscher, D., L.V. Distel, G.G. Grabenbauer, M. Wittlinger, M. Buettner, et al., *Distribution of immune cells in head and neck cancer: CD8+ T-cells and CD20+ B-cells in metastatic lymph nodes are associated with favourable outcome in patients with oro- and hypopharyngeal carcinoma*. BMC Cancer, 2009. **9**: p. 292.
163. Lundgren, S., J. Berntsson, B. Nodin, P. Micke and K. Jirstrom, *Prognostic impact of tumour-associated B cells and plasma cells in epithelial ovarian cancer*. J Ovarian Res, 2016. **9**: p. 21.
164. Carr, J.M., M.J. Carrasco, J.E. Thaventhiran, P.J. Bambrough, M. Kraman, et al., *CD27 mediates interleukin-2-independent clonal expansion of the CD8+ T cell without effector differentiation*. Proc Natl Acad Sci U S A, 2006. **103**(51): p. 19454-9.
165. Peperzak, V., Y. Xiao, E.A. Veraar and J. Borst, *CD27 sustains survival of CTLs in virus-infected nonlymphoid tissue in mice by inducing autocrine IL-2 production*. J Clin Invest, 2010. **120**(1): p. 168-78.
166. Tel, J., E.H. Aarntzen, T. Baba, G. Schreiber, B.M. Schulte, et al., *Natural human plasmacytoid dendritic cells induce antigen-specific T-cell responses in melanoma patients*. Cancer Res, 2013. **73**(3): p. 1063-75.
167. Shaw, J., Y.H. Wang, T. Ito, K. Arima and Y.J. Liu, *Plasmacytoid dendritic cells regulate B-cell growth and differentiation via CD70*. Blood, 2010. **115**(15): p. 3051-7.
168. Jensen, T.O., H. Schmidt, H.J. Moller, F. Donskov, M. Hoyer, et al., *Intratatumoral neutrophils and plasmacytoid dendritic cells indicate poor prognosis and are associated with pSTAT3 expression in AJCC stage I/II melanoma*. Cancer, 2012. **118**(9): p. 2476-85.
169. Labidi-Galy, S.I., I. Treilleux, S. Goddard-Leon, J.D. Combes, J.Y. Blay, et al., *Plasmacytoid dendritic cells infiltrating ovarian cancer are associated with poor prognosis*. Oncoimmunology, 2012. **1**(3): p. 380-382.
170. Fuchs, A., M. Cella, T. Kondo and M. Colonna, *Paradoxical inhibition of human natural interferon-producing cells by the activating receptor Nkp44*. Blood, 2005. **106**(6): p. 2076-82.
171. Sisirak, V., N. Vey, N. Goutagny, S. Renaudineau, M. Malfroy, et al., *Breast cancer-derived transforming growth factor-beta and tumor necrosis factor-alpha compromise interferon-alpha production by tumor-associated plasmacytoid dendritic cells*. Int J Cancer, 2013. **133**(3): p. 771-8.
172. Demoulin, S., M. Herfs, J. Somja, P. Roncarati, P. Delvenne, et al., *HMGB1 secretion during cervical carcinogenesis promotes the acquisition of a tolerogenic functionality by plasmacytoid dendritic cells*. Int J Cancer, 2015. **137**(2): p. 345-58.
173. Bruchhage, K.L., S. Heinrichs, B. Wollenberg and R. Pries, *IL-10 in the microenvironment of HNSCC inhibits the CpG ODN induced IFN-alpha secretion of pDCs*. Oncol Lett, 2018. **15**(3): p. 3985-3990.
174. Conrad, C., J. Gregorio, Y.H. Wang, T. Ito, S. Meller, et al., *Plasmacytoid dendritic cells promote immunosuppression in ovarian cancer via ICOS costimulation of Foxp3(+) T-regulatory cells*. Cancer Res, 2012. **72**(20): p. 5240-9.
175. Aspod, C., M.T. Leccia, J. Charles and J. Plumas, *Plasmacytoid dendritic cells support melanoma progression by promoting Th2 and regulatory immunity through OX40L and ICOSL*. Cancer Immunol Res, 2013. **1**(6): p. 402-15.

176. Yu, H., X. Huang, X. Liu, H. Jin, G. Zhang, et al., *Regulatory T cells and plasmacytoid dendritic cells contribute to the immune escape of papillary thyroid cancer coexisting with multinodular non-toxic goiter*. *Endocrine*, 2013. **44**(1): p. 172-81.
177. Dey, M., A.L. Chang, J. Miska, D.A. Wainwright, A.U. Ahmed, et al., *Dendritic Cell-Based Vaccines that Utilize Myeloid Rather than Plasmacytoid Cells Offer a Superior Survival Advantage in Malignant Glioma*. *J Immunol*, 2015. **195**(1): p. 367-76.
178. Huang, X.M., X.S. Liu, X.K. Lin, H. Yu, J.Y. Sun, et al., *Role of plasmacytoid dendritic cells and inducible costimulator-positive regulatory T cells in the immunosuppression microenvironment of gastric cancer*. *Cancer Sci*, 2014. **105**(2): p. 150-8.